

PEX16: a novel player in adipocyte development and energy metabolism

Master Thesis

by

Dina C. Hofer, BSc



Graz University of Technology
Institute of Biochemistry

supervised by

Assoc.Prof. Mag.rer.nat. Dr.rer.nat. Juliane G. Bogner-Strauß

graded by

Assoc.Prof. Mag.rer.nat. Dr.rer.nat. Juliane G. Bogner-Strauß

Graz, August 2014

STATUTORY DECLARATION

I declare that I have authored this thesis independently, that I have not used other than the declared sources / resources, and that I have explicitly marked all material which has been quoted either literally or by content from the used sources.

Graz,
(date)

.....
(signature)

Acknowledgement

At this point, I would like to express my sincere gratitude for giving me the unique opportunity to work at the institute of biochemistry in such a professional, outstanding and overall affectionate team. Special thanks goes to Juliane Bogner-Strauß, for welcoming me in her team, supervising and guiding me all throughout my work!

To no minor degree, I want to thank Andreas Prokesch, Ariane Pessentheiner and Helmut Pelzmann for their overwhelming support. They not only showed me how to properly work in the cell culture and in the laboratory, they also provided me with know-how, time for discussing results, and good ideas for further experiments and approaches in problem-solving. Thank you very much for always having an open door for me!

Additionally, I really want to thank Claudia Gaug, Florian Stöger and Thomas Schreiner for helping me out in laboratory- and cell culture- work, especially in the last phase of the thesis, when time for finishing the last experiments was running out.

I would also like to thank Madeleine Göritzer from the Medical University of Graz, for the determination of apoptotic markers in protein samples, and of course all the people from the institute who supported me either professionally or socially.

Not to forget, my work has not only been encouraged by members of the institute. I want to say a big "thank you" to all of my friends, who cared for diversion besides work and showed a lot of patience when time for them was limited.

Last but not least, sincere thanks have to be given to my family, and especially my Lucas. They broadened my horizon within lively discussions about my thesis by challenging me to think outside the box. Apart from the shoreless support they gave to me in every phase of my life, they managed to infect me with one important property, that brought me this far: Curiosity!

Thank you very much!

Abstract

English

Keywords: PEX16, peroxisomes, adipogenesis

Adipose tissue, its formation and function have intensively been studied in the past. It represents a promising target for the treatment of obesity and popular health related problems like type 2 diabetes. New players in adipogenesis and lipid metabolism are often discovered comparing adipose tissues of lean and obese mice using high throughput technologies. *Pex16* is one of these candidate genes, as it was shown to be highly upregulated during the differentiation of brown adipocytes in unpublished microarray data of our group. PEX16 protein is involved in peroxisomal de novo formation, growth and fission [1]. Regulation of peroxisomal growth and fission was shown to occur in concert with mitochondrial reorganization and division under stimulations, such as cold exposure and high fat diets in adipose tissue [2][3], suggesting a role in adipose tissue formation and metabolism. However, PEX16 and peroxisomal function have mainly been studied in the liver. The role of PEX16 in adipose tissue has not been investigated until today.

Pex16-expression profiles of murine tissues revealed that *Pex16* is, besides liver, also highly expressed in brown and white adipose tissue (BAT and WAT) and undergoes upregulation in brown adipose tissue and liver under high-fat dietary stimulation. Additionally, *Pex16* was upregulated during differentiation of several adipose cell lines, such as 3T3-L1, iBACs (immortalized brown adipose cell-line), C3H/10 T1/2, SGBS (Simpson Golabi Behmel Syndrome cells), and hMADS (human multipotent adipose-derived stem cells). The highest expression was observed in brown adipose tissue and in iBACs. Overexpression and silencing experiments were performed in models for white (3T3-L1) and brown (iBACs) adipocytes. Both variations of PEX16-expression provoked reduced lipid accumulations during differentiation. Overexpression of PEX16 in 3T3-L1 cells and iBACs caused a decrease in peroxisomal β -oxidation gene expression, such as *Acox1* and *Ehhadh*, and alterations in the expression of the adipogenesis marker gene *Ppar γ* . A reduced cell proliferation was observed for PEX16-overexpressing iBACs. Following hints for direct interactions of *Pex16* and PPAR γ , luciferase assays with putative PPAR γ -binding sites were performed, uncovering two regions of PPAR γ interference. These results indicate a potential role of *Pex16* in (brown) adipogenesis and energy metabolism.

German

Stichwörter: PEX16, Peroxisomen, Adipogenese

Entstehung und Funktion von Fettgewebe wurden aufgrund ihres nachgewiesenen Zusammenhangs mit einer Vielzahl von auf Adipositas zurückgehenden und besonderes herausfordernden Krankheiten des 21. Jahrhunderts, wie zum Beispiel Typ 2 Diabetes, in den letzten Jahren intensiv beforscht. Mittels Hochdurchsatzverfahren konnten bereits einige wichtige Gene aufgefunden werden, die essenziell in der Fettzellentwicklung und im Fettstoffwechsel sind. Im Rahmen eines solchen Microarray-Experiments unserer Arbeitsgruppe wurden wir auf *Pex16* aufmerksam, da es in differenzierenden braunen Fettzellen (iBACs) besonders stark exprimiert war. Das Protein PEX16 ist wesentlich an Neubildung, Wachstum und Teilung von Peroxisomen beteiligt [1]. Es wurde gezeigt, dass sich Peroxisomen im Fettgewebe in Anzahl und Aktivität an äußere Gegebenheiten wie Kälteeinwirkung oder sehr fettreiche Ernährung anpassen, wie es auch schon für Mitochondrien bekannt ist, die maßgeblich für die Funktion von braunem Fettgewebe verantwortlich sind [2][3]. Diese Beobachtung lässt vermuten, dass Peroxisomen und daher auch PEX16 eine relevante Rolle im Fettgewebe spielen könnten. Der Einfluss von PEX16 auf Fettzellentwicklung und deren Stoffwechsel ist indes in der Literatur noch nicht beschrieben.

Expressionsprofile von *Pex16* in verschiedenen Maus-Geweben machten deutlich, dass *Pex16* abgesehen von der Leber auch in braunem und weißem Fettgewebe stark exprimiert ist. Die Expression von PEX16 in braunem Fettgewebe und in der Leber von Mäusen, denen eine High-Fat-Diet verabreicht wurde, ist sogar noch höher. Ebenso konnte eine Hochregulierung während der Differenzierung in allen betrachteten Zelllinien (3T3-L1, iBACs (immortalisierte braune Fettzelllinie), C3H/10 T1/2, SGBS (Simpson Golabi Behmel Syndrom Zellen) und hMADS (humane, multipotente Stammzellen, abgeleitet von Adipozyten) festgestellt werden. Die höchste Expression war in braunem Fettgewebe sowie in braunen Fettzellen (iBACs) vorzufinden. Um einen besseren Einblick in die Rolle von PEX16 im Fettgewebe zu erhalten, wurde versucht, PEX16 in weißen (3T3-L1) und braunen (iBACs) Fettzellen überzuexprimieren und zu silencen. Beide Versuchsanordnungen waren durch verringerte Lipideinlagerungen in die Zellen gekennzeichnet. In PEX16-überexprimierenden Zellen konnte ein Trend zu verringerter Expression von peroxisomalen β -Oxidations-Genen (*Acox1* und *Ehhadh*) sowie eine veränderte *Ppar γ* -Expression festgestellt werden. In iBACs führte die Überexpression von PEX16 zu einer reduzierten Proliferation der Zellen. Da Hinweise für eine potentielle Interaktion zwischen PPAR γ und *Pex16* vorhanden waren, wurde diese im Rahmen von Luciferase Assays untersucht, die schließlich die Existenz von zwei PPAR γ -Bindestellen in der genomischen Sequenz von *Pex16* weitgehend bestätigten. Die erhaltenen Ergebnisse deuten an, dass PEX16 eine wesentliche Rolle in der Entwicklung und im Energie-Stoffwechsel von Fettzellen spielen könnte.

Contents

1	Abbreviations	4
2	Introduction	6
3	Materials & Methods	12
3.1	Materials	12
3.1.1	Buffers, Chemicals and Reagents	12
3.1.2	Cell Lines	15
3.1.3	Culture Media	15
3.1.4	Enzymes	16
3.1.5	Vectors	17
3.1.6	Kits and technical devices	17
3.1.7	Primers	18
	Cloning Primers	18
	qRT-PCR Primers	18
3.1.8	Western Blot reagents and buffers	19
	Antibody solutions	19
3.2	Methods	20
3.2.1	Cloning	20
	Sequence analysis	21
	Primerdesign	22
	PCR	22
	Enzymatic digestion of vectors and inserts	23
	Generation of blunt ends	23
	Ligation	23
	Transformation of NEB5 α Comp. E-Coli cells	23
	Colony PCR	23
	Minipreps and glycerolstocks	24
	Sequencing	24
3.2.2	Cell culture	24
	Handling	24
	Differentiation	25

Stimulation with rosiglitazone and isoproterenol	25
Transfection	26
Transduction	26
Proliferation assay	27
3.2.3 RNA-Isolation	27
3.2.4 cDNA synthesis	27
3.2.5 qRT-PCR	28
3.2.6 Oil Red O staining	28
3.2.7 Protein quantification	28
3.2.8 Triglyceride quantification in cells	28
3.2.9 Free fatty acid quantification in the supernatant of cells	29
3.2.10 Western Blot analysis	29
Gel electrophoresis	29
Transfer	29
Incubation with antibodies	30
Developing the blot	30
3.2.11 Luciferase reporter assays	31
3.2.12 Statistics	31
4 Results	32
4.1 Pex16 expression in murine tissue	32
4.2 PEX16-expression undergoes upregulation during adipogenic differentiation of murine and human cell models	33
4.3 Overexpressing PEX16 in white and brown adipocyte models	35
4.3.1 Overexpression of PEX16 in 3T3-L1-cells	35
Cloning of <i>Pex16</i> -CDS into pMSCVpuro and pHisMaxC-vector	35
Phenotypical changes due to overexpression of PEX16 in white adipocytes	35
4.3.2 Overexpression of PEX16 in iBACs	39
Cloning of <i>Pex16</i> -CDS into pMSCVhygro-vector	39
Phenotypical changes due to overexpression of PEX16 in brown adipocytes via pMSCVpuro	39
4.4 Silencing of PEX16 in models for white and brown adipocytes	46
4.4.1 Silencing of PEX16 in 3T3-L1 adipocytes	46
4.4.2 Silencing of PEX16 in iBACs	48
4.5 Pex16 - a possible PPAR γ target	49
4.5.1 Luciferase assays using pTK-luc - luciferase reporter vector	50
Cloning of putative PPAR γ - target sequences into pPPRE-X3-TK-luc- vector	50
Luciferase-assays using pTK-luc- luciferase reporter vector suggest a potential interaction of PPAR γ and <i>Pex16</i>	51

Contents

4.5.2	Luciferase assays using pGL4.26 - luciferase reporter vector	52
	Cloning of PPAR γ target sequences into pGL4.26-vector	52
	Luciferase-assay using pGL4.26- luciferase reporter vector confirms the suggested binding of Pex16 by PPAR γ	54
5	Discussion	55
5.1	Pex16 is highly expressed in murine adipose tissue and elevated during adipogenesis .	55
5.2	PEX16 overexpression influences adipogenesis	56
5.2.1	Western Blot analysis reveals a reduced protein size of PEX16	58
5.2.2	FFA and Triglyceride measurement	59
5.3	Stable silencing could be accomplished for 3T3-L1 cells, iBACs were not selectable .	59
5.4	Luciferase assays reveal Pex16 as a PPAR γ target gene	60
5.5	Model for PEX16 contribution to lipid metabolism in adipose tissue	61
5.6	Concluding remarks	61
	List Of Figures	66
	List Of Tables	67
6	Appendix	68
	Bibliography	82

1 Abbreviations

ATP	adenosine-5'-triphosphate
BAT	brown adipose tissue
BAX	BCL-2-associated X protein
BCL-2	B-cell lymphoma protein 2
BMI	body mass index (kg/m ²)
BSA	bovine serum albumin
cAMP	cyclic adenosine monophosphate
cDNA	complementary DNA
CDS	coding DNA sequence
ddH₂O	double distilled H ₂ O
Dex	dexamethasone
DMEM	Dulbecco's modified eagle medium
DMSO	dimethylsulfoxide
DNA	deoxyribonucleic acid
dNTP	deoxyribonucleotide triphosphate
DTT	dithiothreitol
ER	endoplasmic reticulum
FA	fatty acid
FBS	fetal bovine serum
FFA	free fatty acid
gDNA	genomic DNA
GM	growth medium
HFD	high fat diet
His-Tag	codon for six histidines in a row
iBAC	immortalized brown adipose cell line
IBMX	3-Isobutyl-1-methylxanthine
Indo	Indomethacin
ko	knockout
mRNA	messenger RNA
MOI	multiplicity of infection
MCS	multiple cloning site
NTC	non targeting control

1 Abbreviations

ob	obese gene
o/e	overexpression
ONC	overnight culture
PBS	phosphate buffered saline
PBST	phosphate buffered saline including Tween20
PCR	polymerase chain reaction
Pex16	Peroxisomal biogenesis factor 16 gene
PEX16	Peroxisomal biogenesis factor 16 protein
PGC-1α	PPAR γ -coactivator 1 α protein/gene
PIC	protease inhibitor cocktail
pMSCV	murine stem cell virus plasmid
PPAR	peroxisome proliferator-activated receptor
PPRE	peroxisome prolifer-activated receptor response element
P/S	penicillin/ streptomycin
qRT-PCR	quantitative real-time polymerase chain reaction
RE	restriction enzyme
Rosi	rosiglitazone maleate
RXRα	retinoid X receptor alpha
SGBS	Simpson-Golabi-Behmel syndrome
SD	standard deviation
SDS	sodium dodecyl sulfate
TBS	tris buffered saline
TG	triglycerides
TNFα	tumor necrosis factor α
TSS	transcription start site
UCP1	uncoupled protein 1
WAT	white adipose tissue
wt	wild-type

2 Introduction

PEX16, peroxin-16 or peroxisomal biogenesis factor 16 are only a few names of a stunning protein, showing various functions reaching from peroxisomal biogenesis to peroxisomal membrane protein (PMP) import, depending on the expressing organism [1]. Absence or mutations of the protein lead to severe, often lethal neurological and developmental diseases.

In humans, *PEX16* gene is located on chromosome 11 (11p11.2)¹, encoding two protein-isoforms (isoform 1: 336aa, \approx 38.6 kDa, isoform 2: 346aa, \approx 39.3 kDa)². Homologs of the gene can be found in almost all eukaryotes, showing about 15-25% sequence identity [1]. In mice, *Pex16* gene is located on chromosome 2 (2E1;2), encoding two transcript variants³, whereas only variant 1 encodes the functional PEX16- protein (336aa, \approx 38.6 kDa)⁴.

The function of PEX16 highly depends on the expressing organism and furthermore on the intracellular localization within these organisms:

PEX16 is commonly targeted to peroxisomes and endoplasmic reticulum [4]. In yeast, PEX16 is a peripheral membrane protein, involved in peroxisomal biogenesis and fission when bound to peroxisomes [1]. This was confirmed by overexpression experiments in yeast, resulting in a decreased number of peroxisomes, which were additionally enlarged in size compared to controls [1][5]. Whereas bound to the endoplasmic reticulum, PEX16 influences cell differentiation and polarity [6][7].

On the contrary, in humans, PEX16 is an integral membrane protein, showing multiple transmembrane domains, with N- and C- termini facing the cytosol [8]. The C-terminal region showed to be essential for the biological function [9], as it seems to play a role in the early phase of peroxisomal de novo synthesis at the endoplasmic reticulum. When integrated into peroxisomes, it influences the attraction of peroxisomal membrane proteins from the cytosol to mature peroxisomes [1]. More precisely, it appears to be a receptor for PEX3 in the endoplasmic reticulum (ER) as well as in mature peroxisomes. Based on this assumption, it enables the PEX3-dependent integration of group I or group II peroxisomal membrane proteins, respectively, either into pre-peroxisomes released from the ER or into mature peroxisomes, promoting growth and fission of these organelles (see figure 2.1). [4][10][11][12].

¹<http://www.ncbi.nlm.nih.gov/gene/9409>, July 2014

²<http://www.uniprot.org/uniprot/Q9Y5Y5>, July 2014

³<http://www.ncbi.nlm.nih.gov/gene/18633>, July 2014

⁴<http://www.uniprot.org/uniprot/Q91XC9>, July 2014

By taking these assumptions into consideration, PEX16 might be the driving force (or "master"-peroxin) in launching peroxisomal biogenesis de novo [1].

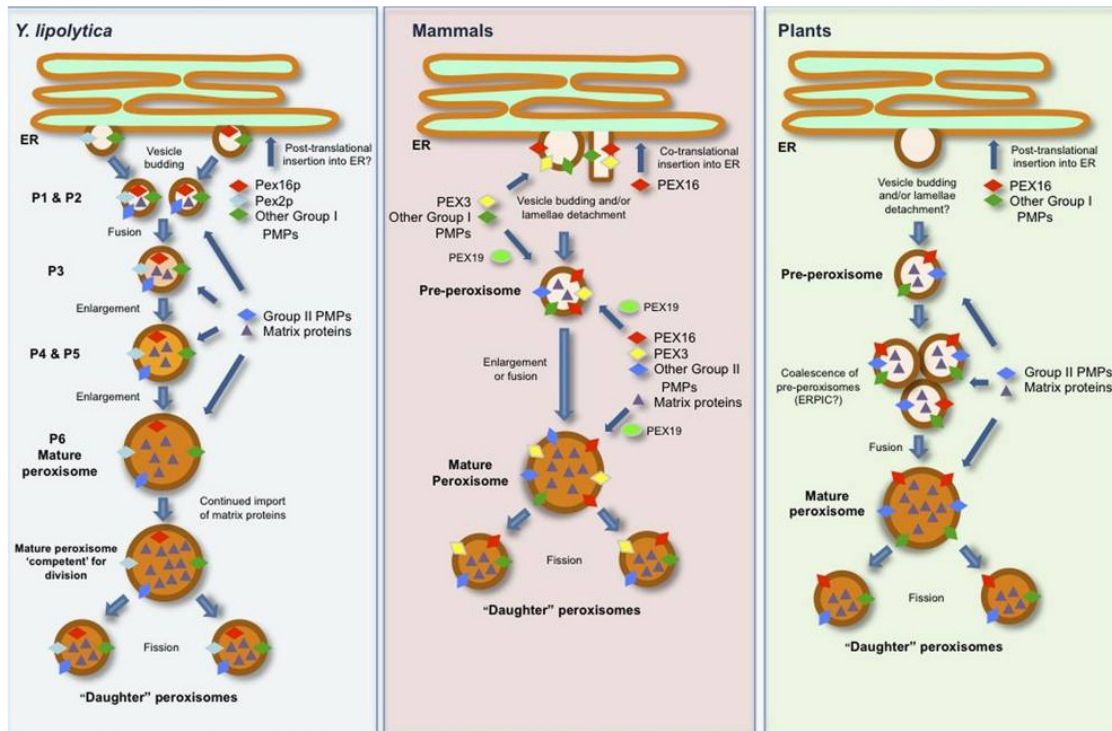


Figure 2.1: Scheme of peroxisomal biogenesis in different organisms: *Y. lipolytica*, *Mammals* and *Plants*. In mammals, PEX16 is co-translationally inserted into the ER by the SEC61-dependent import pathway. At the ER it is integrated into pre-peroxisomes, where it serves as receptor for PEX3 and group 1 PMPs. PEX16 is also directly targeted to pre-peroxisomes, still serving as PEX3 and group 2 PMP receptor and causing the formation of mature peroxisomes, which can now undergo fission for proliferation. [1].

From this point of view, it's no surprise that peroxisomes fail to appear in cells when PEX16 is mutated or absent, which was observed similarly for alterations of PEX3 and PEX19 expression, that are also involved in the early stages of peroxisomal biogenesis [4][8][13][14][15].

Accumulations of toxic substances, like very long-chain fatty acids, phytanic acid and pristanic acid, in the cell caused by a complete or partial loss of peroxisomal functions, culminate in severe developmental and neurological dysfunctions. These are commonly known as peroxisomal biogenesis disorders (PBD) [16][17][18], including fatal Zellweger syndrome, neonatal adrenoleukodystrophy, and infantile Refsum's disease [19][20][21].

Peroxisomes are tiny organelles, that are present in almost all eukaryotic cells and show very complex metabolic functions, reaching from α - and β - oxidation of very long fatty acids over the oxidation of ether lipids, bile acids and cholesterol, to the detoxification of H_2O_2 [4][18][22].

In contrast to their complexity of functions and biosynthesis, the peroxisomal final structure is very simple, composing of a nonhomogenous matrix embedded in a single lipid bilayer membrane (see figure 2.2) [22].

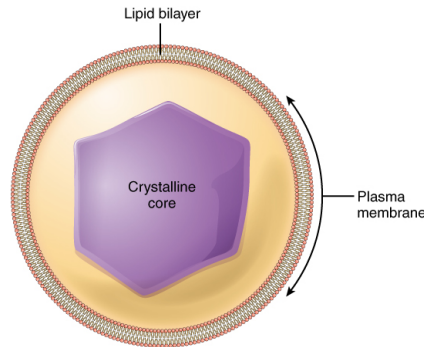


Figure 2.2: Peroxisomal composition: Plasma membrane, nonhomogenous matrix and optional crystalline core.
Source: www.boundless.com/biology/cell-structure/eukaryotic-cells/peroxisomes

By defining stationary levels of multiple signaling lipids like phytanic acid, retinoic acid and especially long-chain fatty acids within the cell, activation of RARs (retinoic acid receptors) and PPARs (peroxisome proliferator-activated receptors) is facilitated, resulting in the transcription of genes necessary for embryonic development and differentiation of various tissues, including adipose, brain, skin, and placental tissues in mammals [23][24][25][26].

Although peroxisomes have long been known for their importance in metabolizing lipids, their functions have primarily been investigated in the liver [27]. Based on the observation, that peroxisomes do not participate at the respiratory chain, and FAD-linked oxidases of the peroxisomal β -oxidation are direct donors of electrons to O_2 , possible roles of these organelles in thermogenesis in brown adipose tissue (BAT) and in the regulation of body weight have been suggested [3][27][28][29][30].

Three different cell organelles are responsible for the oxidation of fatty acids: 1) mitochondria, 2) peroxisomes, both performing β -oxidation, and 3) the endoplasmic reticulum, performing ω -oxidation of fatty acids [20][31][32][33][34]. Fatty acids exhibit crucial functions in a whole set of processes within the cell, such as storage of energy, cellular membrane synthesis and signal transduction [20]. In mitochondria, β -oxidation of short ($<C_8$), medium (C_8 - C_{12}) and long (C_{12} - C_{20})-chain fatty acids takes place, generating acetyl-CoA for energy utilization in form of ATP by oxidative phosphorylation or alternatively in activated brown adipose tissue in form of heat [20][34]. Long-chain fatty acids serve as main energy source in conditions of normal feeding and also in fasting state [20].

Peroxisomal β -oxidation, on the contrary, is probably the only possible way of oxidizing very long-chain fatty acids ($>C_{20}$) and trans-unsaturated acids, which can not be metabolized in mitochondria as they do not feature a very long-chain fatty acyl-CoA synthetase [20][33][34][35]. Two ways of peroxisomal β -oxidation are known: The first one, the "traditional" way, was shown to be inducible by PPAR α , thyroid hormones, cold exposure and high fat diets. The second way is non-inducible and responsible for oxidation of branched-chain fatty acyl-CoAs. [3][20][33][34].

In peroxisomes, three enzymes are mainly involved in the traditional β -oxidation (see figure 2.3): ACOX1 (straight-chain acyl-CoA oxidase or acyl-Coenzyme A oxidase 1) initiates the peroxisomal β -oxidation by oxidizing very long-chain fatty acyl-CoAs.[20][33][34]. EHHADH (enoyl CoA hydratase/3-hydroxyacyl-CoA dehydrogenase) exhibits two different functions. In the second step of peroxisomal β -oxidation it functions N-terminally as enoyl-CoA hydratase. In the third step, it functions C-terminally as 3-hydroxyacyl-CoA dehydrogenase⁵. ACAA1 (acetyl-CoA acyltransferase 1) serves as catalyst in the reversible thiolitic cleavage of 3-ketoacyl-CoA producing acyl-CoA and acetyl-CoA⁶. Generated acetyl-CoA is utilized in anabolic reactions for cholesterol- and bile acid synthesis [36] or is delivered to mitochondria via a "carnitine shuttle" [30], where it can be used for energy production (see figure 2.3). Energy provided via peroxisomal β -oxidation, which generates H_2O_2 , is not preserved in form of ATP, leading to the idea that peroxisomal β -oxidation could eventually be thermogenic, comparable to the energy dissipation in form of heat in mitochondria of brown adipose tissue [20][27].

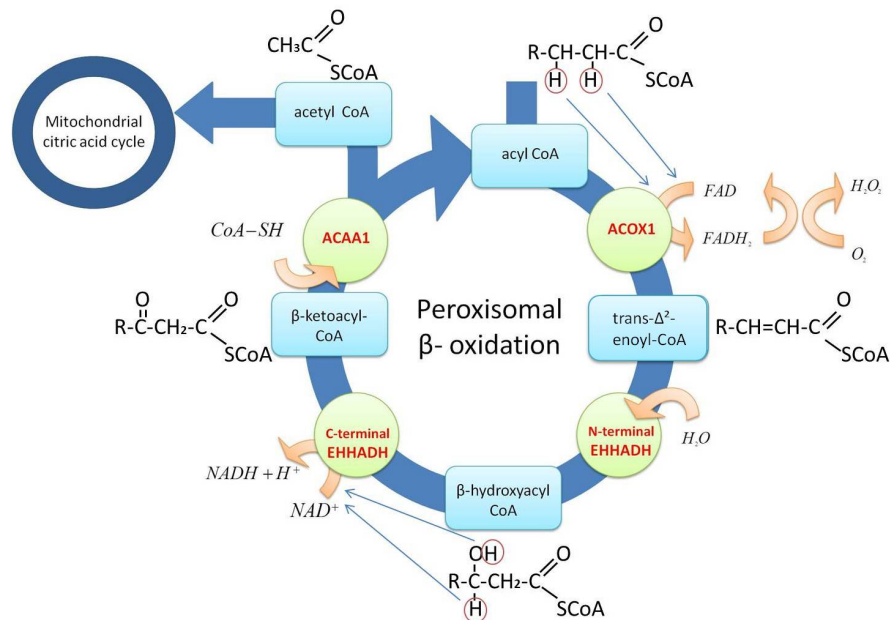


Figure 2.3: Scheme of the peroxisomal β -oxidation. Acyl-CoA is oxidized to acetyl-CoA, which can be delivered to mitochondria where it serves for energy generation. Hydrogen peroxide is generated within the first step of the process.

⁵www.ncbi.nlm.nih.gov/gene/1962, July 2014

⁶www.ncbi.nlm.nih.gov/gene/30, July 2014

It has been shown in the past, that peroxisomes react similarly to mitochondria in response to various stimuli by reorganization and fission [2], suggesting an extensive regulatory linkage between these organelles. Thermogenic, thyroid hormonal stimulation as well as high fat diets and modified expression of PGC-1 α , a transcription cofactor in energy metabolism, led to significant morphological and quantitative changes of peroxisomes [2][3]. Elevated numbers of peroxisomes were observed in brown adipose tissue of mice and rats exposed to cold and in fully differentiated murine fat cells overexpressing PGC-1 α . This observation was accompanied by increased mRNA-levels of peroxisomal β -oxidation and biogenesis genes (*Acox1*, *Acaa1a*, *Ehhadh*, *Pex11 α* , *Pex11 β* , *Pex16*, *Pex19*, *PMP70*, *DLP1*) and important mitochondrial genes (*UCP1*, *PGC-1 α*).[2][28]. The peroxisomal β -oxidation genes *Acox1*, *Acaa1a* and *Ehhadh* were also found increased in adipose tissues of obesity-resistant black 6 mice under high-fat-diet, suggesting a role of peroxisomal β -oxidation in body-fat control [37]. Peroxisomal β -oxidation activity in brown fat was also studied in perinatal rabbits, with the outcome, that peroxisomal activity was highest prior to birth, suggesting, that peroxisomes might not play a role in thermogenesis itself, but in predetermination of brown fat formation [38]. More recently, aP2-Pex5- knockout in mice was performed. The aP2-Pex5- knockout represents an almost adipose tissue specific knockout of *Pex5*. *Pex5* is a peroxisomal gene involved in peroxisomal matrix protein import. [27]. Experiments in aP2-Pex5- knockout mice revealed increased white fat depots and decreased lipolysis, accompanied by defective shivering thermogenesis, motor activity and elevated insulin resistance. However, thermogenesis in BAT was not affected even under long term cold exposure.[27]. Nevertheless, it is not yet verified, whether the elevated fat mass in aP2-Pex5- knockout mice traces back to the deficiency of peroxisomes [27]. Interestingly, knockout of *Pex7*, an additional gene involved in peroxisomal matrix protein import ⁷, in mice displayed reduced lipid accumulations in both, white and brown adipose tissue caused by the absence of ether lipids due to a defective peroxisomal β -oxidation. Lipid stores recovered when mice were fed nutrition rich in ether lipid precursors.[27][39]. Amongst others, *Pex5* and *Pex7* together with *Pex16* belong to the group of PEX-genes, which encode proteins responsible for proper peroxisomal assembly [40].

In general, three distinct types of adipose tissues are known: White adipose tissue (WAT), beige or brite ("brown in white") adipose tissue, and brown adipose tissue (BAT) [41]. White adipose tissue represents the biggest part of adipose tissue in humans and is characterized by a single, large lipid droplet, and only few mitochondria. In brown adipose tissue, multiple smaller lipid droplets and a high number of mitochondria can be found [42]. Accumulations of beige adipocytes can be found within white adipose tissue. These adipocytes share several properties with brown adipocytes, although they do not exhibit full "brown capacity". Their occurrence is considered to be inducible by cold exposure or β 3-adrenergic stimulation [41].

⁷www.ncbi.nlm.nih.gov/gene/5191

Brown adipose tissue has been of great interest for many research teams in the past few years, because of its ability to increase energy consumption by dissipating energy as heat when activated [43][44]. This heat generating process is mediated by uncoupling protein 1 (UCP1), which is located in mitochondria exclusively in beige and brown adipose tissue. By generating a proton leak across the inner mitochondrial membrane, it "uncouples" the oxidation of fuel from the synthesis of ATP [41], and produces heat. Thereby, the activation of BAT offers a great possibility for the treatment of obesity and its associated disorders like type 2 diabetes, heart disease, hypertension, stroke, and multiple types of cancer, making up a majority of the 21st century's complex diseases responsible for the exploding costs in modern healthcare [45].

Many genes participating in brown adipose tissue formation, mitochondrial development and thermogenesis have already been identified. Now, peroxisomes have been shown to represent a promising new player in the complex network of adipocyte development and metabolism, as they are regulated along with mitochondria. PEX16 is highly upregulated in the brown adipose cell line iBACs during adipogenic differentiation, which was shown by microarray experiments of our group (data not published), and is highly expressed in liver, white and brown adipose tissue in mice ⁸. The finding, that it seems to be the initiator of peroxisomal biogenesis and the fact that only little about its role in adipogenesis and lipid metabolism has been described so far, make PEX16 a promising new target to be investigated in the context of adipocyte development and energy metabolism.

⁸www.biogps.org/#goto=genereport&id=18633, July 2014

3 Materials & Methods

3.1 Materials

3.1.1 Buffers, Chemicals and Reagents

- ▷ 1 kb DNA Ladder, Fermentas Inc.
- ▷ 5-(3-aminoallyl)-2'-deoxyuridine-5'-triphosphate (AA-dUTP); Sigma-Aldrich Handels GmbH
- ▷ Aqua bidestillata sterilis. "Fresenius"; Fresenius
- ▷ UltraPureTM Agarose; Life Technologies, Invitrogen corp.
- ▷ Benzonase® Nuclease; Merck Chemicals
- ▷ Bovine Serum Albumine (BSA, Lot.Nr. K00110-1227); PAA Laboratories GmbH
- ▷ Chloroform; Sigma-Aldrich Handels GmbH
- ▷ Dimethylsulfoxide (DMSO); Sigma-Aldrich H. GmbH
- ▷ DEPC treated H₂O for molecular biology; Karl Roth GmbH + Co. KG
- ▷ Dexamethasone (Dex); Sigma-Aldrich Handels GmbH
- ▷ Diethylether; Karl Roth GmbH + Co. KG
- ▷ Dithiothreitol (DTT) 0.1M; Life Technologies, Invitrogen corp.
- ▷ Dithioerythritol (DTE); VWR International (Merck Chemicals)
- ▷ dNTP Set (100mM); Fermentas
- ▷ ECL prime; Amersham, GE Healthcare
- ▷ Ethanol absolute, for analysis; Lactan chemicals and laboratory devices
- ▷ Ethidiumbromidlösung 1%; Karl Roth GmbH + Co. KG
- ▷ 5x First Strand Buffer (5xFS); Life Technologies, Invitrogen corp.
- ▷ Foetal Bovine Serum (FBS, Lot.Nr. 09SB032); Lonza Inc.
- ▷ Formaldehyde; Sigma-Aldrich Handels GmbH
- ▷ Formamide; Sigma-Aldrich Handels GmbH
- ▷ Glycerol 98%; Lactan chemicals and laboratory devices
- ▷ Geneticindisulfat (G418-Sulfat); Karl Roth GmbH + Co. KG
- ▷ HEPES buffer 1M; Life Technologies, Invitrogen corp.
- ▷ Hexadimethrine (Polybrene 8mg/mL); Sigma-Aldrich Handels GmbH

- ▷ 3-isobutyl-1-methylxanthine (IBMX, 1g); VWR International (Merck Chemicals)
- ▷ Indomethacin crystalline (Indo); Sigma-Aldrich Handels GmbH
- ▷ Insulin (10mg/mL); Sigma-Aldrich Handels GmbH
- ▷ Isopropyl alcohol; VWR International (Fisher Scientific U.K. Ltd.)
- ▷ Isoproterenol; Sigma-Aldrich Handels GmbH
- ▷ K_2HPO_4 ; Sigma-Aldrich Handels GmbH
- ▷ KH_2PO_4 ; Sigma-Aldrich Handels GmbH
- ▷ LDS Sample Buffer 4x; Life Technologies, Invitrogen corp.
- ▷ L-Glutamine (L-Glut) 200mM; Life Technologies, Invitrogen corp.
- ▷ Lentiviral MISSION® Transmission Particles NM_145122; Sigma - Aldrich Handels GmbH
- ▷ Mouse anti- β -actin antibody; Sigma-Aldrich H. GmbH
- ▷ Metafectene; Biontex Laboratories GmbH
- ▷ Methanol Normapur for analysis; VWR International (Merck Chemicals)
- ▷ NaCl; Karl Roth GmbH + Co. KG
- ▷ Na_2CO_3 ; VWR International (Merck Chemicals)
- ▷ NaF; VWR International (Merck Chemicals)
- ▷ NaOAc; Sigma-Aldrich Handels GmbH
- ▷ Natriumorthovanadate; Sigma-Aldrich Handels GmbH
- ▷ n-hexane; Karl Roth GmbH + Co. KG
- ▷ Normocin (Normo); Eubio
- ▷ NuPAGE® Antioxidant; Life Technologies, Invitrogen corp.
- ▷ NuPAGE® 10% Bis-Tris Gel 1.0mm X 10 well; Life Technologies, Invitrogen corp.
- ▷ NuPAGE® 4-12% Bis-Tris Gel 1.0mm X 10 well; Life Technologies, Invitrogen corp.
- ▷ NuPAGE® MOPS SDS Running Buffer 20x; Life Technologies, Invitrogen corp.
- ▷ NuPAGE® MES SDS Running Buffer 20x; Life Technologies, Invitrogen corp.
- ▷ Oil Red O; ICN
- ▷ Oligo-dT Primers; Life Technologies, Invitrogen corp.
- ▷ PBS pH 7.4, Life Technologies, Invitrogen corp.
- ▷ Phosphate buffered saline (PBS, pH 7.4); Life Technologies, Invitrogen corp.
- ▷ Penicillin / Streptomycin (P/S) Sol 10.000U/mL per 10.000 μ g/mL; Life Technologies, Invitrogen corp.
- ▷ Poly(A)-DNA; Life Technologies, Invitrogen corp.
- ▷ Polyclonal Goat Anti-Rabbit IgG / HRP, DakoCytomation
- ▷ Polyclonal Goat Anti-Mouse IgG / HRP, DakoCytomation

- ▷ Protease Inhibitor Cocktail Tablets (PIC); Roche Austria GmbH
- ▷ Puromycin dihydrochloride CELL CULTURE; Sigma-Aldrich Handels GmbH
- ▷ Rabbit Polyclonal Anti-PEX16 IgG; Acris Antibodies GmbH
- ▷ Random Hexamer Primers 3µg/µL; Life Technologies, Invitrogen corp.
- ▷ RNaseOUTTM, Life Technologies, Invitrogen corp.
- ▷ Roentogen EUKOBROM (b/w paper developer); Tetanal
- ▷ Roentogen Superfix (fixing bath for rapid processing of b/w materials); Tetanal
- ▷ Rosiglitazone Maleate (Rosi), Ebio
- ▷ 20x Saline-Sodium Citrate (SSC); Sigma-Aldrich Handels GmbH
- ▷ Seebule® Plus2 Prestained Standard; Life Technologies, Invitrogen corp.
- ▷ Skim Milk Powder (NFDM); Fluka analytical AG
- ▷ Sodium Dodecylsulfate (SDS); VWR International (Merck Chemicals)
- ▷ 10% Sodium Dodecyl Sulfate (SDS), Life Technologies, Invitrogen corp.
- ▷ Super Script II Reverse Transcriptase (200U/µL); Life Technologies, Invitrogen corp.
- ▷ Super Signal West Pico Chemoluminescent Substrate; VWR International (Fisher Scientific U.K. Ltd.)
- ▷ SYBR QPCR Supermix W/Rox; Life Technologies, Invitrogen corp.
- ▷ TLC silica gel 60, Merck Chemicals
- ▷ 0.5% Trypsin / EDTA (10x); Life Technologies, Invitrogen corp.
- ▷ Triiodothyronine (T3); Sigma-Aldrich Handels GmbH
- ▷ Tris Glycine Buffer (TGS; 10x), Bio-Rad Laboratories GmbH
- ▷ Tris Ultra Quality, Lactan chemicals and laboratory devices
- ▷ Tween20, VWR International (Merck Chemicals)

TAE-buffer:	242 g Tris Ultra Quality 57,1 g Acetate 16,8 g EDTA 1 L dH ₂ O	LB-medium:	10 g Peptone 10 g NaCl 5 g Yeast 1 L dH ₂ O
-------------	--	------------	---

LB-Medium for agar-plates:	10 g Peptone 10 g NaCl 5 g Yeast 1 L dH ₂ O 15g Agar	Glycerolstock:	25mL LB-medium 25mL Glycerin (>98%)
----------------------------	---	----------------	--

3.1.2 Cell Lines

3H/10 T1/2: mouse embryonic fibroblasts; muscle, adipose, bone or cartilage like

3T3-L1: mouse embryonic fibroblasts; adipose like

Cos7: fibroblasts; recovered from green vervet monkey

hMADS: human multipotent adipose-derived stem cells

iBACs: SV40 T-large antigen immortalized brown adipose cell line, kind gift of Patrick Seale, University of Pennsylvania School of Medicine, Philadelphia

Phoenix: human embryonic kidney cell line, retroviral expression system

SGBS: human Simpson-Golabi-Behmel Syndrome cells, adipose like

3.1.3 Culture Media

Standard Growth Medium (DMEM++++) for 3T3-L1, Cos7 & Phoenix cells:

DMEM (Dulbeccos Modified Eagle Medium, 4,5g Glucose), Invitrogen

+ FBS 10%

+ Normocin 1:500

+ L-Glut 2mM

+ P/S 100U/mL / 100µg/mL

Differentiation/Induction Medium (DM1) for 3T3-L1 cells:

DMEM++++

+ Insulin 2µg/mL

+ Dex 1µM

+ IBMX 0,5mM

Differentiation/Induction Medium 2 (DM2) for 3T3-L1 cells:

DMEM++++

+ Insulin 2µg/mL

Differentiation/Induction Medium 3 (DM3) for 3T3-L1 cells:

DMEM++++

+ Insulin 2µg/mL

+ Dex 1µM

+ IBMX 0,5mM

+ Rosi 1µM

iBACs Growth Medium (iBACs-GM):

DMEM (Dulbeccos Modified Eagle Medium, 4,5g Glucose), Invitrogen

+ FBS 10%

+ HEPES 20mM

+ P/S 100U/mL / 100µg/mL

iBACs Maintenance Medium (iBACs-MM):

iBACs GM
+ Insulin 20nM (1,161 μ L/mL-GM)
+ T3 1nM

iBACs Induction Medium (iBACs-IM):

iBACs MM
+ Dex 500nM
+ IBMX 0,5mM
+ Indo 0,125nM

Freeze Medium (FM) for 3T3-L1, Cos7 & Phoenix cells:

DMEM++++
+ DMSO 5%

iBACs Freeze Medium (iBACs-FM):

iBACs-GM 9%
+DMSO 10%
+FBS 81%

FFA- free Medium:

DMEM (Dulbeccos Modified Eagle Medium, 4,5g Glucose), Invitrogen
+FFA-free BSA 2%

FFA-free Medium + Isoproterenol:

DMEM (Dulbeccos Modified Eagle Medium, 4,5g Glucose), Invitrogen
+FFA-free BSA 2%
+Isoproterenol 10 μ M

3.1.4 Enzymes

- ▷ DNA Polymerase I, Lg (Klenow) Fragment, New England Biolabs, Inc.
- ▷ FastAP; Fermentas
- ▷ Phusion High-Fidelity DNA Polymerase; Thermo Fisher Scientific, Inc.
- ▷ Q5® High Fidelity DNA Polymerase; New England Biolabs, Inc.
- ▷ T4 DNA Ligase; Fermentas
- ▷ Taq DNA Polymerase (recombinant); Fermentas
- ▷ HindIII-HF®, BamHI-HF®, XhoI, KpnI-HF®; New England Biolabs, Inc.
- ▷ BglIII, EcoRI, HpaI, XhoI, NotI; Fermentas

3.1.5 Vectors

- ▷ pMSCVpuro; Clontech Laboratories Inc.
- ▷ pHisMaxC; Invitrogen corp.
- ▷ pMSCVhygro; Clontech Laboratories Inc., kind gift from E.D. Rosen
- ▷ pPPRE X3-TK-luc,(Addgene Plasmid 1015); Addgene, Inc.
- ▷ pGL4.26; Promega, Madison, USA
- ▷ pGL4.75; Promega, Madison, USA

3.1.6 Kits and technical devices

- ▷ 1L 0.22µm cellulose acetate (CA) Filter System; Corning Costar
- ▷ ABI Prism 7000 Sequence Detection System
- ▷ BCA Protein Assay Kit; VWR International (Fisher Scientific U.K. Ltd.)
- ▷ Dual-Luciferase® Reporter Assay System; Promega GmbH
- ▷ FLUOstar Omega microplate reader; BMG LABTECH GmbH
- ▷ Microscope cover glass; Fisher Scientific U.K. Ltd.
- ▷ Mini Trans-Blot® Cell and PowerPac HC Power Supply; Bio-Rad Laboratories, Inc.
- ▷ NanoDrop ND-1000 Spectrophotometer; NanoDrop Technologies, Inc.
- ▷ NEFA-HR R1 Set; Wako Chemicals GmbH
- ▷ NEFA-HR R2 Set; Wako Chemicals GmbH
- ▷ Orion II Microplate Luminometer; Berthold Detection Systems GmbH
- ▷ peqGOLD Total RNA Kit; PEQLAB Biotechnologie GmbH
- ▷ peqGOLD Gel Extraction Kit; PEQLAB Biotechnologie GmbH
- ▷ PureLink® PCR Purification Kit; Life Technologies, Invitrogen corp.
- ▷ PureLinkTM Quick Plasmid Miniprep Kit; Life Technologies, Invitrogen corp.
- ▷ QuantiTect Reverse Transcription Kit; QIAGEN, Inc.
- ▷ Sonicator SONOPULS; Bandelin
- ▷ Thermomixer compact, Eppendorf
- ▷ Triglycerides-kit, Thermo Scientific / Fisher Diagnostics
- ▷ UV-Transilluminator Universal Hood; Bio-Rad Laboratories, Inc.
- ▷ Veriti® 96-Well Thermal Cycler; Applied Biosystems®

3.1.7 Primers

Cloning Primers

Targetvector	Primersname (F = forward, R = reverse)	Sequence	Restriction site
<u>pMSCVpuro:</u>	<i>mPex16_BglII_F</i> <i>mPex16_EcoRI_R</i>	CATCAGAGATCTATGGAGAAGCTACGGCTCC CGGATCGAATTCTCAGCCCAACTGTAGAAATAG	BglII EcoRI
<u>pMSCVhygro:</u>	<i>mPex16_BglII_F</i> <i>mPex16_HpaI_R</i> <i>mPex16_XhoI_R</i>	CATCAGAGATCTATGGAGAAGCTACGGCTCC CGGATCGTTAACTCAGCCCAACTGTAGAAATAG CGGATCCTCGAGTCAGCCCAACTGTAGAAATAG	BglII HpaI XhoI
<u>pHisMaxC:</u>	<i>mPex16_EcoRI_pHM_F</i> <i>mPex16_NotI_pHM_R</i>	CATCAGGAATTCATGGAGAAGCTACGGCTCC CGGATCGGGCCGCTCAGCCCAACTGTAGAAATAG	EcoRI NotI
<u>pPPRE X3-TK-luc:</u>	<i>mPex16_Peak1+2_HindIII_F</i> <i>mPex16_Peak1_BamHI_R</i> <i>mPex16_Peak2_HindIII_F</i> <i>mPex16_Peak1+2_BamHI_R</i> <i>mPex16_Peak3_HindIII_F</i> <i>mPex16_Peak3short_BamHI_R</i> <i>mPex16_Peak3long_XhoI_R</i>	GCCAAGCTTCTGTTTCAGCCTGCCCGCAAGTTGT AGAGGATCCGACGAGTCACATACTCCTGGTAGCG GCCAAGCTTCTGTCCGGCCGGTGGGACTGTC AGAGGATCCCAGAGTCCAACCTTACCCAGTTCAGAC GCCAAGCTTGAGAGCAAAGATGAGTTGGTGGGAC AGACTCGAGTGGGCATGCCTCACTCTCTGAGAC GAGCTCGAGATGGGCATGCCTCACTCTCTGAGAC	HindIII BamHI HindIII BamHI HindIII BamHI XhoI
<u>pGL4.26:</u>	<i>mPex16_Peak1+2_KpnI_F</i> <i>mPex16_Peak1_XhoI_R</i> <i>mPex16_Peak2_KpnI_F</i> <i>mPex16_Peak1+2_XhoI_R</i> <i>mPex16_Peak3long_KpnI_F</i> <i>mPex16_Peak3long_XhoI_R</i>	GCCGGTACCCTGTTTCAGCCTGCCCGCAAGTTGT AGACTCGAGGACGAGTCACATACTCCTGGTAGCG GCCGGTACCCTGTCCGGCCGGTGGGACTGTC AGACTCGAGCAGAGTCCAACCTTACCCAGTTCAGAC GCCGGTACCGAGAGCAAAGATGAGTTGGTGGGAC GAGCTCGAGTGGGCATGCCTCACTCTCTGAGAC	KpnI XhoI KpnI XhoI KpnI XhoI

qRT-PCR Primers

Target Gene (h=human, m=mouse)	Forward Sequence	Reverse Sequence
<i>hβ-Actin</i>	CGCCGCATCCTCCTCTTC	GACACCGGAACCGCTCATT
<i>hPex16</i>	ATGGAGAAGAAGCTGCGGCTCCTG	TCAGCCCAACTGTAGAAGTA
<i>hPex16.2</i>	GTGCGGGGCTTCAGTTACC	GGTTAGAGGCAGAGTACACCA
<i>hTBP</i>	ACGCCAGCTTCGGAGAGTTC	CAAACCGCTTGGGATTATATTCG
<i>mAcaa1a</i>	GATGACCTCGGAGAATGTGG	GCACAATCTCAGCACGGAAG
<i>mAcox1</i>	CACTTGGGCATGTTCTCTGCC	CCTCGAAGATGAGTTCCATGAC
<i>mATGL</i>	GTCCTTACCATCCGCTTGTT	CTCTTGGCCCTCATCACCAG
<i>mEhhadh</i>	CCAATGCAAAGGCTCGTGTTG	AACAGGAACTCCAACGACCC
<i>mPex16</i>	GGATGGAGAAGCTACGGCTC	ACCAGTTCAGACAGCTCGTG
<i>mPPARγ2</i>	TGCCTATGAGCACTTCAACAAGAAAT	CGAAGTTGGTGGCCAGAA
<i>mTFIIβ</i>	GTCACATGTCCGAATCATCCA	TCAATAACTCGGTCCCCTACAA
<i>mUcp1</i>	CTGAGTGAGGCAAAGCTGATTT	TAGGCTGCCCAATGAACACT

3.1.8 Western Blot reagents and buffers

<u>Blocking solution</u> (Pex16 antibody):	TBST	1x	
	+ Milk	5%	
<u>PBST buffer</u> :	PBS		
	+ Tween	0.05%	
<u>SDS Lysis Buffer</u> :	Aqua bidest. steril.	<i>Fresenius</i>	
	+ Glycerol	10%	v/v
	+ β -Glycerophosphate	10mM	
	+ NaF	10mM	
	+ Na orthovanadate	10 μ M	
	+ SDS	2,5%	v/v
	+ Tris-HCL	50mM	
<u>Tris buffered saline (TBS) 10x, pH 7.5</u> :	MilliQ water		
	+ Tris	10mM	
	+ NaCl	150mM	
<u>TBST buffer</u> :	TBS	1x	
	+ Tween20	0.1%	
<u>Transfer buffer</u>	10x TGS buffer	10%	(100mL)
	Methanol	20%	(200mL)
	MilliQ water	70%	(700mL)

Antibody solutions

PEX16 antibody was diluted 1:500 in TBST buffer containing 1% milk. β -Actin antibody was diluted 1:250000 in PBST buffer. Anti-rabbit antibody was diluted 1:2000 in TBST containing 1% milk for PEX16 antibody and anti-mouse antibody was diluted 1:3000 in PBST containing 1% milk for β -Actin antibody.

3.2 Methods

3.2.1 Cloning

For the purpose of PEX16-overexpression in various cell lines, plasmids including the coding sequence of *Pex16* had to be designed. pMSCVpuro-Pex16 vector constructs could be used for the PEX16 overexpression in 3T3-L1 cells, which received a puromycin resistance for later selection due to the vector-properties. As iBACs show a partial resistance against puromycin, a pMSCVhygro-Pex16 vector construct was designed for the overexpression of PEX16 in this cell line. HisMaxC-Pex16-plasmid was used for transfections of Cos7-cells as a control for PEX16-overexpression on protein level, due to the high expression rate of HisMaxC. The used vectors can be seen in figure 3.1.

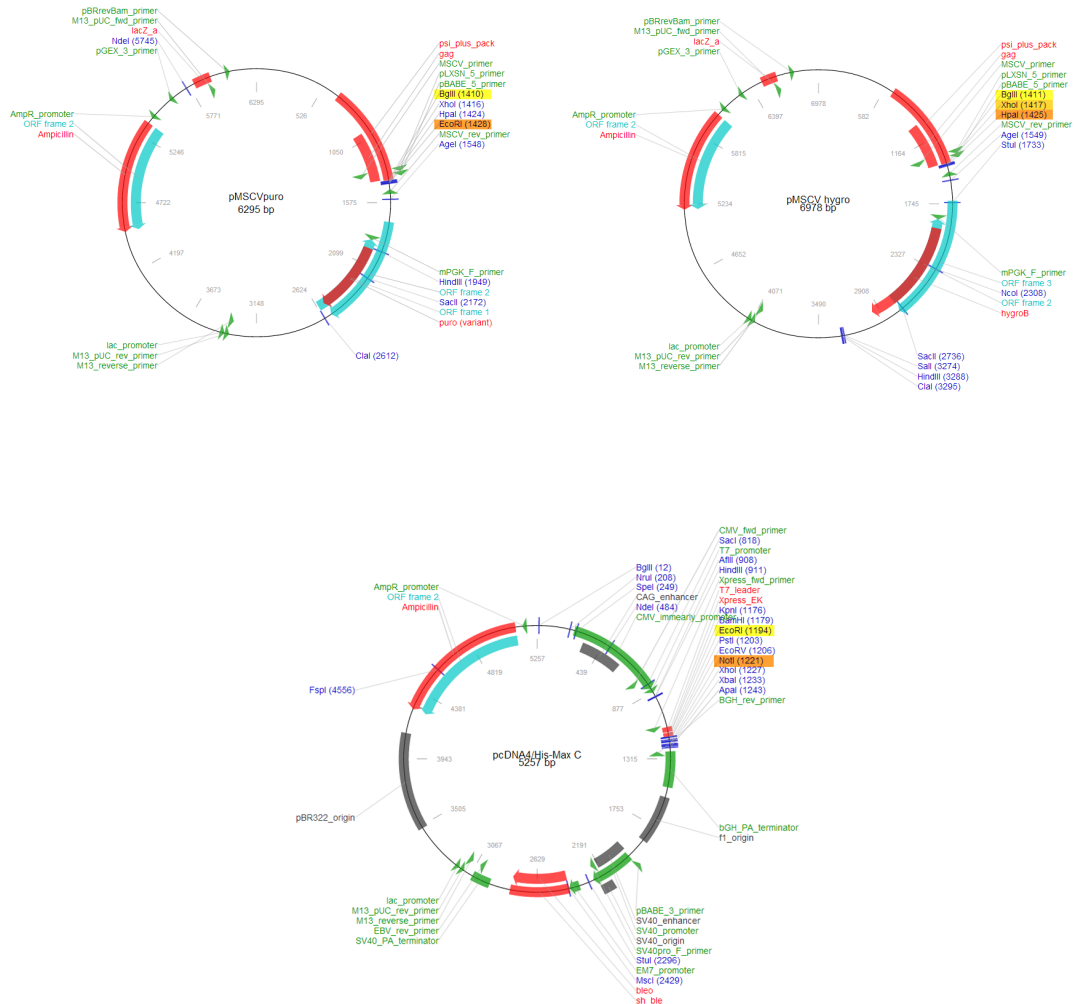


Figure 3.1: Vector maps of cloning plasmids pMSCVpuro, pMSCVhygro and HisMaxC. Yellow and orange labels represent the used restriction sites. Source: www.addgene.org/vector-database

The potential PPAR γ - binding sequences of *Pex16* were cloned into pPPRE- X3-TK-luc and pGL4.26 luciferase reporter vectors for subsequent luciferase reporter assays (see figure 3.2). By removing the 3x PPRE-sequence, the empty pTK-luc vector served as control in luciferase reporter assays. These vectors constructs encode the firefly luciferase reporter gene and can be used for the detection of PPAR γ binding sites. The pGL4.26-vector also contains a minimal promoter sequence to initiate the transcription of the inserted sequences.

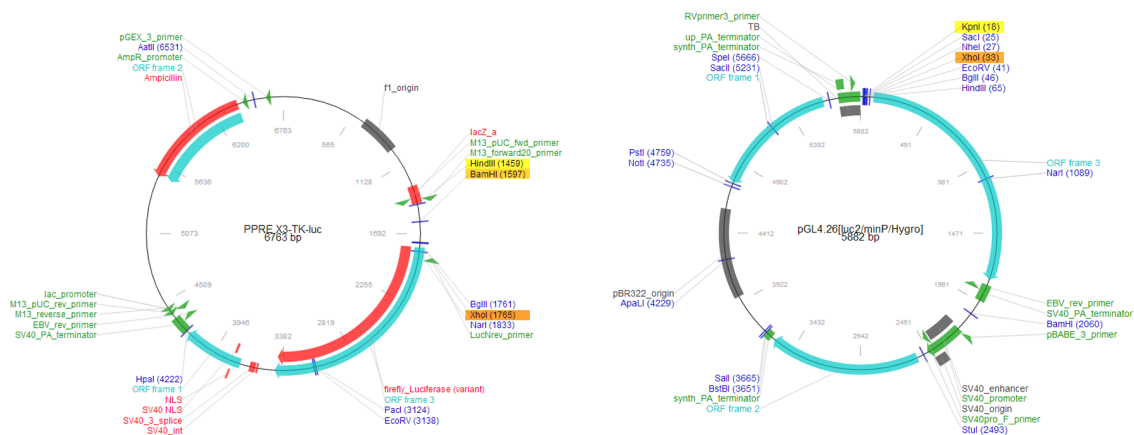


Figure 3.2: Vector maps of cloning plasmids pPPRE X3-TK-luc and pGL4.26. Yellow and orange labels represent the used restriction sites. Source: www.addgene.org/vector-database

All of the vectors harboured ampicillin resistance. This characteristic was used in the transformation of NEB5 α Competent E.Coli cells for selection.

Sequence analysis

Genome organization around the *Pex16* transcription start site (TSS) was visualized using the UCSC genome browser (NCBI37/mm9). Custom tracks include CHIP-Seq data (chromatin immunoprecipitation followed by sequencing) for PPAR γ in iWAT and eWAT derived adipocytes and 3T3-L1 cells on day 6 of differentiation, see figure 4.17. Sequences of three potential PPAR γ targets downstream TSS were generated and used for primer design.

Primerdesign

For cloning *Pex16*-inserts in sense direction into the multiple cloning site (MCS) of pMSCVpuro, pMSCVhygro, pHisMaxC, pPPRE-X3-TK-luc, and pGL4.26-vectors, restriction enzyme cutting sequences corresponding to the cutting sequences provided in the vector-MCS had to be attached to the CDS during PCR, which could be achieved by a well-considered primer design. The used restriction enzymes are listed in section 3.1.7 and labelled yellow and orange in figure 3.1.

For designing the cloning primers, various programs and online-tools were used.^{1,2,3}

It was important to avoid self-complementarity and non-specificity of the primers, in order to get high yields of specific PCR products. It was also necessary to make sure that the chosen restriction enzymes do not cut in the *Pex16*-sequence. Ideal PCR primers have a length of 18-22 bp and melting temperatures around 70°C, primer-pairs (forward and reverse primer) should be similar in melting temperature and size.

Based on the UCSC Genome Browser information (see figure 4.17), primers for four luciferase reporter assay constructs were designed, one for each peak in the graph ("Peak1", "Peak2", "Peak3") and one construct covering the first two peaks ("Peak1+2").

PCR

100ng of gDNA (for luciferase assay constructs) or cDNA from murine brown adipose and liver tissue served as PCR templates. 0.3µL of Phusion or Q5® High-Fidelity DNA Polymerase, 5µL of (5x) Phusion HF Buffer or (5x) Q5 Reaction Buffer, 0.5µL of 10mM dNTP-mix and 1µL of 20µM primer-mix were used in the PCR reaction. The implemented PCR temperature profiles are shown in table 3.1, steps 2-4 were repeated 35x. Temperature profile 1 was used for pMSCVpuro, pMSCVhygro and pHisMaxC inserts, temperature profile 2 for pPPRE X3-TK-luc and pGL4.26 inserts.

Steps	Temperature profile 1			Temperature profile 2		
	Temperature in °C	Time		Temperature in °C	Time	
1	98	3 min	1x	98	3 min	1x
2	98	10 s	35x	98	10 s	35x
3	62	30 s		64	30 s	
4	72	90 s		72	40 s	
5	72	10 min	1x	72	10 min	1x
6	4	∞		4	∞	

Table 3.1: Temperature profiles used in PCR reactions.

¹Serial Cloner 2.5

²OligoCalc: <http://www.basic.northwestern.edu/biotools/oligocalc.html>

³NCBI Primer-BLAST: www.ncbi.nlm.nih.gov/tools/primer-blast/

Enzymatic digestion of vectors and inserts

The amplification step was followed by the digestion of PCR products and vectors. Ideal digestion conditions for the particular enzymes (see section 3.1.4) were determined via "Double Digest" online-tools^{4,5}. The samples were cut for 1h at 37°C. Vectors were then dephosphorylated for 10min at 37°C using 1µL (= 1U) of FastAP enzyme and subsequently purified via agarose-gel-electrophoresis (1% agarose gel, 105V, 45min). Inserts were purified using the PureLink® PCR Purification Kit.

Generation of blunt ends

In order to produce blunt ends of digested pPPRE X3-TK-luc vector, restriction enzymes were deactivated after 1h of digestion at 70°C for 10min. 0.5µL 20mM dNTP-mix, 1µL Klenow Polymerase (= 5U) and 18.5µL aqua bidest. sterilis "Fresenius" were added to the sample, followed by incubation for 10min at 37°C to fill up the sticky ends. The enzyme was inactivated for 10min at 75°C afterwards. The product was purified via agarose gel electrophoresis.

Ligation

The received, purified products were ligated for 1h at room temperature using 0.5µL (= 2.5U) of T4 DNA Ligase and 1x T4 DNA Ligase Buffer. For blunt end ligations, 2µL PEG4000 were added. Required insert amounts for 40ng of vector DNA were determined using the "Ligation Calculator"-online-tool⁶. The chosen molar vector/insert ratio was 1:3.

Transformation of NEB5α Comp. E-Coli cells

The transformation of NEB5α Comp. E-Coli cells for the propagation of the plasmids was realized according to the "High Efficiency Transformation Protocol (C2987H/C2987I)"⁷. The transformation was followed by an overnight selection on ampicillin selection plates (50µg/mL), spreading 100µL of each dilution per plate.

Colony PCR

In order to test the colonies for successful ligations, a colony PCR was performed and the tested colonies were plated on new selection plates. The colony PCR was performed using 2µL (= 10U) of Taq DNA Polymerase (recombinant), 1.2µL (25mM) MgCl₂, 1.6µL (2.5mM) dNTP-mix, 2µL (2µM) primer-mix, 1x Taq Buffer (+KCl - MgCl₂) and Aqua bidest. ster. "Fresenius". The temperature profile used for colony PCR reactions is shown in table 3.2.

⁴Double Digest Finder; New England Biolabs, Inc.

⁵Double Digest; Thermo Fisher Scientific, Inc.

⁶Ligation Calculator: www.insilico.uni-duesseldorf.de/Lig_Input.html

⁷"High Efficiency Transformation Protocol (C2987H/C2987I)"; New England Biolabs, Inc.

Temperature °C	Time	
94	2 min	1x
94	30 s	35x
62	1 min	
72	4 min	
72	10 min	1x
4	∞	

Table 3.2: Temperature profile for Colony PCR reactions.

Minipreps and glycerolstocks

The amplified plasmids were isolated and purified, using the PureLinkTM Quick Plasmid Miniprep Kit. Therefore, cultures (5mL LB-medium + 50µg/mL ampicillin per colony) were prepared and incubated overnight at 37°C, rotating at 250rpm. For glycerol stocks, 1mL per overnight- culture was centrifuged for 20 min at 4°C and 1500xg. The resulting pellet was then re-suspended in 1mL of glycerol + 1µL of ampicillin and stored at -80°C. The remaining 4mL of the overnight cultures (ONCs) were used for minipreps.

Sequencing

For sequencing, 1.2µg of miniprep-DNA + 6µL 5µM forward or reverse primer, filled up with ddH₂O to 21µL total volume were sent to Microsyth AG for sequencing. Results were viewed with *Sequence Scanner Software v1.0*, Applied Biosystems® and tested via *Align Sequences Nucleotide BLAST-search*⁸.

3.2.2 Cell culture

Handling

Storage, freezing and thawing: Cells were held in special cryovials in liquid nitrogen tanks for long time storage. In order to avoid cell death due to crystallization of the media, special DMSO-containing freeze media were used (FM and iBACs-FM).

Before freezing the cells, cultured cells were washed with PBS twice, and trypsin solution (1mL for a 75cm² culture flask) was added in order to detach the cells from the bottom of the culture plates. Either DMEM++++ or iBACs-GM was used to stop the trypsin reaction and suspend the cells in medium. The cell-suspensions were centrifuged for 5min at 1200rpm and the resulting pellet was then re-suspended in FM or iBACs-FM. The cell-suspension was aliquoted in special cryovials, each 1mL (or 0.5mL for smaller cell amounts). For gentle freezing, cells were stored in isopropanol chambers at -80°C overnight before transferring them to the liquid nitrogen tanks.

⁸<http://blast.ncbi.nlm.nih.gov/Blast>

During the thawing process, it was essential to dilute the still partially frozen cells immediately in a ratio of about 1:12 with fresh, preheated media. 24h after thawing, the medium was changed in order to remove the cell-toxic DMSO residues.

Cultivation: 3T3-L1, Cos7, and Phoenix cells were cultivated in DMEM++++ and iBACs in iBACs-GM. Medium change was carried out every 2-3 days as long as splitting was not required.

Splitting: To preserve full differentiation potential, it was necessary to avoid 100% cell confluence, especially for 3T3-L1 and iBACs cell lines, by spitting the cells at 60-80% of confluence. For this purpose, all medium was removed, the cells were washed gently with PBS, and trypsin solution (1mL for a 75cm² culture flask) was added to detach the cells from the bottom of the culture plates. Either DMEM++++ or iBACs-GM was used to stop the trypsin reaction and to seed the cells onto appropriate culture plates.

Differentiation

3T3-L1 cells were induced to differentiation 48h after 100% of confluence (day 0), using the standard hormonal cocktail DM1. Medium was changed on day 3 to DM2, and on day 5 to DMEM++++. 3T3-L1 cells were differentiated longest until day 8.

iBACs were induced to differentiation at 100% of confluence or latest 24h after confluence, using iBACs-IM (day 0). The medium was changed to iBACs-MM after 48h and from day 4 every day. iBACs were differentiated until day 7.

Stimulation with rosiglitazone and isoproterenol

The effect of rosiglitazone on 3T3-L1 gene expression has been reviewed during differentiation via qRT-PCR. The stimulation was done using 1 μ M Rosiglitazone in DM1 permanently applied to the cells.

The influence of isoproterenol on FFA- release and TG- content during differentiation was measured using free fatty acid and triglyceride-assays. Therefore, the medium had to be changed 1h before stimulation to iBACs-MM. The stimulation was done by applying 10 μ M isoproterenol (final concentration) in FFA-free Medium for 4h and/or 12h to the cells.

Transfection

METAFACTENE® PRO-transfection was used to transiently integrate plasmid DNA into Cos7 and Phoenix cells. The poly-cationic molecular characteristic of Metafectene leads to the formation of DNA/lipid-complexes, which can easily enter the cells. Furthermore, the transfection reagent leads to the destabilisation of the DNA-coating lipid membrane by repulsive electrostatic forces and makes the DNA available in the cell. Phoenix cells were transfected at 30-50%, Cos7 cells at 60-80% of confluence. One hour before transfection, a medium change was performed (DMEM++++). For 24-well plates, 400ng DNA and 1µL metafectene (1µg : 2.5µL) per well, each in 50µL PBS, were combined and pipetted up and down twice. The DNA/metafectene-mix was incubated for 20min at room temperature and then pipetted dropwise into the cell medium. Empty vectors were transfected as negative controls. After 24h, a medium change to DMEM++++ was performed and 48-72h after the transfection, the maximal expression results were obtained.

Via transfection of Phoenix cells with pMSCVpuro and pMSCV-Pex16, amphotrophic lentiviral particles were produced in the supernatant, which were collected and used for transduction of 3T3-L1 cells and iBACs. The lentiviral particles were stored at -80°C in order to preserve the transduction capacity. The transfection of Cos7 cells with pHixMaxC and pHixMaxC-Pex16 was used to control protein production via Western Blot.

Transduction

Lentiviral transduction is a common method to stably integrate foreign DNA into the genomic DNA of 3T3-L1 cells and iBACs.

Overexpression(o/e) and silencing (si) of PEX16 in 3T3-L1 cells: 3T3-L1 cells were seeded in 6-well plates and transduced with lentiviral particles at about 30% of confluence. The addition of polybrene (8µg/mL final conc.) to the medium can increase the retroviral transduction efficiency by neutralizing the charge interactions between the pseudoviral capsid and the sialic acid of the cell membrane due to its poly-cationic characteristic. In order to achieve a stable overexpression of PEX16 in 3T3-L1 cells, 1mL of lentiviral supernatant obtained from transfected phoenix cells and 1mL of DMEM++++ containing 8µg/mL polybrene per well of a 6-well, were applied to the cells for 16-24h. Testing for successful overexpression of *Pex16* was done via qRT-PCR.

For stable silencing of PEX16, 3T3-L1 cells were infected with approximately 7.5 MOI (multiplicity of infection) of shRNA lentiviral particles (NM_145122) and non-targeting control (NTC) per cell (=90.000 MOI per well). The lentiviral particles were pipetted directly into 1mL DMEM++++ plus 8µg/mL polybrene per well of a 6-well and incubated for 16-24h. After the transduction, medium was changed and a selection was performed with 3µg/mL (final conc.) puromycin for at least 5-6 days for overexpression. Selection during silencing was performed with 1.5mg/mL geneticin (G418) for 72h. Cells were split at 60-70% of confluence in order to preserve their capacity to differentiate. Testing for successful silencing of *Pex16* was done via qRT-PCR.

Overexpression (o/e) and silencing(si) of PEX16 in iBACs: For overexpression of PEX16 in iBACs, cells were seeded into 6-well plates and transduced at about 30% of confluence with pMSCVpuro (=controls) and pMSCV-Pex16 lentiviral particles. In order to achieve a stable overexpression of PEX16 in iBACs, 1mL of the lentiviral supernatant from transfected phoenix cells was added to 1ml of iBACs-GM containing 8µg/mL polybrene and applied to the cells for 16-24h, followed by a medium change to iBACs-GM. After another 24h, cells were detached from the bottom, counted and two dilution steps were carried out: 1) 100 cells/10mL iBACs-GM, 2) 10 or 20 cells/mL iBACs-GM (\approx 1 or 2 cells/100µL). Then 100µL of cell suspension were seeded per well in a 96-well plate. Cells were grown with iBACs-GM and split at 60-70% of confluence. Testing for successful overexpression of *Pex16* was done via qRT-PCR.

For stable silencing of *Pex16*, iBACs were infected with approximately 7.5 MOI per cell (=90.000 MOI per well) of shRNA lentiviral particles and NTC for 16-24h followed by a medium change. As about one third of iBACs show puromycin resistance, selection was done using 1.5mg/mL geneticin (G418) for 7 days. Testing for successful silencing of *Pex16* was done via qRT-PCR.

Proliferation assay

For testing the proliferation of transduced iBACs, 20.000 and 40.000 cells of each, iBACs-puro and iBACs-Pex16, were seeded into 6-well plates and grown with iBACs-GM. As soon as cells reached 100% of confluence, they were induced to differentiate with iBACs-IM and differentiated as described above. Starting 24h after cell-seeding, cells of one well per sample were counted every 48h.

3.2.3 RNA-Isolation

Before RNA was harvested using 400µL of RNA Lysis Buffer T (in a 12-well or 6-well plate), cells were washed with PBS once. For the isolation of RNA, the "peqGOLD Total RNA Kit" was used. In contrast to the kit-instructions, RNA was eluted with 30µL DEPC treated H₂O and incubated for 3 minutes at room temperature before centrifugation at 5000xg for 1min. RNA concentrations were measured using NanoDrop spectrophotometer. The samples were stored at -20°C.

3.2.4 cDNA synthesis

Reverse transcription was performed using the QuantiTect Reverse Transcription Kit. 400ng of RNA were transcribed into cDNA per sample following the kit-instructions. After the transcription, samples were diluted to a final concentration of 1ng/µL with DEPC treated H₂O and stored at -20°C.

3.2.5 qRT-PCR

Via PCR (polymerase chain reaction), DNA sequences up to 3000bp can be amplified by the use of typical polymerases. Special polymerases allow the amplifications of even longer sequences. Based on fluorescence technology, a quantification of the amplified sequences is possible (qRT-PCR). SYBR-green fluorescent absorbs blue light (maximum wavelength = 498nm) and emits green light (maximum wavelength = 522nm) when bound to double stranded DNA. Measurable fluorescence signal increases proportionally to the amount of double stranded DNA generated during PCR. Correct quantification can only be done during the exponential phase of the dsDNA-formation. Housekeeping genes used in qRT-PCR reactions as reference were *TFII β* for murine samples, *β -actin* and *TBP* for human samples. All qRT-PCR primer sequences can be found in section 3.1.7. Per reaction, 4.5 μ L of 1ng/ μ L cDNA, 4.5 μ L of 800nM primer-mix and 9 μ L of SYBR green were used. The temperature program for qRT-PCR reactions is shown in table 3.3.

Temperature °C	Time	
50	2 min	1x
95	10 min	
95	15 s	40x
60	1 min	

Table 3.3: Temperature profile for qRT-PCR reactions.

3.2.6 Oil Red O staining

For staining of cells with Oil Red O, cells had to be washed with PBS twice and fixed with 10% formaldehyde (\approx 1mL in a 6-well) for 30min. For the Oil Red O stock, Oil Red O powder (0.25g) was diluted in 50mL isopropyl alcohol. The Oil Red O dilution was filtered through filter paper. The staining was performed for one hour using 1mL Oil Red O stock, diluted 3:2 with ddH₂O, per well in a 6-well. The dyed cells were stored covered with 1mL ddH₂O at 4°C.

3.2.7 Protein quantification

Protein quantification was done using the *BCA Protein Assay Kit*, Pierce. The sample-quantities were measured with FLUOstar Omega microplate reader; BMG LABTECH GmbH at a wavelength of 562nm.

3.2.8 Triglyceride quantification in cells

Triglyceride (TG) quantification was done using the *Triglycerides-kit* from Thermo Scientific / Fisher Diagnostics. Cells were harvested with 150 μ L of PBS per well in a 6-well after washing the cells twice with PBS. Cell- samples had to be treated with ultrasound for 10s twice, cooling in ice, in order to open the cells and release the triglycerides. 10 μ L per sample were used for the measurement. The TG content was measured with the FLUOstar Omega microplate reader; BMG LABTECH GmbH at a wavelength of 500nm.

3.2.9 Free fatty acid quantification in the supernatant of cells

Free fatty acid (FFA) quantification was done using *NEFA-HR R1 Set + NEFA-HR R2 Set*, Wako Chemicals GmbH. To measure FFA in the supernatant of cells, cells were washed with PBS twice and incubated at 37°C for either 4h or 12h with FFA-free Medium. Afterwards, the supernatant was harvested and centrifuged for 15min at 4°C at 12,000xg. The supernatant was transferred to new Eppendorf tubes. 20µL per sample were mixed with 100µL of Reagent 1 (0.06g/mL buffer 1) and incubated for 10min at 37°C. Afterwards, 150µL of Reagent 2 (0,01g/mL buffer 2) were added and again incubated at 37°C for 10min. The FFA-content was measured with the FLUOstar Omega microplate reader; BMG LABTECH GmbH at a wavelength of 546nm.

3.2.10 Western Blot analysis

After washing cells 3x with PBS, protein samples were harvested with 100µL SDS-Lysis Buffer + 1x Protease Inhibitor Cocktail (PIC), in order to improve protein stability. The samples had to be stored on ice for further processing. Protein samples were inactivated at 95°C for 5min and placed back on ice afterwards. For an easier handling, protein samples were digested using 3-5µL benzonase per 100µL sample. After the digest, samples were centrifuged for 3min at 13.000xg.

Gel electrophoresis

Proteins can be separated by gel electrophoresis based on differences in charge and size. Therefore, 50-70µg of protein was used for Western Blot experiments. Gels were inserted in the Bio-Rad Western Blot chamber, which was filled with 700mL of diluted (1x) NuPAGE® MOPS buffer. Additionally, 500µL antioxidant were pipetted directly into the buffer. Protein samples, 8µL (4x) LDS and 1µL DTE were filled up to 35µL with ddH₂O, mixed gently and incubated at 70°C for 10 min, with the purpose of protein denaturation. The protein standard consisted of 10µL of Seebblue® Plus2, 20µL sterile H₂O and 5µL of 4x LDS. Before sample and standard were applied to the gel, the gel slots had to be rinsed with a pipette tip in order to remove antioxidant-residues from the slots. The gel was run at 175V for ≈1h.

Transfer

Proteins need to be blotted onto a nitrocellulose membrane to get accessible to the detection with antibodies. The negative net charge of proteins in the gel enables the transfer from the gel to the membrane within an electric field.

The membrane had to be incubated in ddH₂O for ≈5min before the transfer. Three filter papers, nitrocellulose membrane, gel and two sponges were applied to the transfer buffer and fixed in the right order in a gel holder cassette (as to see in figure 3.3).

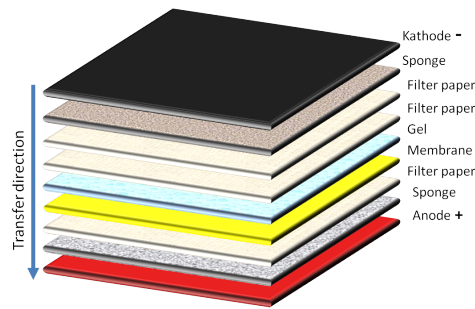


Figure 3.3: Arrangement of sponges, filters, gel and membrane for the blotting procedure.

Gel holder cassettes and cooling unit were placed in the transfer tank, which was then filled with transfer buffer. The transfer was performed within 1.5h at an electric current of 500mA and at 4°C.

Blocking: To avoid the binding of antibodies to the nitrocellulose membrane instead of the antigen, the membrane had to be blocked for 1h with an antibody-dependent blocking solution (see 3.1.8).

Incubation with antibodies

The membrane was incubated with two different types of antibodies. Incubation with a primary antibody specific to the target protein was done over night, rotating at 4°C. Thereafter, the membranes were washed three times with TBST (PEX16) or PBST (β -ACTIN) for 10min on a shaking plate. Incubation with a secondary antibody, α -rabbit for PEX16 and α -mouse for β -ACTIN, was done for 2h, rotating the blots at room temperature. The secondary antibody binds to the primary antibody and can be used for chemiluminescent detection of the target protein due to an attached enzymatic reporter molecule. The last step was once more a three times washing procedure using the appropriate buffer.

Developing the blot

Western Blots were developed using *Amersham ECL prime* or *Super Signal West Pico-* Western Blot detection reagents. For both types of detection reagents, 750-850 μ L of each of the chemiluminescent substrates were mixed and applied to the membranes for 5min. Chemiluminescence signals at the location of the target protein hit the photo paper, which could be developed with Roentogen EUKOBROM and Roentogen Superfix. The exposure time at the developing chamber was dependent on the signal intensity. The photo paper was washed with ddH₂O.

3.2.11 Luciferase reporter assays

Four regions downstream the *Pex16* - TSS (transcription start site) (Peak1: 1052-1379bp, Peak2: 1349-1676bp, Peak1+2: 1052-1676bp, Peak3: 2160-2554bp) were cloned into luciferase reporter vectors (pGL4.26 and pPPRE X3-TK-luc). The 3x PPRE- sequence of the pPPRE X3-TK-luc vector was removed in order to get an empty control vector for the assays, see section 3.2.1.

Cos7 cells were transfected according to section 3.2.2 in 24-well plates. 200ng of the cloned plasmids or empty luciferase reporter vectors were co-transfected with 100ng/well pCMX_PPAR γ 2 and 100ng/well pCMX_RxR α expression vectors. In controls, 200ng of empty pCMX vector were co-transfected instead of pCMX_PPAR γ 2 and pCMX_RxR α . Co-transfection of renilla luciferase reporter vector pGL4.75 in a ratio of 1:50 (=2ng/well) to the luciferase reporter vectors in all experiments served as control for varying efficiencies in transfections.

Luciferase reporter assays were performed 48h after transfection using the *Dual-Luciferase® Reporter Assay System*, Promega. Before starting, buffers and substrates had to be prepared. Passive lysis buffer (5x) was diluted with aqua bidest. sterilis "Fresenius" in a ratio of 1:5. LARII reagent was diluted with Luciferase Assay buffer, remaining substrate was stored in 2mL-aliquots at -80°C. Stop&Glo substrate (50x) was diluted with Stop&Glo Buffer in a 1:50 ratio. Both substrates had to be protected from light.

Cells were washed with PBS twice and lysed with 100 μ L (1x) passive lysis buffer per well on a shaking-plate for 20min at room temperature. 10 μ L per sample were used for measurement in a 96-well assay-plate.

Luminescence measurement was done using "Berthold Orion II" luminometer. Relative luciferase activities were calculated by relating renilla-normalized values of PPAR γ 2/RxR α - cotransfected cells to measured values for pCMX-transfected cells for each construct individually.

3.2.12 Statistics

Mean value and standard deviation (SD) for qRT-PCR results were calculated from 2-3 biological replicates. For representative experiments, SD was calculated from technical replicates. Significance levels were set to *p < 0.05, **p < 0.01, and ***p < 0.001 only for n=3.

4 Results

In humans, *Pex16* gene (peroxisomal biogenesis factor 16, [Homo sapiens], gene ID: 9409)¹ is located on chromosome 11 (11p11.2). Two human protein encoding transcript variants are known (isoform 1: 336 aa, \approx 38.6 kDa, isoform 2: 346 aa, \approx 39.3 kDa)². All herein shown experiments were carried out with murine models, and for that reason, further mentioned "*Pex16* gene" refers to "*Pex16* peroxisomal biogenesis factor [Mus musculus]" (gene ID:18633), located on mouse chromosome 2 (2 E1;2)³. According to NCBI³, only transcript variant 1 of 2 existing variants in mus musculus encodes the functional PEX16-protein (336 aa, \approx 38.6 kDa⁴).

4.1 Pex16 expression in murine tissue

Various murine tissues were screened for *Pex16* mRNA-expression via qRT-PCR. Expression was highest in white adipose tissue (WAT) (ct-levels: 25-26) and in brown adipose tissue (BAT) (ct-levels: 24-25), and lower in cardiac muscle (CM) (ct-levels: 27-28), skeletal muscle (SM) (ct-levels: 27-28) and liver (ct-levels: \approx 26) in fed samples (see figure 4.1A). A trend for elevated *Pex16* mRNA-expression could be determined in brown adipose tissue and liver in high-fat-diet fed mice compared to chow diet fed mice (see figure 4.1B). No difference in WAT and BAT between ob/ob and wildtype (wt) mice could be observed. Additionally, the nutrition status did not change the expression pattern (see figure 4.1C).

¹<http://www.ncbi.nlm.nih.gov/gene/9409>

²<http://www.uniprot.org/uniprot/Q9Y5Y5>

³<http://www.ncbi.nlm.nih.gov/gene/18633>

⁴<http://www.uniprot.org/uniprot/Q91XC9>

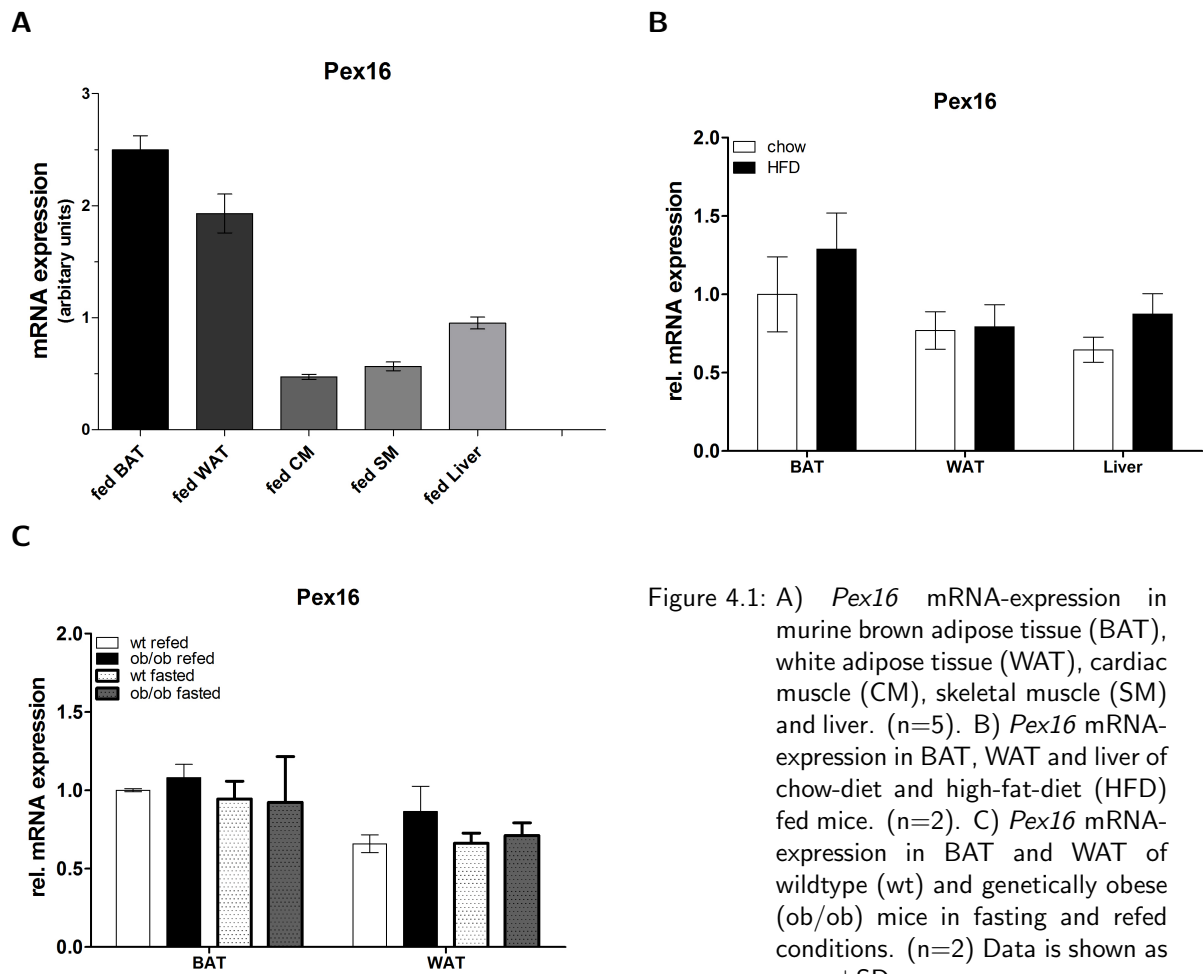


Figure 4.1: A) *Pex16* mRNA-expression in murine brown adipose tissue (BAT), white adipose tissue (WAT), cardiac muscle (CM), skeletal muscle (SM) and liver. (n=5). B) *Pex16* mRNA-expression in BAT, WAT and liver of chow-diet and high-fat-diet (HFD) fed mice. (n=2). C) *Pex16* mRNA-expression in BAT and WAT of wildtype (wt) and genetically obese (ob/ob) mice in fasting and refeed conditions. (n=2) Data is shown as mean \pm SD.

4.2 PEX16-expression undergoes upregulation during adipogenic differentiation of murine and human cell models

In addition to murine tissues, also human and murine cell models for adipogenesis were screened for *Pex16* mRNA-expression during their differentiation process. The qRT-PCR results showed an up-regulation of *Pex16* during early stages of adipogenesis in the murine cell models 3T3-L1, iBACs and C3H/10 T1/2 (see figure 4.2A-C). Stimulation of *Ppar γ* , an important marker gene of adipogenesis, by rosiglitazone in 3T3-L1 cells lead to an increased *Pex16* mRNA-expression on day 3 and day 5 of differentiation (see figure 4.2A). In iBACs, β 3-adrenergic stimulation by isoproterenol led to an elevated mRNA-expression of *Pex16* on day 5 of differentiation (see figure 4.2B). *PEX16* expression in human SGBS cells and hMADS was lower (ct-levels: 26-29), when compared to murine adipocytes (ct-levels: 24-26), but increased with progress of differentiation (see figure 4.2D,E).

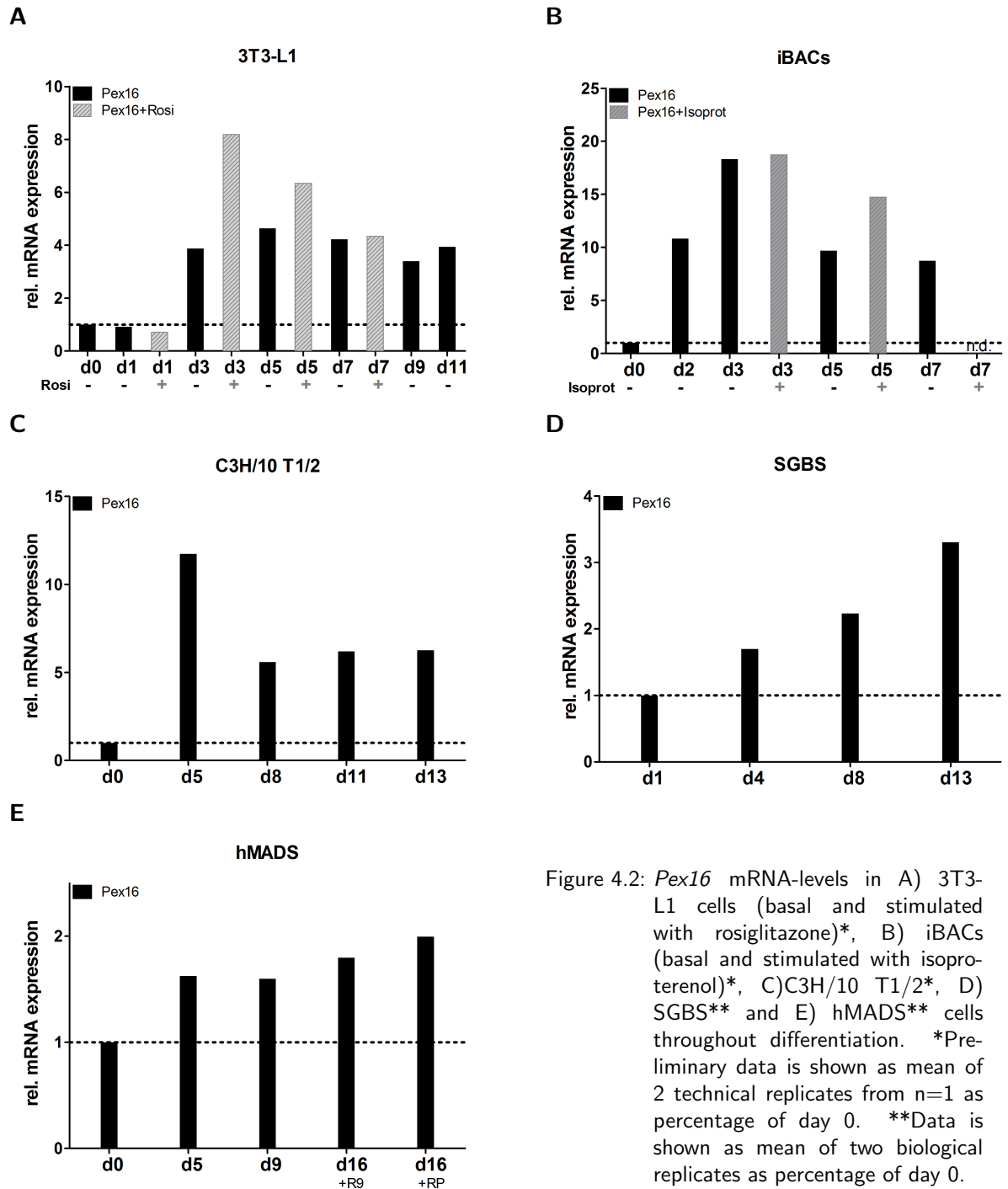


Figure 4.2: *Pex16* mRNA-levels in A) 3T3-L1 cells (basal and stimulated with rosiglitazone)*, B) iBACs (basal and stimulated with isoproterenol)*, C) C3H/10 T1/2*, D) SGBS** and E) hMADS** cells throughout differentiation. *Preliminary data is shown as mean of 2 technical replicates from n=1 as percentage of day 0. **Data is shown as mean of two biological replicates as percentage of day 0.

4.3 Overexpressing PEX16 in white and brown adipocyte models

As an up-regulation of PEX16 during adipogenic differentiation of cellular models for adipogenesis as well as a high expression of PEX16 in murine brown and white adipose tissue was found, PEX16 was further investigated in order to gain insight into the function of PEX16 in adipocyte development and energy metabolism.

The first step was to test the effects of overexpression. PEX16 was overexpressed in 3T3-L1 cells (white adipose cells), and iBACs (brown adipose cells). To accomplish the overexpression of PEX16 in these cell lines, several preparative steps had to be done: The *Pex16*-CDS had to be cloned into transporter vectors pMSCVpuro and pMSCVhygro (see section 3.2.1). By transfection of Phoenix cells with the generated pMSCV-Pex16 plasmids, amphotrophic lentiviral particles were produced, which could then be used for transduction of 3T3-L1 cells and iBACs according to section 3.2.2. Cells transduced with pMSCVpuro plasmid served as control.

4.3.1 Overexpression of PEX16 in 3T3-L1-cells

Cloning of *Pex16*-CDS into pMSCVpuro and pHisMaxC-vector

Cloning of *Pex16*-CDS into pMSCVpuro and pHisMaxC was done during a practical prior to the master thesis. Positive clones were confirmed via colony PCR and sequencing. Sequencing results can be found in the appendix.

Phenotypical changes due to overexpression of PEX16 in white adipocytes

In order to overexpress PEX16 in 3T3-L1 cell line, two distinct lines of amphotrophic lentiviral particles were tested. As transduction with line 1 exhibited the highest *Pex16*-expression in 3T3-L1 cells, this line was used for all further experiments (see figure 4.3A).

First, three biological replicates of *Pex16*-o/e cells and controls from line 1 were differentiated ("time-series 1") and mRNA-levels of *Pex16* (\pm rosiglitazone-stimulation) were measured. The overexpression was confirmed over the whole differentiation process (see figure 4.3B). *PEX16*-o/e cells showed no further increase in *Pex16* mRNA-levels upon rosiglitazone-stimulation when compared to controls (figure 4.3B). Furthermore, reduced lipid accumulations were found for *PEX16*-o/e cells on day 7 of differentiation in pictures of Oil-red-O stained cells when compared to controls (figure 4.3C).

Again, 3 biological replicates of *PEX16*-o/e cells and controls from line 1 were differentiated ("time-series 2") to investigate *Pex16* mRNA-expression, protein expression, free fatty acid (FFA) release and triglyceride (TG) content. The overexpression was confirmed throughout differentiation on mRNA-level (see figure 4.3D). Moreover, the overexpression was shown on protein level within Western Blots on day 0, day 3 and day 8 of differentiation as well (see figure 4.3E). Pictures of Oil-red-O (ORO) stained cells on day 8 of differentiation showed again a reduction in lipid accumulation in *PEX16*-o/e cells compared to controls (see figure 4.3F).

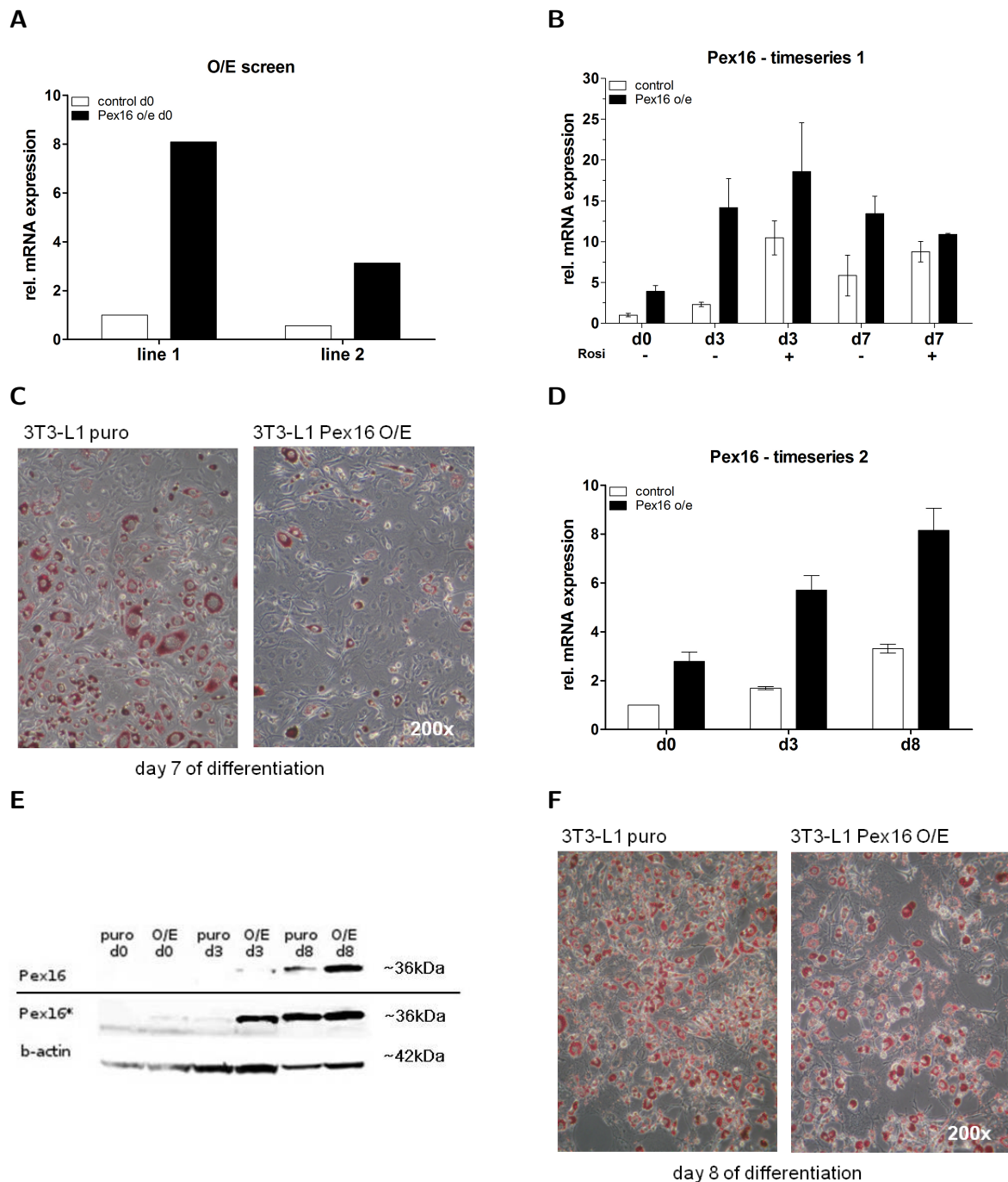


Figure 4.3: A) mRNA-level-screen for *Pex16*-overexpression on day 0 of differentiation. 3T3-L1 cells were transduced with lentiviral particles. Preliminary data is shown as mean of two technical replicates as percentage of pMSCV-puro control on day 0 of differentiation. B) *Pex16* mRNA-levels during differentiation of PEX16-o/e line 1-3T3-L1 cells and controls with and without rosiglitazone (=Rosi) stimulation, referred to as "timeseries 1". C) Oil-red-O stainings from PEX16-o/e 3T3-L1 cells and controls of timeseries 1 on day 7 of differentiation. D) *Pex16* mRNA-levels during the second differentiation of PEX16-o/e line 1-3T3-L1 cells and controls, referred to as "timeseries 2". E) Western Blot of timeseries 2-protein samples (puro= control, O/E= PEX16-o/e, "Pex16": developed with Super Signal, "Pex16*": developed with ECL Prime). F) Oil-red-O stainings from PEX16-o/e 3T3-L1 cells and controls of timeseries 2 on day 8 of differentiation. qRT-PCR-data is shown as mean \pm SD as percentage of pMSCVpuro-control (d0) which was set to 1. (n=3)

As ORO staining showed reduced lipid accumulations in PEX16-o/e cells, triglyceride (TG) content and free fatty acid (FFA) release were determined as well. Results of the measurement show hardly any differences in TG content as well as in FFA release between PEX16-o/e cells and controls under basal conditions. However, on day 8 of differentiation a small but significant decrease in FFA release was observed (see figure 4.4A,B). After β 3-adrenergic stimulation with isoproterenol a trend to a reduction in TG content and to an increase in FFA release in PEX16-o/e cells could be seen on day 8 of differentiation (see figure 4.4A,B).

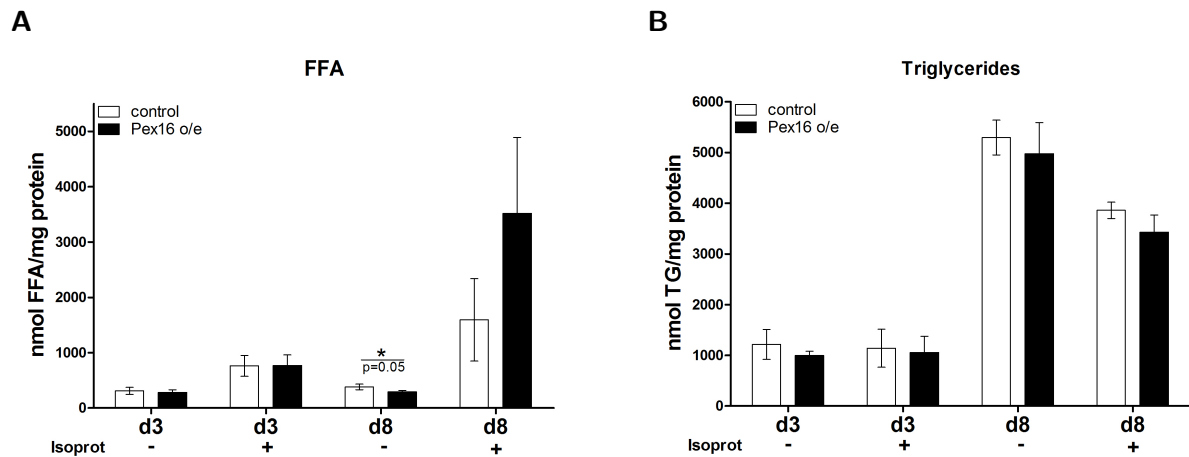


Figure 4.4: A) Free fatty acid and B) triglyceride measurement on day 3 and day 8 of differentiation of Pex16-o/e 3T3-L1 cells and controls (timeseries 2) with and without isoproterenol (=Isoprot) stimulation. Free fatty acid contents are presented in nmol FFA/mg protein, triglyceride contents in nmol TG/mg protein. (n=3) *p<0.05

In addition, marker gene expression for adipogenesis (*Ppar γ 2*) and lipolysis (*ATGL*) as well as peroxisomal β -oxidation gene expression (*Acox1*, *Ehhadh*, *Acaa1a*) were tested via qRT-PCR. Corresponding to the noticed reduction in lipid accumulation of PEX16-o/e cells, *Ppar γ 2* mRNA-levels showed a trend to reduction as shown in figure 4.5A, hinting at a reduced differentiation of PEX16-o/e cells. mRNA-expression of lipolysis gene *ATGL* was significantly reduced in PEX16-o/e cells compared to controls on day 0 and day 3 of differentiation (see figure 4.5B). Peroxisomal β -oxidation gene *Acox1* mRNA-levels were decreased in PEX16-o/e cells throughout differentiation (figure 4.5C). mRNA-levels of another peroxisomal β -oxidation gene *Ehhadh* were also decreased in PEX16-o/e cells (figure 4.5D), but the expression of *Ehhadh* in 3T3-L1 cells was very low, as only one of three biological replicates showed detectable mRNA-levels (ct-values: 25-31). The third peroxisomal β -oxidation gene *Acaa1a* showed a trend to elevated mRNA-levels in PEX16-o/e cells on day 3 of differentiation (figure 4.5E).

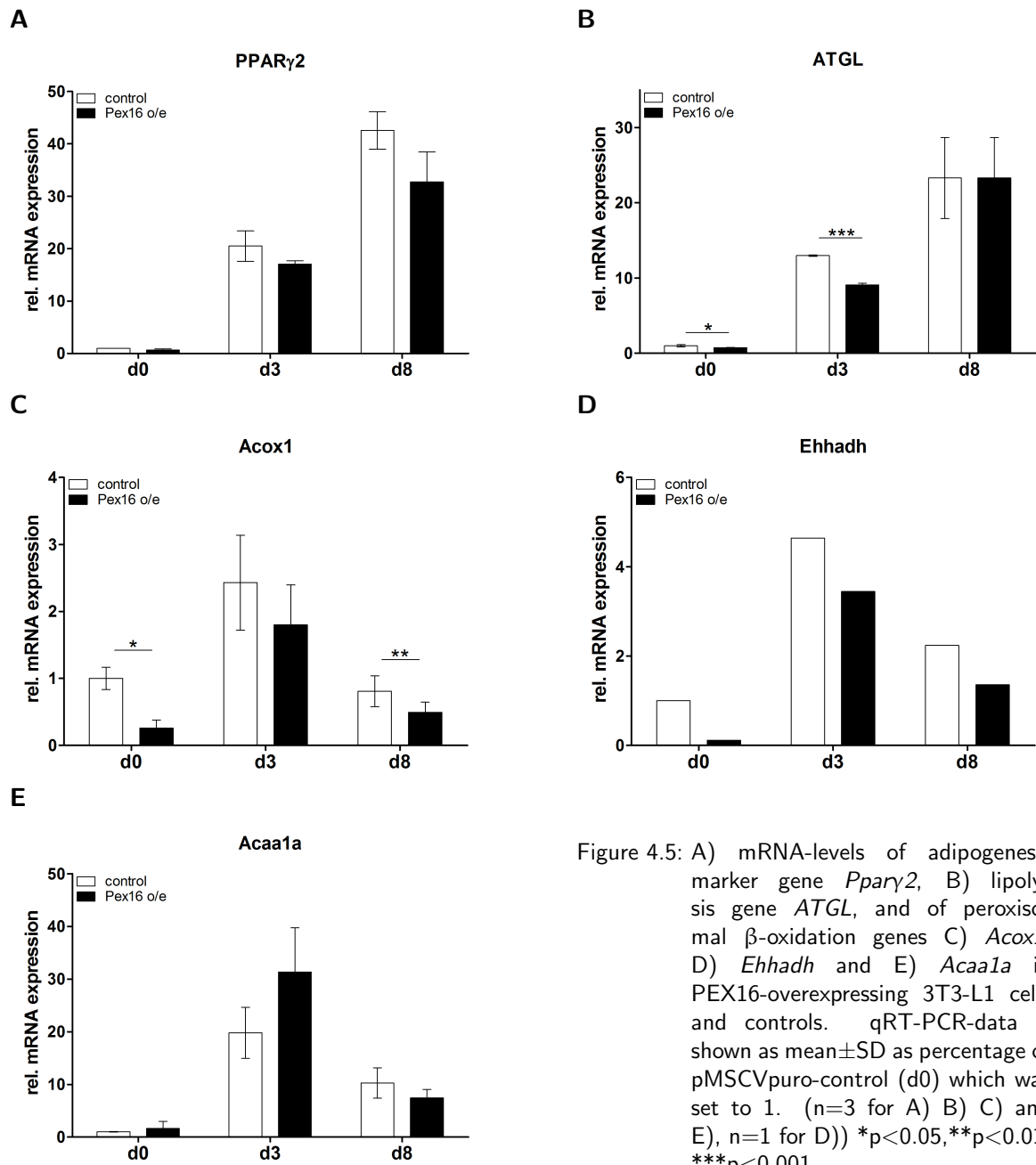


Figure 4.5: A) mRNA-levels of adipogenesis marker gene *Ppar γ 2*, B) lipolysis gene *ATGL*, and of peroxisomal β -oxidation genes C) *Acox1*, D) *Ehhadh* and E) *Acaa1a* in PEX16-overexpressing 3T3-L1 cells and controls. qRT-PCR-data is shown as mean \pm SD as percentage of pMSCVpuro-control (d0) which was set to 1. (n=3 for A) B) C) and E), n=1 for D)) *p<0.05, **p<0.01, ***p<0.001

Western Blots for PEX16 did not show the expected size of 38.6 kDa. Instead a band at ≈ 36 kDa was detected (see figure 4.6A). The His-tagged control showed the right size of ≈ 39 kDa (figure 4.6A). We used *SignalP 4.1*⁵, an online tool for protein cleavage-site predictions, to find reasons for the reduced protein size. However, no potential cleavage sites were detected (see figure 4.6B).

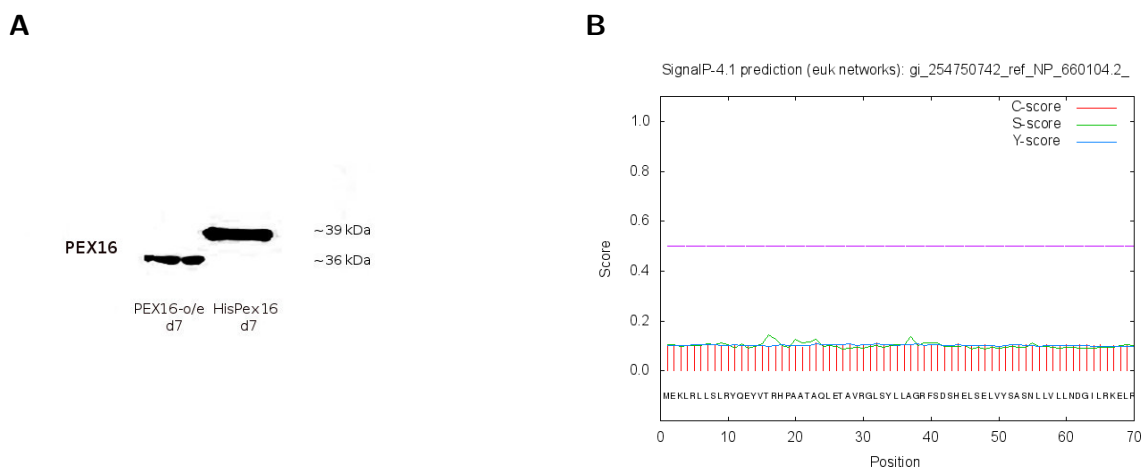


Figure 4.6: A) Western Blot of PEX16 overexpressing 3T3-L1 cells (PEX16 o/e) and Cos7 cells (HisPex16) on day 7 of differentiation using α -PEX16-antibody. The pMSCV-Pex16 transduced 3T3-L1 cells express a ≈ 36 kDa- protein, HisPex16 transfected Cos7 cells express a protein at the size of ≈ 39 kDa. B) Cleavage site prediction for PEX16-protein generated via *SignalP4.1* prediction tool: no cleavage sites could be detected within the aminoacid sequence. C-score: raw cleavage site score, S-score: signal peptide score, Y-score: combined cleavage site score.

4.3.2 Overexpression of PEX16 in iBACs

For further elucidation of PEX16 function in adipocyte development and metabolism, overexpression of PEX16 in the immortalized brown adipose cell line "iBACs" was performed.

Cloning of Pex16-CDS into pMSCVhygro-vector

Cloning of *Pex16*-CDS into pMSCVhygro at BglII/HpaI or BglII/XhoI- restriction sites was not successful. No positive NEB5 α Comp.E-Coli colonies could be found within several repetitions of the experiment.

Phenotypical changes due to overexpression of PEX16 in brown adipocytes via pMSCVpuro

iBACs exhibit a partial resistance against puromycin, as they were selected with puromycin throughout the immortalization process and developed a resistance [46]. In addition, integration of *Pex16*-CDS into pMSCVhygro for selection with hygromycin could not be accomplished. Thus, another option for stably overexpressing PEX16 in iBACs had to be found: A dilution experiment. iBACs were transduced with pMSCVpuro and pMSCV-Pex16. Transduced cells were diluted to a final concentration of approx. 1 cell per 100 μ L. Single cells were then grown in 96-wells without puromycin

⁵<http://www.cbs.dtu.dk/services/SignalP/>

selection and subsequently screened for PEX16 overexpression on mRNA-level at 100% of confluence. Three promising PEX16-overexpressing cell lines (H2, E12, F5) resulted from two iterations of this experiment, as shown in figure 4.7.

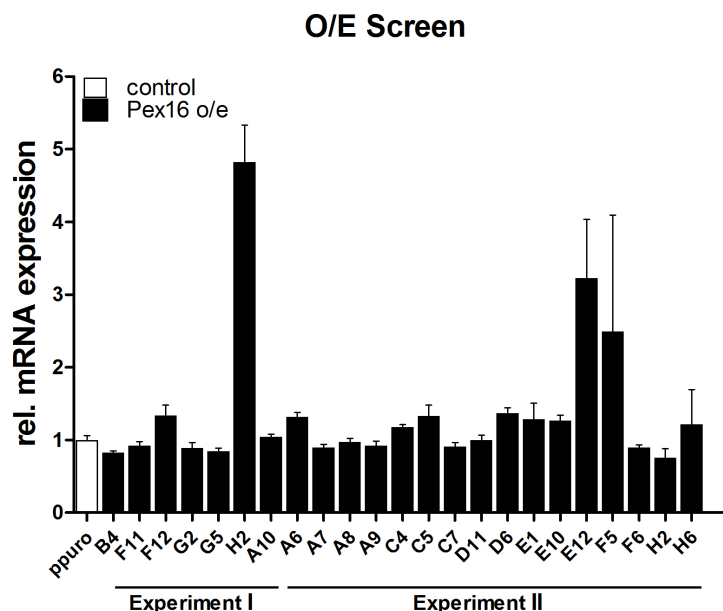


Figure 4.7: qRT-PCR-screen for PEX16 overexpression in iBACs compared to controls after two repetitions of a dilution experiment ("Experiment I", "Experiment II"). iBACs were transduced with lentiviral particles (pMSCVpuro and pMSCV-Pex16) and diluted to 1 cell/100 μ L. Single cells were grown without antibiotic selection and tested for overexpression at 100% of confluence via qRT-PCR. mRNA-levels of PEX16-o/e iBACs are shown as percentage of pMSCVpuro-control, which was set to 1. Preliminary data is shown as mean \pm SD of two technical replicates from n=1.

A 1:1:1 mix of these three cell lines was grown to confluence and differentiated until day 7. qRT-PCR analysis of *Pex16* mRNA-levels throughout this differentiation process show a loss of the overexpression on day 3, which was partially regained on day 7 of differentiation (see figure 4.8A). Oil-red-O stainings of the cells show again a reduction in lipid accumulation of PEX16-o/e cells comparable to the one seen in 3T3-L1 cells overexpressing PEX16 (see figure 4.8E,F). However, and that was true for puro and PEX16-o/e cells, many cells died during day 3 and day 7 of differentiation, as visually observed. The surviving cells displayed a high content of lipid accumulations (see figure 4.8E,F). Only on day 3 of differentiation, Western Blot showed a signal around the expected protein size of \approx 36kDa, but the signal for PEX16-o/e samples was even reduced when compared to controls (see figure 4.8B). The reduced protein amount seen in the β -actin control on day 7, probably due to a biased protein-amount determination caused by the high lipid-content of the samples, could be responsible for not detecting PEX16-protein on day 7 (see figure 4.8B). Differences between PEX16-o/e cells and pMSCVpuro controls concerning free fatty acid-release were hardly existent (see figure 4.8C). However, there was a trend to increased fatty acid release and reduced triglyceride content nearly throughout all timepoints measured (see figure 4.8C,D). On day 3 of differentiation, TG content was even significantly reduced after 12h incubation with FFA-free Medium in PEX16-o/e cells when compared to controls (see figure 4.8D).

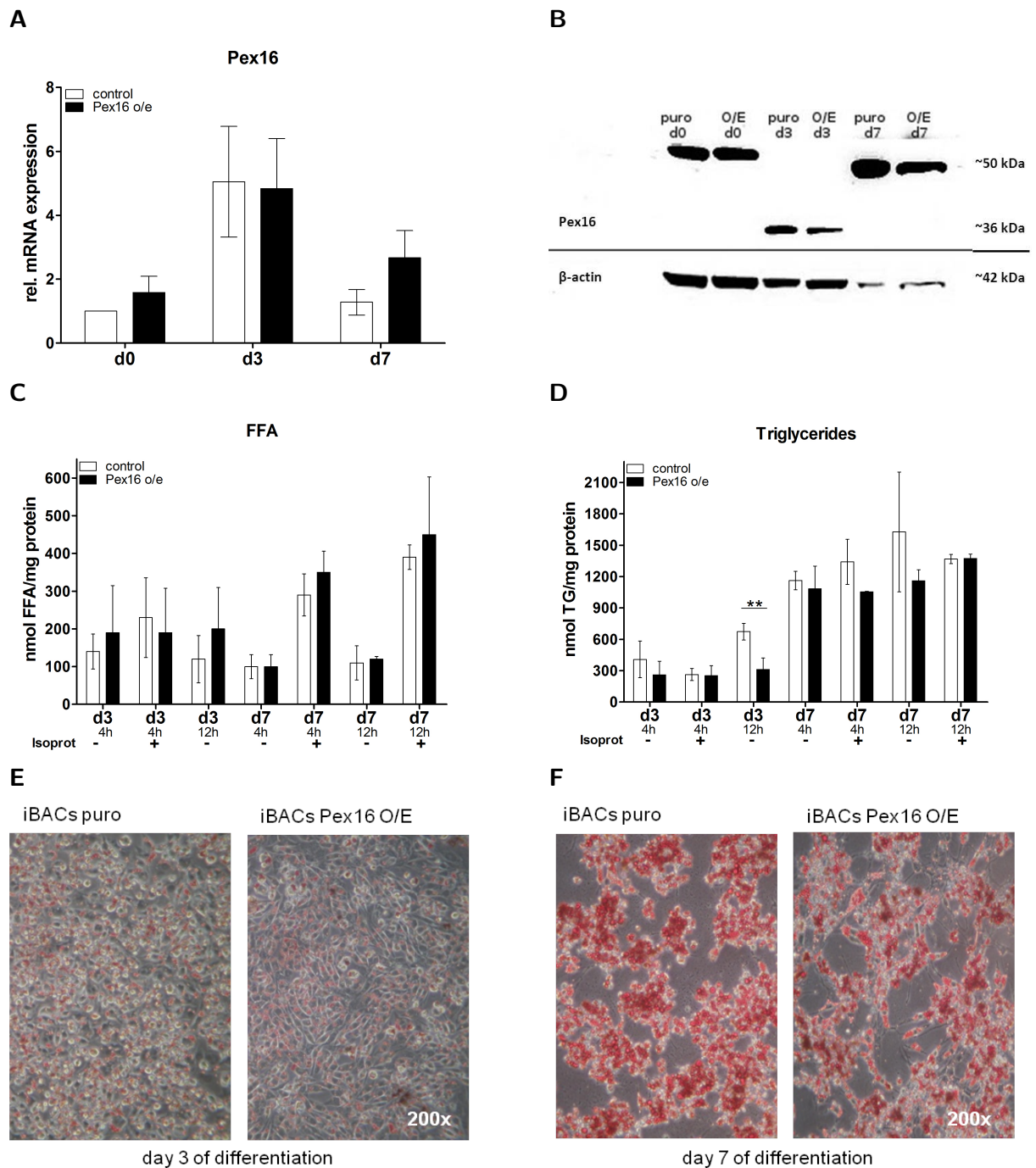


Figure 4.8: Combination of the three highest PEX16-o/e iBACs lines H2, E12 and F5 compared to pMSCVpuro-controls: A) mRNA-levels of *Pex16* in PEX16-overexpressing cells compared to controls throughout differentiation. B) Western Blot analysis of protein samples from PEX16-o/e cells (=O/E) and controls (=puro) on d0, d3 and d7 of differentiation, developed with ECL Prime. C) Free fatty acid (FFA) and D) triglyceride-measurement of PEX16-o/e cells compared to controls after 4h or 12h incubation with FFA-free Medium with and without stimulation with isoproterenol (=Isoprot) on day 3 and day 7 of differentiation. Oil-Red-O staining of PEX16-o/e cells and controls E) on day 3 and F) on day 7 of differentiation. qRT-PCR-data is shown as mean \pm SD as percentage of pMSCVpuro-control (d0) which was set to 1. Free fatty acids are presented in nmol FFA/mg protein, triglycerides are presented in nmol TG/mg protein.(n=3) **p<0.01

Additionally, mRNA-expression of adipocyte marker gene *Ppar γ 2*, brown adipocyte marker gene *UCP1* and peroxisomal β -oxidation genes *Acox1*, *Ehhadh* and *Acaa1a* was investigated via qRT-PCR. Interestingly, *Ppar γ 2* expression was elevated in PEX16-o/e cells throughout the differentiation (see figure 4.9A), contradicting the impression gained in Oil-red-O-pictures, that PEX16-o/e cells showed less differentiation and would therefore express less *Ppar γ* (figure 4.8E,F). A trend of elevated *UCP1*-expression could be observed on day 7 of differentiation (figure 4.9B). Differences of *Acox1*, *Ehhadh* and *Acaa1a* expression between PEX16-o/e cells and controls were not significant due to very high standard deviations (figure 4.9C,D,E). However, a trend to reduced *Acox1* and *Ehhadh* mRNA-levels and to elevated *Acaa1a* mRNA-levels in PEX16-o/e iBACs was detected nearly throughout all measured timepoints when compared to controls (figure 4.9C,D,E).

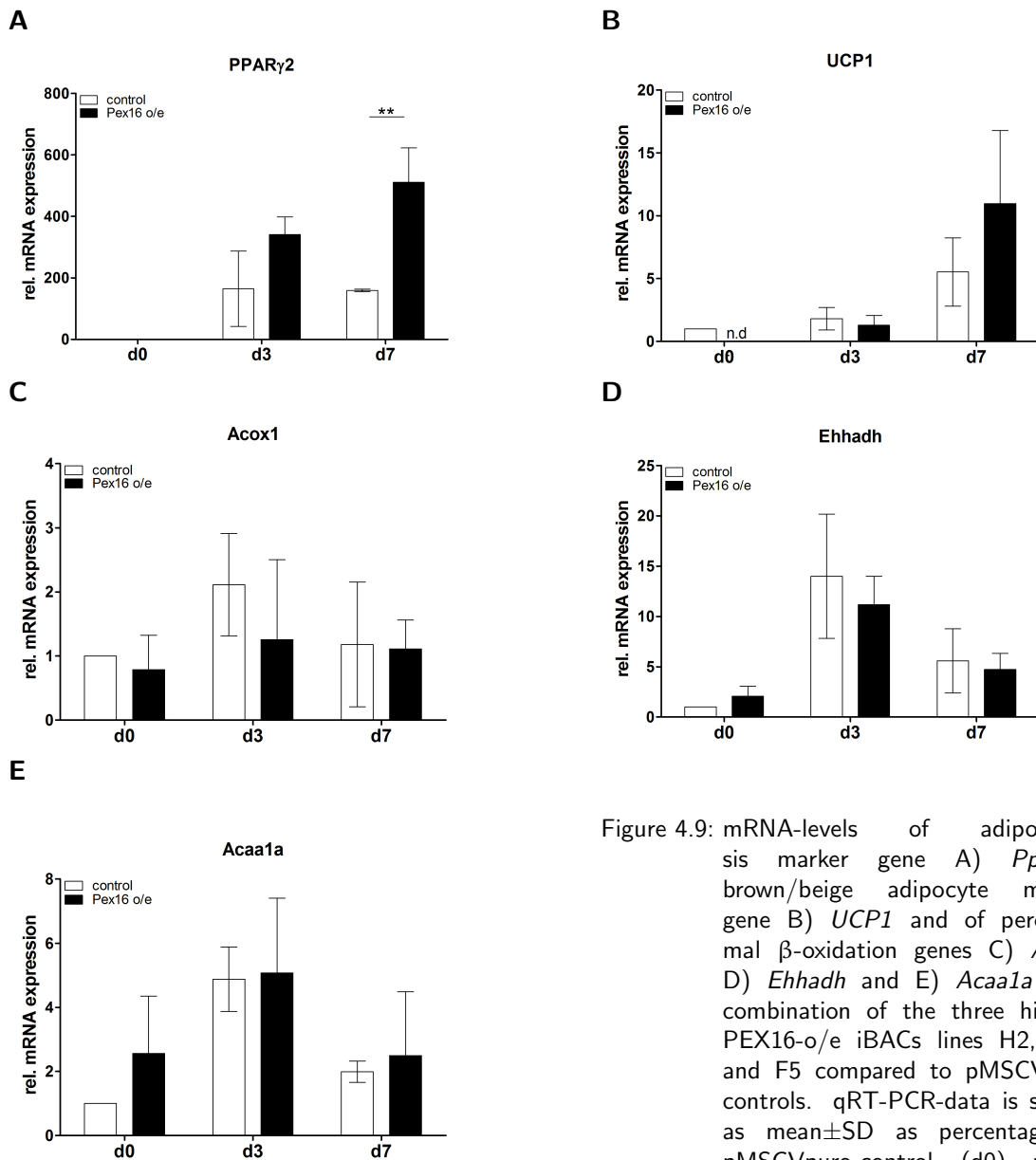


Figure 4.9: mRNA-levels of adipogenesis marker gene A) *Ppar γ 2*, brown/beige adipocyte marker gene B) *UCP1* and of peroxisomal β -oxidation genes C) *Acox1* D) *Ehhadh* and E) *Acaa1a* in a combination of the three highest PEX16-o/e iBACs lines H2, E12 and F5 compared to pMSCVpuro controls. qRT-PCR-data is shown as mean \pm SD as percentage of pMSCVpuro-control (d0) which was set to 1. (n=3)

As the overexpression of PEX16 on day 0 was already less than 2-fold in the combined PEX16-o/e iBACs, in persuasive experiments only the highest PEX16-o/e iBACs-line H2 was used. During differentiation of the H2-cell line a clear overexpression of *Pex16* mRNA could be seen (figure 4.10A). Again, PEX16-o/e cells seemed to accumulate less lipids than controls (figure 4.10B). Furthermore, mRNA expression of *Ppar γ 2* was measured to see, whether the changes in cell morphology can be related to an altered adipogenesis, but again elevated *Ppar γ 2* mRNA-levels were found in PEX16-o/e iBACs when compared to controls (figure 4.10C). From visual observation, we concluded that cells died throughout differentiation, which gave reason to perform a proliferation assay. The assay confirmed the observation of decreasing cell amounts for PEX16-o/e iBACs starting about 72h after induction of differentiation (figure 4.10D).

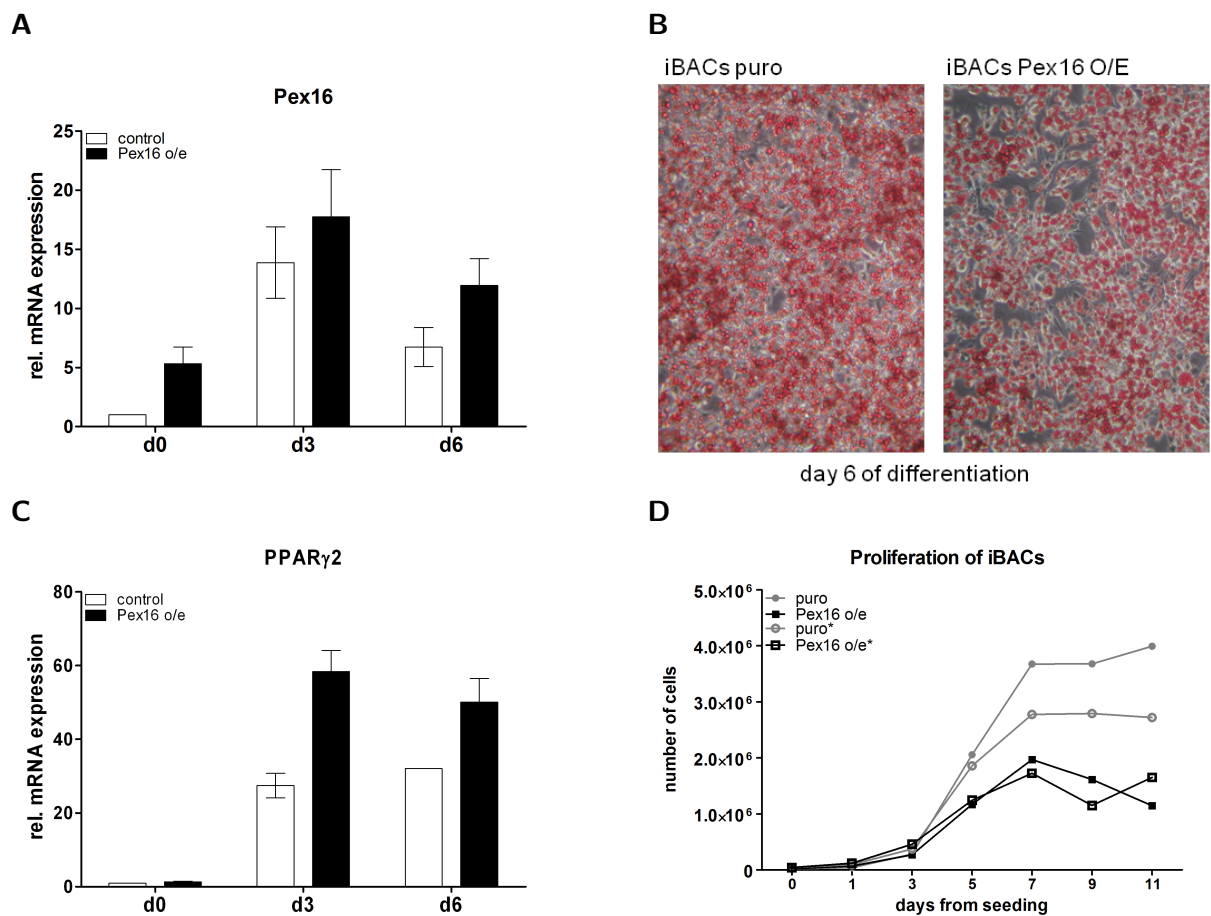


Figure 4.10: A) mRNA levels of *Pex16* in PEX16-o/e iBACs cell line H2 compared to pMSCVpuro controls during differentiation. B) Oil-red-O pictures of control cells and PEX16-o/e cells on day 6 of differentiation. C) mRNA levels of *Ppar γ 2* in PEX16-o/e iBACs cell line H2 compared to controls during differentiation. D) Proliferation testing by counting the cell amount of iBACs during growth and differentiation ("puro"/"Pex16 o/e": 20.000 cells seeded, induction on day 5, "puro*"/"Pex16 o/e*": 40.000 cells seeded, induction on day 4). Preliminary qRT-PCR-data is shown as mean \pm SD of two technical replicates as percentage of pMSCVpuro-control (d0), which was set to 1.

Furthermore, mRNA-expression of brown adipocyte marker gene *UCP1* and peroxisomal β -oxidation genes *Acox1*, *Ehhadh* and *Acaa1a* in the PEX16-o/e iBACs line H2 and controls was measured via qRT-PCR. Intriguingly, *UCP1* mRNA-levels were clearly decreased in PEX16-o/e cells on day 3 and on day 6 of differentiation when compared to controls (ct-levels: PEX16-o/e: d3: ≈ 34.7 , d6: ≈ 29.6 , control: d3: ≈ 29 , d6: ≈ 26.7), as to see in figure 4.11A. *Acox1* mRNA-expression showed again a trend to reduction in PEX16-o/e iBACs throughout all measured timepoints (figure 4.11B). Furthermore, a trend to increased *Acaa1a* mRNA-expression on day 0 and day 3 of differentiation was observed again, *Ehhadh* was not changed in PEX16-o/e cells compared to controls (figure 4.11C,D).

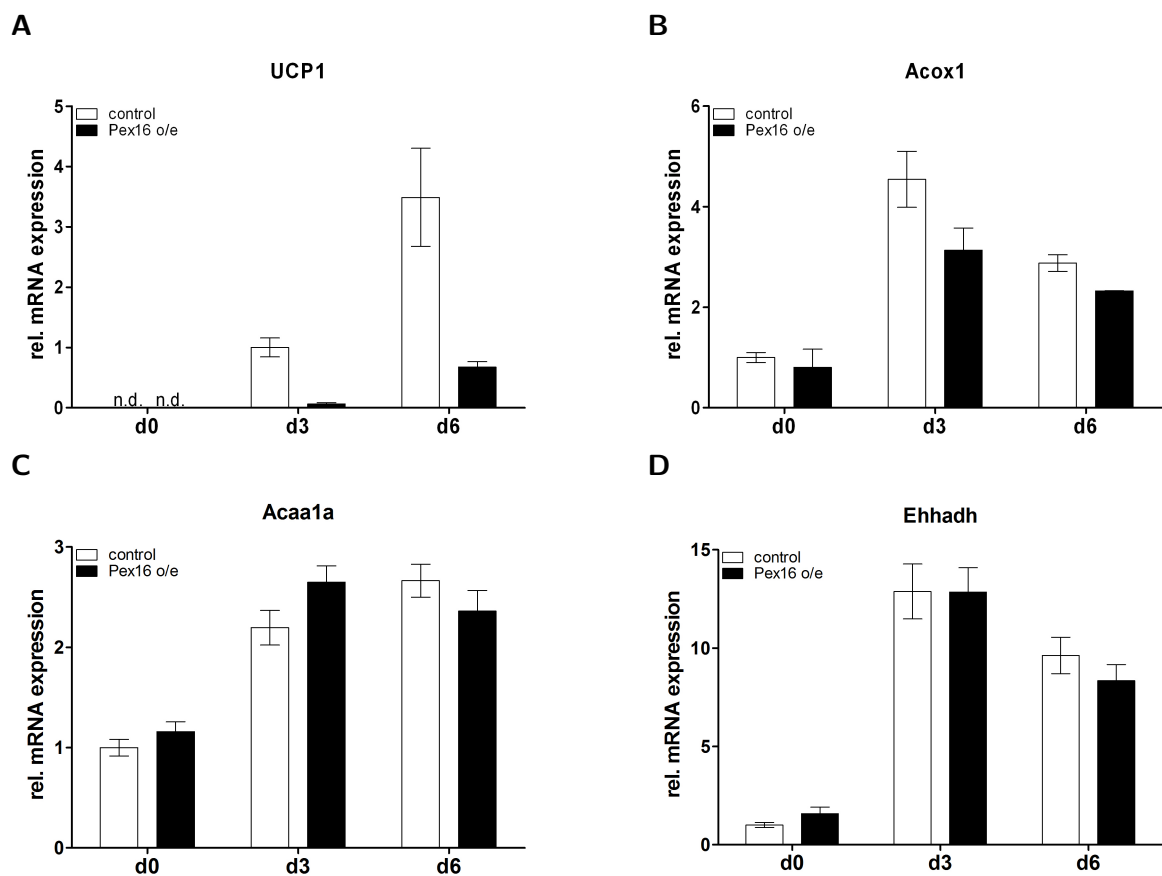


Figure 4.11: A) mRNA levels of *UCP1* in PEX16-o/e iBACs cell line H2 compared to pMSCVpuro controls. Preliminary qRT-PCR-data is shown as mean \pm SD of two technical replicates as percentage of pMSCVpuro-control (d3), which was set to 1. B) mRNA levels of *Acox1* C) *Acaa1a* and D) *Ehhadh* in PEX16-o/e iBACs cell line H2 compared to pMSCVpuro controls. Preliminary qRT-PCR-data is shown as mean \pm SD of two technical replicates as percentage of pMSCVpuro-control(d0), which was set to 1.

Based on the observation, that PEX16-overexpression gets almost lost during the differentiation process, cells were differentiated until day 4 and RNA samples were harvested every day. The qRT-PCR results show a loss of overexpression already 24h after induction and a regeneration on day 4 of differentiation (figure 4.12A). *Ppar γ 2* expression of PEX16-o/e cells was clearly decreased on day 0 and day 1 of differentiation (ct-levels for PEX16-o/e cells: d0: \approx 38, d1: \approx 33, ct-levels for controls: d0: \approx 33, d1: \approx 31) (figure 4.12B). However, starting on day 2 of differentiation, *Ppar γ 2*-expression of overexpressing cells was boosted to higher levels than in controls (figure 4.12B).

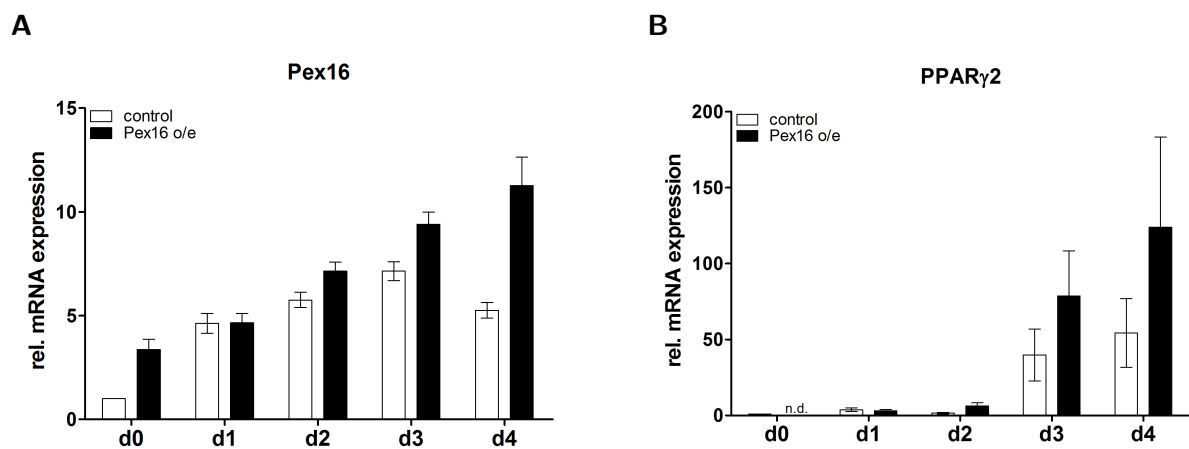


Figure 4.12: mRNA-levels of A) *Pex16* and B) *Ppar γ 2* during differentiation of the PEX16-o/e iBACs line H2 compared to pMSCVpuro-controls. The graphic represents mean \pm SD of 2 technical replicates as percentage of controls on day 0, which were set to 1.

In order to find an explanation for the cell death of PEX16 overexpressing iBACs after induction, Western Blots with day 0-protein samples for pro- and anti-apoptotic markers BAX and BCL-2 were performed by Madeleine Görtzer, Medical University of Graz. PEX16-o/e cells of passage 19 showed an approx. 50%-reduced expression of the pro-apoptotic protein BAX when compared to controls (figure 4.13A). With higher passages, the BAX-expression in PEX16-o/e cells increased, resulting in an even higher BAX expression in PEX16-o/e cells of passage 21 than in controls (figure 4.13A). Anti-apoptotic BCL-2 expression in PEX16-o/e cells of passage 19 was higher than in controls, and decreased with elevating passage (figure 4.13B). PEX16-o/e cells of passage 21 showed BCL-2 expression levels that were decreased to approximately 70% of the levels observed in controls (figure 4.13B).

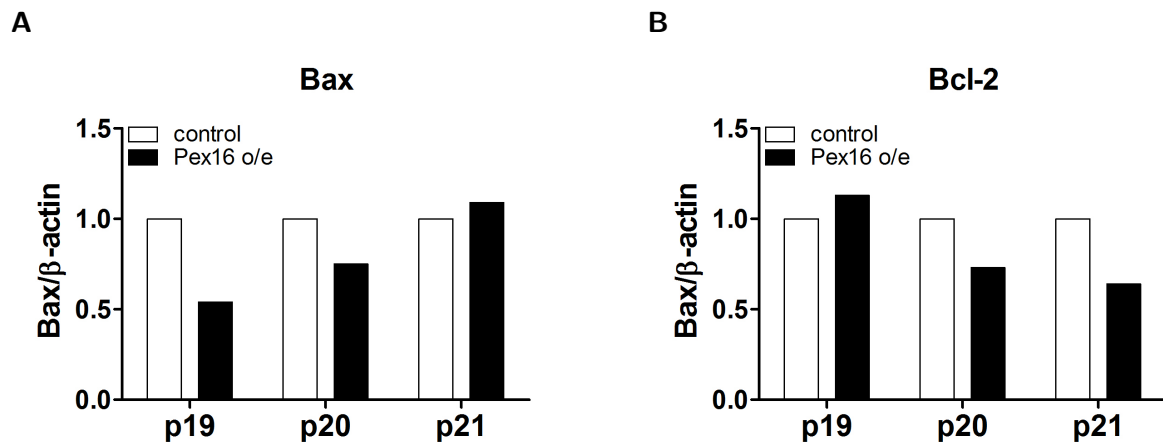


Figure 4.13: Results obtained from densitometric determination of BAX-and BCL-2 expression on day 0 of differentiation via Western Blots, normalized to β -actin. Controls were set to 1. The graphic shows 3 biological replicates.

4.4 Silencing of PEX16 in models for white and brown adipocytes

As PEX16 overexpression in 3T3-L1 cells and iBACs already showed slight alterations in growth, morphology and lipid metabolism, we were also interested in the effects of silencing PEX16 in these cell lines. Therefore, lentiviral transduction particles, encoding *Pex16*-targeting small hairpin RNA (shRNA), were used for generation of 3T3-L1 and iBACs cell lines with stably silenced PEX16 expression. Cells transduced with non targeting control (NTC)-lentiviral particles served as control.

4.4.1 Silencing of PEX16 in 3T3-L1 adipocytes

Silencing of PEX16 in 3T3-L1 cells was performed with 7.5 MOI (multiplicity of infection) per cell using 5 different shRNA lentiviral constructs. Subsequent selection with G418 had to be abandoned 72h after selection-start due to a massive loss of cells. Surviving cells were grown to 100% of confluence, and differentiated until day 7. qRT-PCR analysis was performed with day 0 and day 7 samples. On day 0 and on day 7 of differentiation a clear reduction of *Pex16* mRNA expression up to more than 50% was observed for all 5 lentiviral particles (figure 4.14A,B).

PEX16 silenced 3T3-L1 cells differentiated worse than control cells, as to see in ORO-pictures in figure 4.15. Thus, PEX16 seems to play a critical role in white adipocyte differentiation. On protein level silencing has not been verified yet.

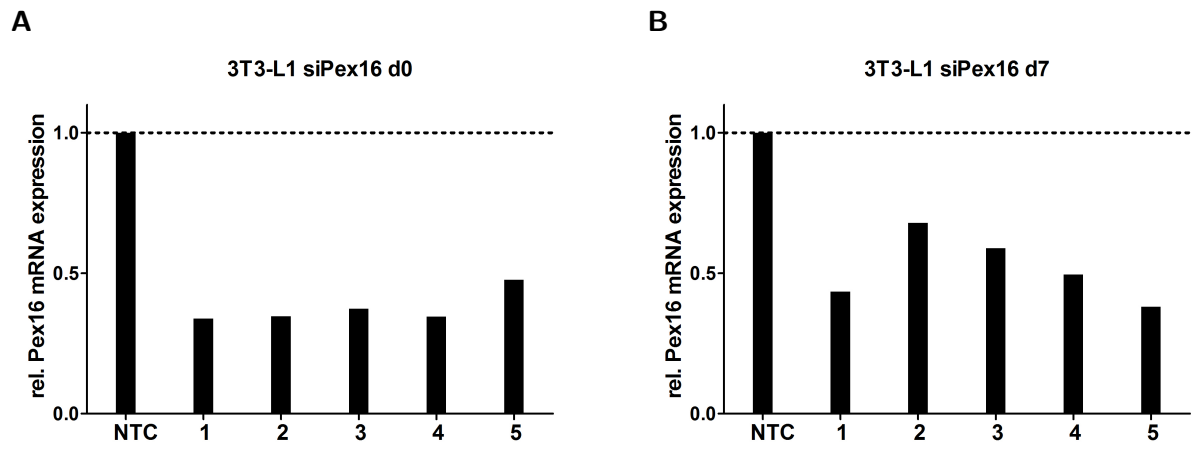


Figure 4.14: mRNA-levels of *Pex16* in 3T3-L1 cells on A) day 0 and B) day 7 of differentiation, silenced with 5 different lentiviral lines or transduced with non targeting control determined by qRT-PCR. Data is shown as mean of two technical replicates as percentage of not targeting control (NTC), which was set to 1.

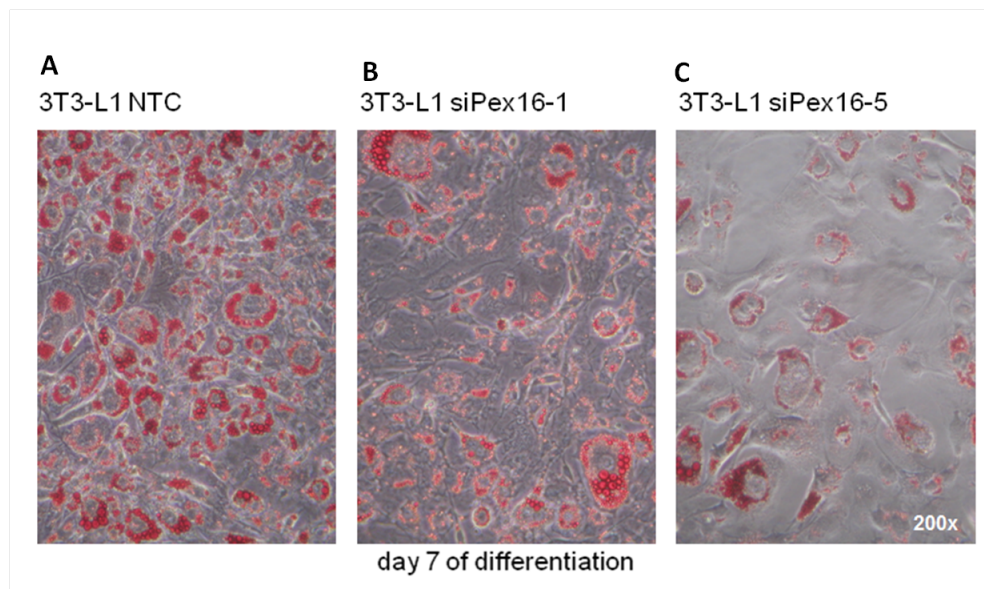


Figure 4.15: Effect of PEX16-silencing in 3T3-L1 cells on lipid accumulation shown in Oil-Red-O pictures of cells on day 7 of differentiation. A) Non targeting control (NTC) B) silencing construct 1 C) silencing construct 5. 200x magnification.

4.4.2 Silencing of PEX16 in iBACs

As PEX16-expression is even higher in BAT than in WAT (figure 4.1A), silencing effects in iBACs were expected to be more significant than in 3T3-L1 cells. Silencing of PEX16 in iBACs was tried with the same *Pex16*-targeting shRNA-expressing lentiviral particles used for 3T3-L1 cells. Due to the partial resistance of iBACs to puromycin, selection was done using 1.5mg/mL G418, but cells did not respond to the selection. Nevertheless, a screen for transduction efficiency was made on day 7 of differentiation via qRT-PCR, which confirmed that selection was inefficient. No reduction in *Pex16* mRNA-expression could be observed (figure 4.16).

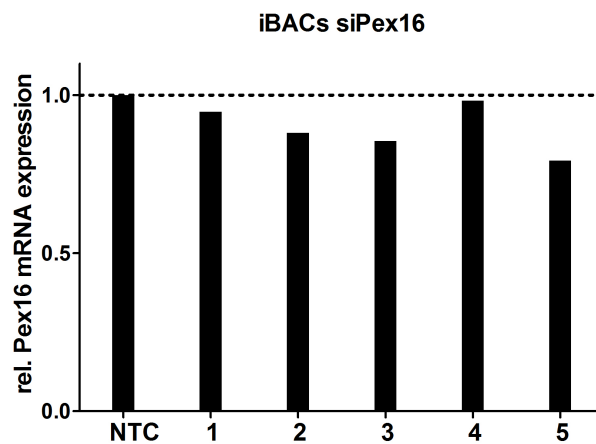


Figure 4.16: mRNA-levels of *Pex16* in iBACs on day 7 of differentiation, transduced with 5 different PEX16-targeting lentiviral lines and non targeting control. Data is shown as mean of two technical replicates as percentage of not targeting control (NTC), which was set to 1.

4.5 Pex16 - a possible PPAR γ target

As elevated levels of *Pex16* mRNA-expression during adipogenesis and an increase of *Pex16* mRNA-expression under PPAR γ -stimulation with rosiglitazone could be observed by qRT-PCR, a linkage between PPAR γ and *Pex16* seemed likely. For that purpose, the region around TSS of *Pex16* gene was observed via UCSC genome browser and three estimated PPAR γ binding targets downstream the TSS were discovered, referred to as "Peak1" (1052-1379bp downstream TSS) and "Peak2" (1349-1676bp downstream TSS), both located in intron 1, and "Peak3" (2160-2554bp downstream TSS), located in intron 2/exon 3 -transition (see figure 4.17).

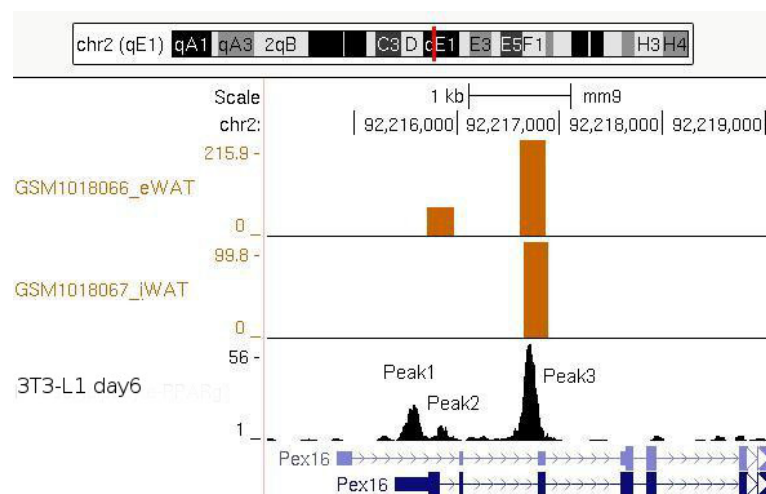


Figure 4.17: UCSC genome browser information on *Pex16* showing the region around *Pex16*-transcription start site. Three potential PPAR γ -targets, labelled as "Peak1", "Peak2" and "Peak3" were detected.

The genomic regions a) 1052-1379bp (Peak1), b) 1349-1676bp (Peak2), c) the combined version 1052-1676bp (Peak1+2), and d) 2160-2554bp (Peak3) downstream the TSS, according to figure 4.18 were cloned into luciferase reporter vector pTK-luc.

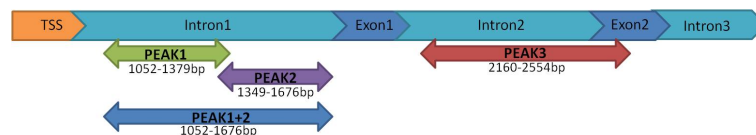


Figure 4.18: Location of the potential PPAR γ -target regions "Peak1", "Peak2", "Peak1+2", and "Peak3" downstream the transcription start site.

Luciferase assays with these constructs were performed, but only very low read-outs could be achieved in these experiments due to a missing minimal promoter in the vector system. This realization gave reason to re-clone the sequences into another vector system (pGL4.26), providing a minimal promoter in its sequence, and to repeat the luciferase assays.

4.5.1 Luciferase assays using pTK-luc - luciferase reporter vector

Cloning of putative PPAR γ - target sequences into pPPRE-X3-TK-luc- vector

The genomic regions were successfully amplified via PCR using primers with restriction-site extensions (see section 3.1.7) for HindIII (fw) and BamHI (rv) restriction enzymes (see figure 4.19A). Enzymatic digestion, ligation and transformation of NEB5 α Comp. E.Coli-cells were carried out as described in section 3.2.1. In order to have an empty control vector of pTK-luc for subsequent luciferase assays, the triple PPRE-region in the pPPRE-X3-TK-luc plasmid was removed and the empty plasmid was then ligated via blunt end ligation. Ampicillin-selection on agar-selection-plates was performed over night at 37°C and resulted in growth of several potentially plasmid-containing colonies. Three colonies per plasmid were used for miniprep-production. To evaluate whether the generated plasmids contain the desired DNA-sequences, control cuts with HindIII and BamHI were performed (see figure 4.19B). Positive results were obtained for Peak1 (2 colonies), Peak2 (1 colony) and Peak1+2 (3 colonies). Peak3 was \approx 150bp shorter than expected. This observation was confirmed by the sequencing results, which can be found in the appendix. An overlooked restriction site of BamHI within the Peak3-sequence was found to be responsible for the sequence-abbreviation. Cloning of full Peak3-sequence was finally successful at HindIII (fw) and XhoI (rv)-restriction sites (data not shown).

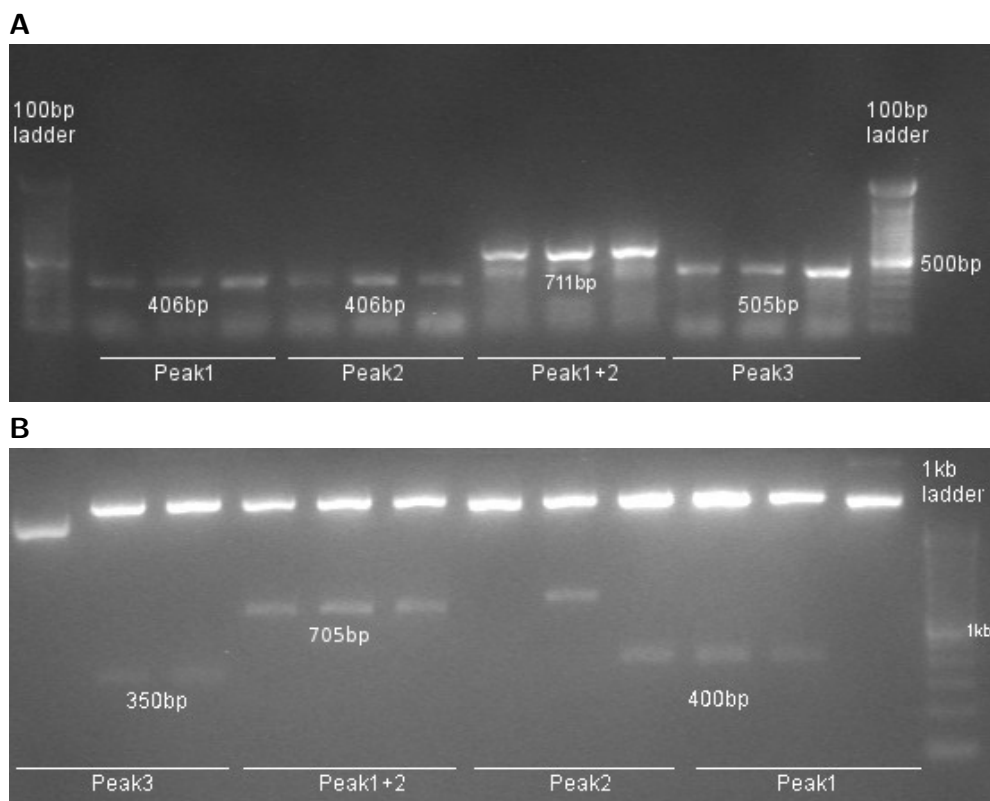


Figure 4.19: Electrophoresis gel: A) Genomic regions of *Pex16* used for testing of PPAR γ -interactions amplified via PCR. B) Control digest of minipreps containing the putative PPAR γ target regions using HindIII and BamHI restriction enzymes. Peak3 sequence is \approx 150bp shorter than expected.

Luciferase-assays using pTK-luc- luciferase reporter vector suggest a potential interaction of PPAR γ and Pex16

The luciferase activities of pTK-luc-Peak3l construct of PPAR γ /RxR α - cotransfected cells with and without rosiglitazone-stimulation were significantly elevated compared to the pCMX-cotransfected samples (see figure 4.20). Stimulation with rosiglitazone resulted in a significant increase in luciferase activity at Peak3s- and Peak3l- constructs compared to the unstimulated construct of the PPAR γ /RxR α cotransfected samples (see figure 4.20). In addition, luciferase activity of rosiglitazone-stimulated pTK-luc-Peak3s construct of PPAR γ /RxR α - cotransfected cells was significantly increased compared to the pCMX-cotransfected samples and a trend for elevated luciferase activities under basal conditions was observed as well (figure 4.20). Peak1+2 of PPAR γ /RxR α - cotransfected cells showed a trend to increased luciferase activity with and without rosiglitazone-stimulation. Peak1- and Peak2- constructs did not react to PPAR γ - stimulation. These results suggest, that *Pex16* might be a target of PPAR γ .

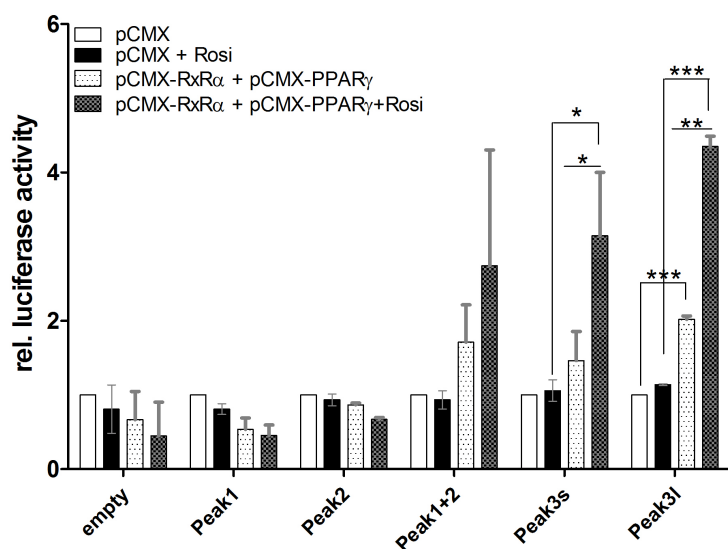


Figure 4.20: Luciferase assay results for PPAR γ binding. Five potential target regions downstream transcription start site were cloned into luciferase reporter vector pTK-luc (Peak1, Peak2, Peak1+2, Peak3s (truncated sequence) and Peak3l (full sequence)). pCMX-vectors expressing PPAR γ and RxR α , or the empty pCMX-vecor respectively, were co-transfected into Cos7 cells. Preliminary data show two (Peak1, Peak2, Peak3l) or three (empty pGL4.26 and Peak3s) biological replicates. Luciferase activity is shown as percentage of pCMX-luciferase activity, which was set to 1, for each construct individually. * $p < 0.05$, ** $p < 0.01$, *** $p < 0.001$

As the number of counts in these experiments was very low, the results could not be seen as reliable and had to be repeated, using an appropriate luciferase reporter vector, which harbours a minimal promoter.

4.5.2 Luciferase assays using pGL4.26 - luciferase reporter vector

Cloning of PPAR γ target sequences into pGL4.26-vector

To solve the problem of low read-outs obtained from previous luciferase assays, the sequences were re-cloned at KpnI (fw) and XhoI (rv) restriction sites into pGL4.26 vector, containing a minimal promoter. The four generated constructs are represented schematically in figure 4.21. The figures were generated via *Serial Cloner*-program, which was used for imaginary test-runs of the cloning procedure including PCR, enzymatic digestion of vectors and inserts, and ligation, in order to avoid mistakes as in previous cloning attempts of the Peak3-sequence into pTK-luc vector.

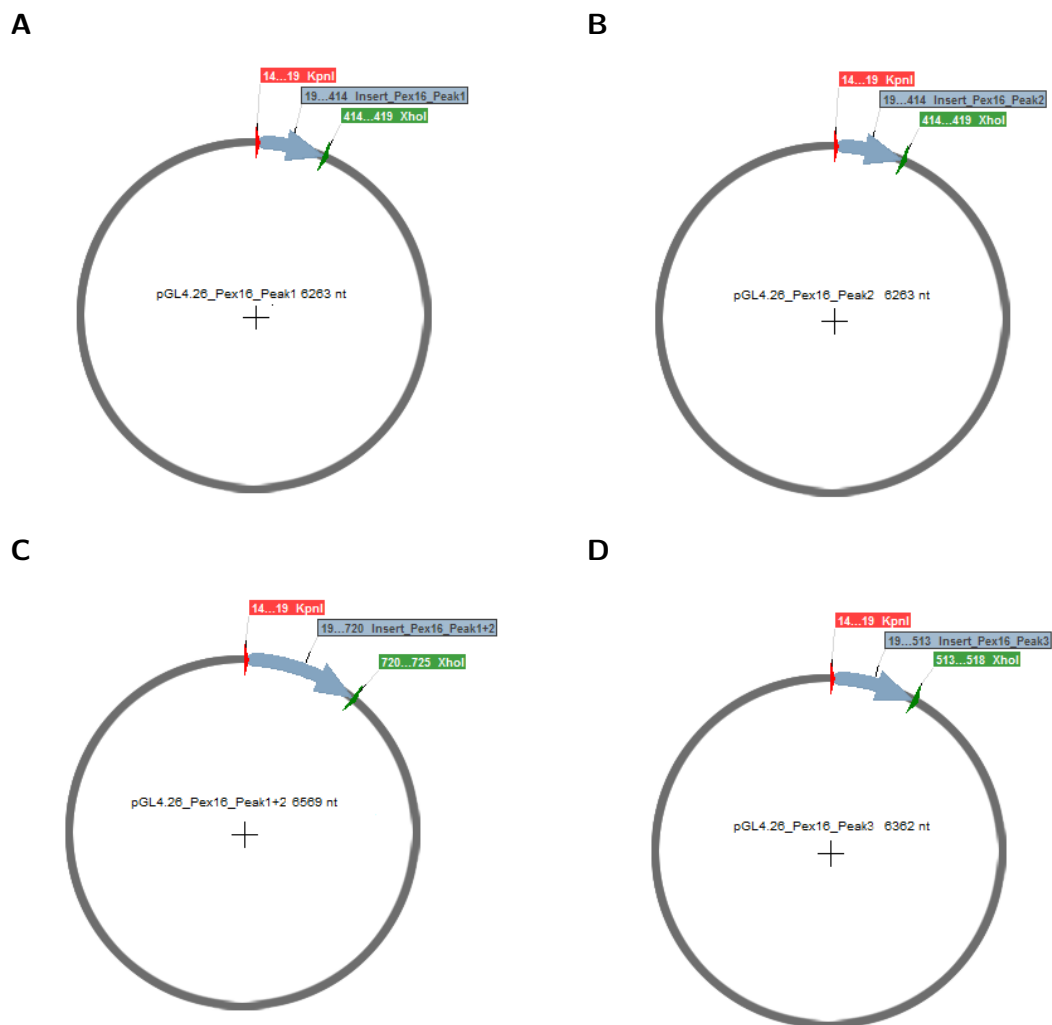


Figure 4.21: Scheme of plasmids generated by cloning *Pex16*-regions A) Peak1, B) Peak2, C) Peak1+2, and D) Peak3 into pGL4.26 vector at KpnI and XhoI restriction sites.

Pex16-inserts were amplified via PCR. Minipreps of pTK-luc constructs served as template, and primers with restriction-site extensions for KpnI and XhoI restriction enzymes (see section 3.1.7) were used for the amplification (see figure 4.22).

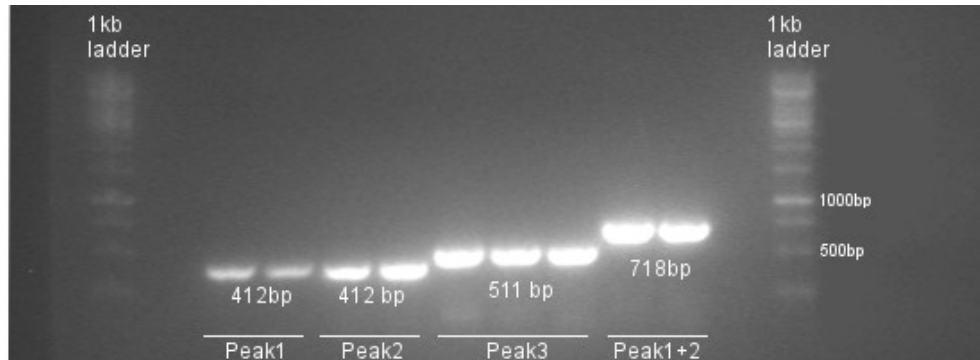


Figure 4.22: Electrophoresis gel: Inserts for pGL4.26-vector amplified via PCR.

Transformation of NEB5 α Comp. E.Coli-cells with the generated plasmids and subsequent colony PCR of 6 colonies per construct revealed a well-functioning cloning of *Pex16*-inserts into pGL4.26-vector (see figure 4.23).

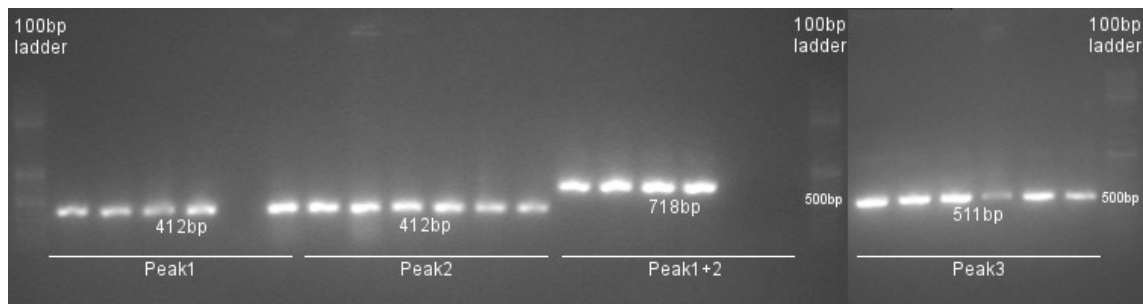


Figure 4.23: Electrophoresis gel: Colony PCR results for pGL4.26-Pex16 (Peak1, Peak2, Peak1+2, and Peak3) constructs.

Control digest with KpnI and XhoI restriction enzymes (see figure 4.24) and sequencing of the minipreps confirmed the integration of all of the four potential PPAR γ target sequences into pGL4.26 vector. Sequencing results can be found in the appendix.

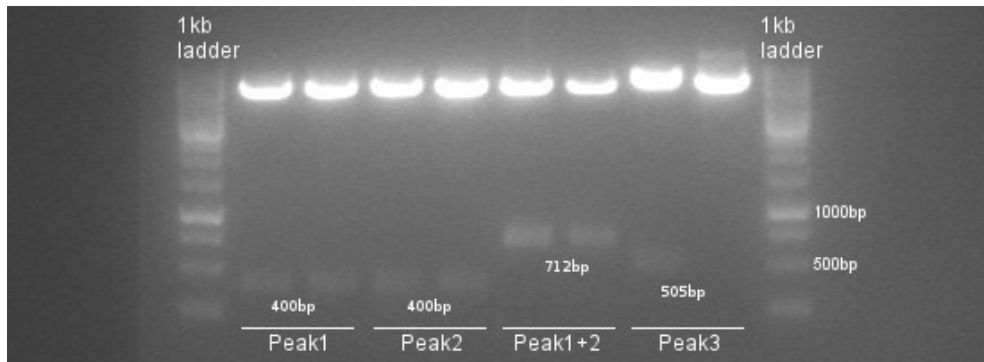


Figure 4.24: Electrophoresis gel: Control digest of the generated pGL4.26- constructs with KpnI and XhoI restriction enzymes confirms the integration of all putative PPAR γ target regions (Peak1, Peak2, Peak3, and Peak1+2).

Luciferase-assay using pGL4.26- luciferase reporter vector confirms the suggested binding of Pex16 by PPAR γ

Corresponding to the results from previous luciferase assays using pTK-luc-vector, the luciferase activity of pGL4.26 - Peak1+2- and Peak3- constructs of PPAR γ /R α - cotransfected cells was elevated compared to the pCMX-cotransfected samples (figure 4.25). A clear increase under stimulation with rosiglitazone was detected for Peak3-samples cotransfected with PPAR γ /R α compared to the unstimulated samples. In addition, a tendency to increase was observed for Peak1+2-constructs when stimulated with rosiglitazone (figure 4.25).

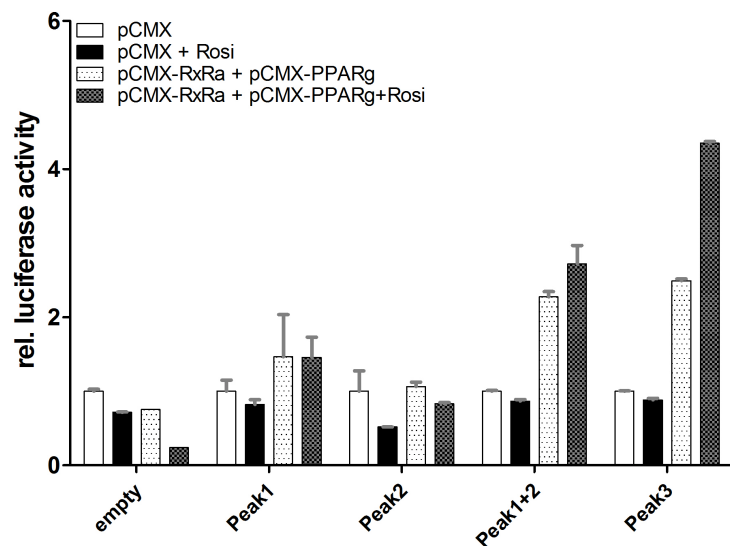


Figure 4.25: Luciferase assay results for PPAR γ binding. Four potential target regions downstream transcription start site were cloned into luciferase reporter vector pGL4.26 (Peak1, Peak2, Peak1+2 and Peak3 (full sequence)). pCMX-vectors expressing PPAR γ and R α , or the empty pCMX-vector respectively, were co-transfected into Cos7 cells. Preliminary data show the mean \pm SD of two technical replicates. Luciferase activity is shown as percentage of pCMX-luciferase activity, which was set to 1, for each construct individually.

5 Discussion

PEX16 is known to be essential for peroxisomal biogenesis, growth and fission. Although function and composition of peroxisomes as well as several peroxisomal proteins have been studied in the liver extensively in the past, not much is known about the role of peroxisomes, and especially PEX16, in adipose tissue. As PEX16 was highly upregulated in differentiating iBACs as observed via microarray experiments performed in our group and hints for an influence of peroxisomes in adipocyte development and energy metabolism were found in literature, *Pex16* seemed to represent an interesting new candidate gene to investigate.

5.1 *Pex16* is highly expressed in murine adipose tissue and elevated during adipogenesis

The first step of investigation was to screen various tissues for *Pex16* mRNA-expression. High levels of *Pex16*-mRNA could be detected in white and brown adipose tissue, while expression in liver, skeletal muscle and cardiac muscle tissue was rather low. Additionally, *Pex16*-expression was significantly higher in BAT than in WAT. Further, mice on high-fat diet for 16-20 weeks showed trends of elevated *Pex16* mRNA-expression in brown adipose tissue as well as in the liver (see figure 4.1). Thus, a role of PEX16, and consequentially peroxisomes, in adipocyte, and especially brown adipocyte energy metabolism was assumed. Reports of elevated numbers of peroxisomes and increased *Pex16* mRNA-expression in brown adipose tissue in literature, as consequence of various stimuli, including high-fat diets and cold exposure [2][3], substantiate the suspicion, that PEX16 might contribute to adipocyte lipid metabolism and eventually also to thermogenesis. In BAT and WAT, *Pex16*-expression was the same in fasting (overnight) or refed (1h free access to food after overnight fasting) conditions of wildtype mice. Also genetic obesity, like in ob/ob-mice, had no impact on BAT and WAT expression of *Pex16*- mRNA. Eventually a longer fasting for 24h would lead to perceivable changes of *Pex16* mRNA-expression.

Further, we were interested in *Pex16* mRNA-expression in various adipose cell lines during differentiation and eventual expression-changes under stimulation of PPAR γ by rosiglitazone or by β 3-adrenergic stimulation with isoproterenol. In murine 3T3-L1 cells, iBACs and C3H/10 T1/2, an increase in *Pex16*-expression on the first few days of differentiation could be observed. Stimulation of PPAR γ in 3T3-L1 cells with rosiglitazone and β 3-adrenergic stimulation of iBACs with isoproterenol lead to an further increase in *Pex16*-expression. PPAR γ represents the "master-regulator"

of adipogenesis. A linkage of *Pex16* mRNA-expression and PPAR γ -stimulation gives evidence to a contribution of PEX16 to adipogenic differentiation. The increase of *Pex16* expression under β 3-adrenergic stimulation suggests a role of PEX16 also in brown fat metabolism and eventually even in thermogenesis. In human Simpson-Golabi-Behmel-syndrome cells (SGBS) and human multipotent adipose-derived stem cells (hMADS), *Pex16*-expression was lower compared to murine cell lines, although mRNA-levels were also increasing with progressive differentiation. This result is congruent with the finding on www.biogps.org, that *Pex16* seems to be hardly expressed in human tissues¹.

5.2 PEX16 overexpression influences adipogenesis

Although expression in human cell lines was comparatively low, we wanted to further investigate the role of PEX16 in murine adipose cell lines, as the results for *Pex16*-expression in murine tissues and cell lines seemed very promising. Therefore, we overexpressed PEX16 in models for brown and white adipocytes, namely iBACs and 3T3-L1 cells.

As pMSCV-plasmids including the *Pex16* coding sequence for the overexpression in 3T3-L1 cell line were already cloned within a practical prior to the master thesis, overexpression of PEX16 was first accomplished in 3T3-L1 cells. Cells stably overexpressing PEX16 were differentiated twice (three passages each). The first trial of differentiation was characterized by low lipid accumulations in control and PEX16-o/e cells. However, PEX16-overexpressing cells accumulated even less lipid droplets. Application of an unnoticed wrong differentiation cocktail or a too early induction could be possible reasons for the weak differentiation. Nevertheless, overexpression of PEX16 could still be observed and stimulation with rosiglitazone led to an even higher *Pex16* mRNA-expression in PEX16-overexpressing cells compared to controls on day three of differentiation. The second trial showed enhanced differentiation, but as in the first trial, PEX16-overexpressing cells seemed to exhibit reduced lipid accumulation. This observation was also accompanied by reduced *Ppar γ 2* mRNA-expression, suggesting a role of PEX16 in adipogenic differentiation. Here it has to be mentioned that also the reduced differentiation of PEX16-o/e cells might be responsible for the reduced *Ppar γ* expression. When stimulated with isoproterenol PEX16-overexpressing cells showed a trend to reduced triglyceride content and increased free fatty acid release on day 8 of differentiation, indicating a possible contribution of PEX16 to an elevated lipid turnover in response to β 3-adrenergic stimulation. Quite the contrary was witnessed for basal conditions, as on day 8 free fatty acid release was significantly decreased in overexpressing cells. This observation was supported by a tendency to reduced mRNA-expression of *ATGL*, the main enzyme for adipogenic lipolysis, and a reduction in peroxisomal β -oxidation genes (*Acox1*, *Acaa1a*, *Ehhadh*) in PEX16-o/e cells. We expected, that overexpressing PEX16 would result in a higher peroxisomal activity and subsequently a higher peroxisomal β -oxidation within cells, but this was at least not the case under basal conditions. In future, isoproterenol stimulated mRNAs have to be measured. Taken together, overexpression of PEX16

¹www.biogps.org/#goto=genereport&id=9409

seems to interfere with peroxisomal function. In which way this happens remains to be investigated. Experiments in yeast revealed an increase of peroxisomes in size, and a reduction of peroxisomal number caused by the overexpression of PEX16 [5]. Eventually, electron microscopy- experiments could illuminate the effect of PEX16-overexpression on peroxisomal structure, size and morphology.

PEX16- overexpression in iBACs, a brown adipocyte model, seemed to be more difficult than PEX16-o/e overexpression in 3T3-L1 cells. iBACs already possess a resistance against puromycin [46], making a selection of transduced cells using puromycin impossible. Therefore, *Pex16*-CDS had to be cloned into the vector system pMSCVhygro, providing a hygromycin-resistance-gene as selectable marker. Multiple trials of cloning the sequence into pMSCVhygro vector at various restriction sites failed, presumably due to a malfunctioning ligase. Thus, an alternative way for overexpressing PEX16 in iBACs had to be found. For this purpose, a dilution experiment with cells transduced with lentiviral particles for pMSCVpuro and pMSCV-Pex16 plasmids was performed. The subsequent screening for PEX16-overexpressing cell lines via qRT-PCR revealed three candidate cell lines, exhibiting an up to 5-fold overexpression of PEX16. Since we did not want to base further conclusions only on results received from one single overexpressing cell line, differentiation of the cells was performed with a combination of all three overexpressing cell lines. Interestingly, the previously explored 3- to 5-fold overexpression of *Pex16* on mRNA-level almost vanished and accordingly differences in FFA- release and TG- content, as seen in 3T3-L1 cells, could not be observed. A slight trend to augmented "browning" of the overexpressing cells was detected on day 7 of differentiation by elevated *UCP1* mRNA-levels. The expression of β - oxidation genes was not changed in PEX16-o/e iBACs.

Although Oil-red-O pictures suggested a worse differentiation of PEX16 overexpressing iBACs, *Ppar γ 2* mRNA-expression was elevated although the opposite would have been expected. The experiments were repeated with the H2-overexpressing iBAC line. Overexpression was maintained throughout differentiation, although the overexpression on day 3 was not significant. Again, reduced lipid accumulation was found in PEX16 overexpressing iBACs, although *Ppar γ 2*- expression was still increased in these cells. Interestingly, *UCP1*-expression in PEX16-o/e cells was not comparable to the previous results observed in the combined PEX16-overexpressing iBACs, as mRNA levels of *UCP1* were hardly detectable. Peroxisomal β -oxidation gene expression was again hardly altered in PEX16-o/e iBACs compared to controls. RNA samples from day 0 to day 4 were harvested in order to investigate, at which point of differentiation the overexpression disappears. The clear 3 to 4-fold overexpression of PEX16 on day 0 disappeared on day 1, and was slowly regained in the next few days. I assume, that this observation might be caused by a reduced differentiation or proliferation of overexpressing iBACs. *Ppar γ 2*- levels in PEX16-o/e cells were lower than in control cells on day 0 and day 1. On day 2, the overexpressing cells executed a delayed boost of *Ppar γ 2*- expression, which was then also preserved on day 3 and 4. This delayed *Ppar γ* expression could eventually explain the delayed differentiation and the accompanied loss of PEX16 overexpression on day 2 and day 3 of differentiation. The boost in *Ppar γ 2*-expression might justify the regain of PEX16 overexpression on day 4.

A proliferation assay, which should be repeated in the future for more reliable results, revealed that growth of PEX16-overexpressing iBACs was actually reduced compared to controls, or that some of the cells died in the first few days of growth. Additionally, a massive cell death starting three days after induction could be observed visually for PEX16-o/e overexpressing cells and controls. Microscopy pictures from ORO-stainings show that there were holes in the cell monolayer of PEX16-o/e cells and controls.

In order to find a reason for the enormous loss of cells, we asked Madeleine Göritzer from the Medical University of Graz to screen our day 0 protein samples for the apoptose markers BAX (pro-apoptotic) and BCL-2 (anti-apoptotic). Intriguingly, hardly a difference or even reduced pro-apoptotic protein-levels for overexpressing cells could be detected. The pro-apoptotic BAX protein levels increased with every passage of the cells. I assume, that another screen for day 3 and/or day 7 protein samples for apoptotic marker genes would be necessary to detect alterations, as the massive cell death started three days after induction.

The facts, that many control cells died as well and that detached cells were still connected to the bottom by structures, reminding of extracellular matrix, indicate another reason for the cell death. Possible explanations could be the exorbitant lipid accumulations in the cells, causing cells to detach from the bottom, or the way the dilution experiment was performed, as cells were exposed to trypsin repeatedly during this process, or, not to forget, an unidentified infection. However, typical infections like mycosis or bacterial infections could not be observed by microscopy, and a mycoplasma-test was negative.

As the overexpression of PEX16 in iBACs was very conflicting, the repetition of these experiments with an appropriate vector-system would be reasonable. By considering that the accomplished overexpression in 3T3-L1 cells was also not very high, a repetition of this experiments with higher PEX16-overexpressing cells would eventually lead to more significant results.

5.2.1 Western Blot analysis reveals a reduced protein size of PEX16

Western Blot analysis was performed for both overexpression experiments in 3T3-L1 cells as well as in iBACs. The observed protein bands were found 2-3kDA below the expected protein size of 38.6kDA. Neither cleavage site analysis using *SignalP4.1* prediction tool could explain the reduction in size, nor could the sequencing results of the pMSCV-Pex16 plasmids. If there was an undetected cleavage of PEX16, it could only be C-terminally, as the N-terminally His-tagged control could be detected and had the right size using anti-His-antibody (data not shown) and anti-PEX16-antibody. According to Honsho et al. (1998), the C-terminal region of PEX16 is responsible for the biological function of PEX16. The loss of a C-terminal region would subsequently lead to a loss of PEX16 protein function. There was apparently no cleavage in the His-tagged PEX16-proteins. Thus, a cleavage in the untagged samples seems unlikely. Until now we have no explanation for the reduced protein size. Mass spectrometry could eventually clarify whether the detected protein is PEX16 or not.

In iBACs, PEX16 overexpression could not be verified on protein level. For day 0 and day 7, signals at the size of ≈ 50 kDA were observed, indicating a possible dimerization of PEX16, which has not been described so far in literature. However, on day 3 a band at the right size was detected, but this band suggested reduced PEX16 concentration in PEX16-o/e cells.

Anyway, reasons for the reduced PEX16-protein size should be further investigated, as drawing conclusions regarding PEX16-overexpression based on an eventually malfunctioning protein would quite simply be wrong.

5.2.2 FFA and Triglyceride measurement

Free fatty acid release and triglyceride content were determined using intracellular protein-amounts for normalization. As protein amounts were consistently reduced in PEX16-overexpressing cells, variations of FFA-release and TG- content could also arise from this normalization method. It would be necessary to consider additional normalization parameters, such as the cell number, for the determination of more reliable results.

5.3 Stable silencing could be accomplished for 3T3-L1 cells, iBACs were not selectable

As the overexpression of PEX16 in 3T3-L1 cells and iBACs already interfered with adipocyte differentiation, we were also interested in silencing effects of PEX16. Mutations and absence of PEX16 were shown to result in the complete loss of peroxisomal structures [4][8][13][14][15].

Five different lentiviral strains were tested for their silencing efficiencies in 3T3-L1 cells and iBACs. Silencing of PEX16 in 3T3-L1 was successful for all five lentiviral particles compared to the non targeting control, although antibiotic selection had to be abandoned 72h after selection start, due to the appearance of an enormous cell death. It remains to be investigated, whether the cell death under selection pressure traces back to bad transduction efficiencies, or if this occurrence represents the first effect of complete silencing of PEX16. Non targeting controls remained in large parts alive during selection. Silencing efficiencies up to $>50\%$ could be observed for all lentiviral strains on day 0, and for strains 1 and 5 also on day 7 of differentiation. Additionally, reduced lipid accumulations of silenced cells could be observed using Oil-red-O-stainings. In future experiments, silencing should be confirmed on protein level. Additionally, the expression of adipogenic and peroxisomal marker genes and FFA- release and TG- content in basal and stimulated conditions should be investigated in these cells. Transduced iBACs were not selectable with geneticin (G418), possibly caused by a developed resistance against the antibiotic, or due to the use of defective G418 antibiotic. The unselected cells were differentiated until day 7. Silencing of PEX16 could not be detected. Selection should be repeated with new antibiotic in the future.

5.4 Luciferase assays reveal Pex16 as a PPAR γ target gene

As multiple hints for possible interactions of PPAR γ and *Pex16* were found in literature and previous experiments, we wanted to investigate these interactions using luciferase assays.

Cloning of putative PPAR γ target sequences (Peak1, Peak2, Peak1+2, and Peak3) into luciferase reporter vector pTK-luc and the blunt end ligation for the generation of an empty vector turned out to be very time consuming, as in initial trials the same malfunctioning ligase as for cloning *Pex16*-CDS into pMSCVhygro was used. Additionally, an overlooked restriction site for BamHI in the Peak3-sequence lead to another necessary cloning repetition of the complete Peak3-sequence into pTK-luc vector.

However, luciferase assay results received for experiments using the generated pTK-luc plasmids indicate a PPAR γ interaction at Peak1+2 and Peak3 sequence, as significantly increased firefly luciferase activities could be observed compared to controls. The luciferase activities for cells transfected with Peak1 and Peak2 sequences were hardly altered when PPAR γ /RxR α were present, suggesting that the putative PPAR γ - target sequence of Peak1+2 might be located between Peak1 and Peak2 region. In these experiments, only very low read outs (several hundred counts) for firefly luciferase activity were generated. A non-existent minimal promoter in the pTK-luc sequence might be the cause of these low read outs. The fact, that still differences in luciferase activity could be observed, can be explained by the existence of a thymidine kinase promoter lying several hundred basepairs upstream the target region in the vector [47], which could be sufficient for generation of at least some transcripts of these regions.

In order to get more reliable results, the sequences were re-cloned into pGL4.26 vector, providing a minimal promoter in its sequence. The performed luciferase assay confirmed the results obtained for pTK-luc constructs, finally showing reliable counts for firefly luciferase activity. The regions of Peak1+2 and Peak3 seem to represent direct targets of PPAR γ . By knowing this, a linkage of PEX16 to adipogenesis seems very likely. This results needs to be verified within prospective repetitions of the experiment in the future.

5.5 Model for PEX16 contribution to lipid metabolism in adipose tissue

The idea of how PEX16 might contribute to (brown) adipocyte metabolism, is drawn schematically in figure 5.1. PEX16 is integrated into pre-peroxisomes at the endoplasmic reticulum. It contributes to peroxisomal formation and growth by serving as receptor for PEX3, which subsequently attracts peroxisomal membrane proteins from the cytosol to the peroxisomal membrane [1][4][10][11][12]. Peroxisomes perform β -oxidation of very long chain fatty acids, in an acetyl-CoA providing and potentially thermogenic way [3]. Acetyl-CoA is then transported into mitochondria, where it is processed in order to generate ATP or heat (only in brown adipocytes). The expression of PEX16 can be regulated by PPAR γ .

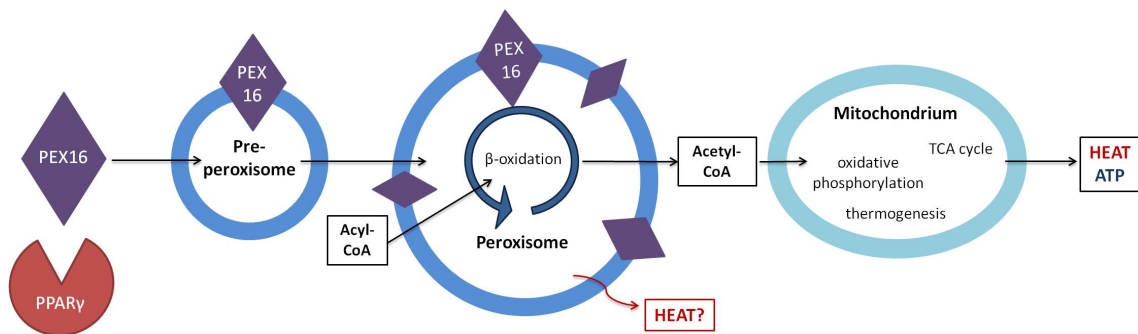


Figure 5.1: Scheme of the potential influence of PEX16 to peroxisomal development and lipid metabolism in (brown) adipose tissue.

5.6 Concluding remarks

Many fascinating facts about PEX16 and its possible contribution to adipogenesis and energy metabolism have been collected throughout the research for this thesis. *Pex16* seems to be a direct target of PPAR γ , which makes it a promising new player in adipogenesis. Overexpression and silencing of PEX16 in models for white and brown adipocytes also gave hints for this assumption. Nevertheless, for unraveling questions, like the impact of PEX16 in priming adipocyte development and if so, how it might contribute to adipocyte metabolism, more research needs to be done in the future.

List of Figures

2.1	Scheme of peroxisomal biogenesis in different organisms: <i>Y. lipolytica</i> , <i>Mammals</i> and <i>Plants</i> . In mammals, PEX16 is co-translationally inserted into the ER by the SEC61-dependent import pathway. At the ER it is integrated into pre-peroxisomes, where it serves as receptor for PEX3 and group 1 PMPs. PEX16 is also directly targeted to pre-peroxisomes, still serving as PEX3 and group 2 PMP receptor and causing the formation of mature peroxisomes, which can now undergo fission for proliferation. [1].	7
2.2	Peroxisomal composition: Plasma membrane, nonhomogenous matrix and optional crystalline core. Source: www.boundless.com/biology/cell-structure/eukaryotic-cells/peroxisomes	8
2.3	Scheme of the peroxisomal β -oxidation. Acyl-CoA is oxidized to acetyl-CoA, which can be delivered to mitochondria where it serves for energy generation. Hydrogen peroxide is generated within the first step of the process.	9
3.1	Vector maps of cloning plasmids pMSCVpuro, pMSCVhygro and HisMaxC. Yellow and orange labels represent the used restriction sites. Source: www.addgene.org/vector-database	20
3.2	Vector maps of cloning plasmids pPPRE X3-TK-luc and pGL4.26. Yellow and orange labels represent the used restriction sites. Source: www.addgene.org/vector-database	21
3.3	Arrangement of sponges, filters, gel and membrane for the blotting procedure.	30
4.1	A) <i>Pex16</i> mRNA-expression in murine brown adipose tissue (BAT), white adipose tissue (WAT), cardiac muscle (CM), skeletal muscle (SM) and liver. (n=5). B) <i>Pex16</i> mRNA-expression in BAT, WAT and liver of chow-diet and high-fat-diet (HFD) fed mice. (n=2). C) <i>Pex16</i> mRNA-expression in BAT and WAT of wildtype (wt) and genetically obese (ob/ob) mice in fasting and refeed conditions. (n=2) Data is shown as mean \pm SD.	33
4.2	<i>Pex16</i> mRNA-levels in A) 3T3-L1 cells (basal and stimulated with rosiglitazone)*, B) iBACs (basal and stimulated with isoproterenol)*, C) C3H/10 T1/2*, D) SGBS** and E) hMADS** cells throughout differentiation. *Preliminary data is shown as mean of 2 technical replicates from n=1 as percentage of day 0. **Data is shown as mean of two biological replicates as percentage of day 0.	34

4.3	<p>A) mRNA-level-screen for <i>Pex16</i>-overexpression on day 0 of differentiation. 3T3-L1 cells were transduced with lentiviral particles. Preliminary data is shown as mean of two technical replicates as percentage of pMSCV-puro control on day 0 of differentiation. B) <i>Pex16</i> mRNA-levels during differentiation of PEX16-o/e line 1-3T3-L1 cells and controls with and without rosiglitazone (=Rosi) stimulation, referred to as "timeseries 1". C) Oil-red-O stainings from PEX16-o/e 3T3-L1 cells and controls of timeseries 1 on day 7 of differentiation. D) <i>Pex16</i> mRNA-levels during the second differentiation of PEX16-o/e line 1-3T3-L1 cells and controls, referred to as "timeseries 2". E) Western Blot of timeseries 2-protein samples (puro= control, O/E= PEX16-o/e, "Pex16": developed with Super Signal, "Pex16*": developed with ECL Prime). F) Oil-red-O stainings from PEX16-o/e 3T3-L1 cells and controls of timeseries 2 on day 8 of differentiation. qRT-PCR-data is shown as mean±SD as percentage of pMSCVpuro-control (d0) which was set to 1. (n=3)</p>	36
4.4	<p>A) Free fatty acid and B) triglyceride measurement on day 3 and day 8 of differentiation of Pex16-o/e 3T3-L1 cells and controls (timeseries 2) with and without isoproterenol (=Isoprot) stimulation. Free fatty acid contents are presented in nmol FFA/mg protein, triglyceride contents in nmol TG/mg protein. (n=3) *p<0.05 . . .</p>	37
4.5	<p>A) mRNA-levels of adipogenesis marker gene <i>Pparγ2</i>, B) lipolysis gene <i>ATGL</i>, and of peroxisomal β-oxidation genes C) <i>Acox1</i>, D) <i>Ehhadh</i> and E) <i>Acaa1a</i> in PEX16-overexpressing 3T3-L1 cells and controls. qRT-PCR-data is shown as mean±SD as percentage of pMSCVpuro-control (d0) which was set to 1. (n=3 for A) B) C) and E), n=1 for D)) *p<0.05,**p<0.01, ***p<0.001</p>	38
4.6	<p>A) Western Blot of PEX16 overexpressing 3T3-L1 cells (PEX16 o/e) and Cos7 cells (HisPex16) on day 7 of differentiation using α-PEX16-antibody. The pMSCV-Pex16 transduced 3T3-L1 cells express a ≈36 kDa- protein, HisPex16 transfected Cos7 cells express a protein at the size of ≈39 kDa. B) Cleavage site prediction for PEX16-protein generated via <i>SignalP4.1</i> prediction tool: no cleavage sites could be detected within the aminoacid sequence. C-score: raw cleavage site score, S-score: signal peptide score, Y-score: combined cleavage site score.</p>	39
4.7	<p>qRT-PCR-screen for PEX16 overexpression in iBACs compared to controls after two repetitions of a dilution experiment ("Experiment I", "Experiment II"). iBACs were transduced with lentiviral particles (pMSCVpuro and pMSCV-Pex16) and diluted to 1 cell/100µL. Single cells were grown without antibiotic selection and tested for overexpression at 100% of confluence via qRT-PCR. mRNA-levels of PEX16-o/e iBACs are shown as percentage of pMSCVpuro-control, which was set to 1. Preliminary data is shown as mean±SD of two technical replicates from n=1.</p>	40

4.8	Combination of the three highest PEX16-o/e iBACs lines H2, E12 and F5 compared to pMSCVpuro-controls: A) mRNA-levels of <i>Pex16</i> in PEX16-overexpressing cells compared to controls throughout differentiation. B) Western Blot analysis of protein samples from PEX16-o/e cells (=O/E) and controls (=puro) on d0, d3 and d7 of differentiation, developed with ECL Prime. C) Free fatty acid (FFA) and D) triglyceride-measurement of PEX16-o/e cells compared to controls after 4h or 12h incubation with FFA-free Medium with and without stimulation with isoproterenol (=Isoprot) on day 3 and day 7 of differentiation. Oil-Red-O staining of PEX16-o/e cells and controls E) on day 3 and F) on day 7 of differentiation. qRT-PCR-data is shown as mean±SD as percentage of pMSCVpuro-control (d0) which was set to 1. Free fatty acids are presented in nmol FFA/mg protein, triglycerides are presented in nmol TG/mg protein.(n=3) **p<0.01	41
4.9	mRNA-levels of adipogenesis marker gene A) <i>Pparγ2</i> , brown/beige adipocyte marker gene B) <i>UCP1</i> and of peroxisomal β-oxidation genes C) <i>Acox1</i> D) <i>Ehhadh</i> and E) <i>Acaa1a</i> in a combination of the three highest PEX16-o/e iBACs lines H2, E12 and F5 compared to pMSCVpuro controls. qRT-PCR-data is shown as mean±SD as percentage of pMSCVpuro-control (d0) which was set to 1. (n=3)	42
4.10	A) mRNA levels of <i>Pex16</i> in PEX16-o/e iBACs cell line H2 compared to pMSCVpuro controls during differentiation. B) Oil-red-O pictures of control cells and PEX16-o/e cells on day 6 of differentiation. C) mRNA levels of <i>Pparγ2</i> in PEX16-o/e iBACs cell line H2 compared to controls during differentiation. D) Proliferation testing by counting the cell amount of iBACs during growth and differentiation ("puro"/"Pex16 o/e": 20.000 cells seeded, induction on day 5, "puro*"/"Pex16 o/e*": 40.000 cells seeded, induction on day 4). Preliminary qRT-PCR-data is shown as mean±SD of two technical replicates as percentage of pMSCVpuro-control (d0), which was set to 1.	43
4.11	A) mRNA levels of <i>UCP1</i> in PEX16-o/e iBACs cell line H2 compared to pMSCVpuro controls. Preliminary qRT-PCR-data is shown as mean±SD of two technical replicates as percentage of pMSCVpuro-control (d3), which was set to 1. B) mRNA levels of <i>Acox1</i> C) <i>Acaa1a</i> and D) <i>Ehhadh</i> in PEX16-o/e iBACs cell line H2 compared to pMSCVpuro controls. Preliminary qRT-PCR-data is shown as mean±SD of two technical replicates as percentage of pMSCVpuro-control(d0), which was set to 1.	44
4.12	mRNA-levels of A) <i>Pex16</i> and B) <i>Pparγ2</i> during differentiation of the PEX16-o/e iBACs line H2 compared to pMSCVpuro-controls. The graphic represents mean±SD of 2 technical replicates as percentage of controls on day 0, which were set to 1.	45
4.13	Results obtained from densitometric determination of BAX-and BCL-2 expression on day 0 of differentiation via Western Blots, normalized to β-actin. Controls were set to 1. The graphic shows 3 biological replicates.	46

4.14	mRNA-levels of <i>Pex16</i> in 3T3-L1 cells on A) day 0 and B) day 7 of differentiation, silenced with 5 different lentiviral lines or transduced with non targeting control determined by qRT-PCR. Data is shown as mean of two technical replicates as percentage of not targeting control (NTC), which was set to 1.	47
4.15	Effect of PEX16-silencing in 3T3-L1 cells on lipid accumulation shown in Oil-Red-O pictures of cells on day 7 of differentiation. A) Non targeting control (NTC) B) silencing construct 1 C) silencing construct 5. 200x magnification.	47
4.16	mRNA-levels of <i>Pex16</i> in iBACs on day 7 of differentiation, transduced with 5 different PEX16-targeting lentiviral lines and non targeting control. Data is shown as mean of two technical replicates as percentage of not targeting control (NTC), which was set to 1.	48
4.17	UCSC genome browser information on <i>Pex16</i> showing the region around <i>Pex16</i> -transcription start site. Three potential PPAR γ -targets, labelled as "Peak1", "Peak2" and "Peak3" were detected.	49
4.18	Location of the potential PPAR γ -target regions "Peak1", "Peak2", "Peak1+2", and "Peak3" downstream the transcription start site.	49
4.19	Electrophoresis gel: A) Genomic regions of <i>Pex16</i> used for testing of PPAR γ -interactions amplified via PCR. B) Control digest of minipreps containing the putative PPAR γ target regions using HindIII and BamHI restriction enzymes. Peak3 sequence is \approx 150bp shorter than expected.	50
4.20	Luciferase assay results for PPAR γ binding. Five potential target regions downstream transcription start site were cloned into luciferase reporter vector pTK-luc (Peak1, Peak2, Peak1+2, Peak3s (truncated sequence) and Peak3l (full sequence)). pCMX-vectors expressing PPAR γ and RxR α , or the empty pCMX-vecor respectively, were co-transfected into Cos7 cells. Preliminary data show two (Peak1, Peak2, Peak3l) or three (empty pGL4.26 and Peak3s) biological replicates. Luciferase activity is shown as percentage of pCMX-luciferase activity, which was set to 1, for each construct individually. * $p < 0.05$, ** $p < 0.01$, *** $p < 0.001$	51
4.21	Scheme of plasmids generated by cloning <i>Pex16</i> -regions A) Peak1, B) Peak2, C) Peak1+2, and D) Peak3 into pGL4.26 vector at KpnI and XhoI restriction sites. . . .	52
4.22	Electrophoresis gel: Inserts for pGL4.26-vector amplified via PCR.	53
4.23	Electrophoresis gel: Colony PCR results for pGL4.26- <i>Pex16</i> (Peak1, Peak2, Peak1+2, and Peak3) constructs.	53
4.24	Electrophoresis gel: Control digest of the generated pGL4.26- constructs with KpnI and XhoI restriction enzymes confirms the integration of all putative PPAR γ target regions (Peak1, Peak2, Peak3, and Peak1+2).	54

4.25	Luciferase assay results for PPAR γ binding. Four potential target regions downstream transcription start site were cloned into luciferase reporter vector pGL4.26 (Peak1, Peak2, Peak1+2 and Peak3 (full sequence)). pCMX-vectors expressing PPAR γ and RxR α , or the empty pCMX-vecor respectively, were co-transfected into Cos7 cells. Preliminary data show the mean \pm SD of two technical replicates. Luciferase activity is shown as percentage of pCMX-luciferase activity, which was set to 1, for each construct individually.	54
5.1	Scheme of the potential influence of PEX16 to peroxisomal development and lipid metabolism in (brown) adipose tissue.	61

List of Tables

3.1	Temperature profiles used in PCR reactions.	22
3.2	Temperature profile for Colony PCR reactions.	24
3.3	Temperature profile for qRT-PCR reactions.	28

6 Appendix

Sequencing results (Query = Pex16-sequence, Subject= Sequencing results)

pMSCVpuro_Pex16_fw

Alignments

[1_puro_Pex16_1_f_pMSCV_fw.fasta-1.txt - 1114 bp] 1_puro_Pex16_1_f_pMSCV_fw - Selection From [1] To Sequence ID: lcl229737 Length: 1114 Number of Matches: 1 Range 1: 39 to 1049

Score	Expect	Identities	Gaps	Strand	Frame
1884 bits(100%)	0.0()	1010/1011(99%)	0/1011(0%)	Plus/Plus	
Features:					
Query 1	ATGGAGAAGCTACGGCTCCTGAGCCTCCGCTACCAGGAGTATGTGACTCGTCATCCAGCC	60			
Sbjct 39	ATGGAGAAGCTACGGCTCCTGAGCCTCCGCTACCAGGAGTATGTGACTCGTCATCCAGCC	98			
Query 61	GCCACGGCCAGTTGGAGACGGCTGTGCGGGCCCTCAGTTACTGCTGGCAGGTGCGCTTC	120			
Sbjct 99	GCCACGGCCAGTTGGAGACGGCTGTGCGGGCCCTCAGTTACTGCTGGCAGGTGCGCTTC	158			
Query 121	TCCGATTACACGAGCTGTCTGAACTGGTGTACTCTGCCTCGAACCTGCTGGTGTGCTC	180			
Sbjct 159	TCCGATTACACGAGCTGTCTGAACTGGTGTACTCTGCCTCGAACCTGCTGGTGTGCTC	218			
Query 181	AATGACGGGATCCTGAGGAAAGGAGCTTCGAAAAAAGTTGCCCTGTGCTGCTGCCAGCAG	240			
Sbjct 219	AATGACGGGATCCTGAGGAAAGGAGCTTCGAAAAAAGTTGCCCTGTGCTGCTGCCAGCAG	278			
Query 241	AAGTTGCTGACATGGCTGAGTGTACTGGAGTGTGTGGAGGTGTTTCATGGAGATGGGGCT	300			
Sbjct 279	AAGTTGCTGACATGGCTGAGTGTACTGGAGTGTGTGGAGGTGTTTCATGGAGATGGGGCT	338			
Query 301	GCCAAAGTGTGGGGCGAAGTAGGCCGTTGGCTCGTCATTGCTCTCATCCAGTTGGCCAAAG	360			
Sbjct 339	GCCAAAGTGTGGGGCGAAGTAGGCCGTTGGCTCGTCATTGCTCTCATCCAGTTGGCCAAAG	398			
Query 361	GCCGTCCTGCGCATGCTCCTGTTGATCTGGTTCAGGCTGGCATTGACATCACCCCCC	420			
Sbjct 399	GCCGTCCTGCGCATGCTCCTGTTGATCTGGTTCAGGCTGGCATTGACATCACCCCCC	458			
Query 421	ATTGTTCCACTGGACAGGGAAACTCAGGCCACAGCCCTTGGATGGTGACCCACAATCCGGGC	480			
Sbjct 459	ATTGTTCCACTGGACAGGGAAACTCAGGCCACAGCCCTTGGATGGTGACCCACAATCCGGGC	518			
Query 481	AGCCAGGAGCCATCATATGTGGGGAAAACGGTACACAGAGTGGTGGCAACCTCCAGAAC	540			
Sbjct 519	AGCCAGGAGCCATCATATGTGGGGAAAACGGTACACAGAGTGGTGGCAACCTCCAGAAC	578			
Query 541	AGCCCATCCCTGCACCTACGGTACTGGGGAGCCCTCAGCAGCGGGAAATTCGGCAGAAA	600			
Sbjct 579	AGCCCATCCCTGCACCTACGGTACTGGGGAGCCCTCAGCAGCGGGAAATTCGGCAGAAA	638			
Query 601	CAGCAGCAGGAGAACTGAGCACACCCCAACACCTCTGGGGTTGCAGGAGACCAATTGCA	660			
Sbjct 639	CAGCAGCAGGAGAACTGAGCACACCCCAACACCTCTGGGGTTGCAGGAGACCAATTGCA	698			
Query 661	GAGTCTTTGTACATCGCCCGCCCTGCTGCACTTGCTCAGCCTGGGCTTATGGGGTCAG	720			
Sbjct 699	GAGTCTTTGTACATCGCCCGCCCTGCTGCACTTGCTCAGCCTGGGCTTATGGGGTCAG	758			
Query 721	CGATCGTGGACACCCCTGCTACTGTCTGGTGTGGTAGATATGACTAGCCTGAGTCTCCTG	780			
Sbjct 759	CGATCGTGGACACCCCTGCTACTGTCTGGTGTGGTAGATATGACTAGCCTGAGTCTCCTG	818			
Query 781	AGTGACAGGAAAGAACTTGACCCGGAGGGAGCGGCTAGAACTGAGGCGTTCGCACAATCCTG	840			
Sbjct 819	AGTGACAGGAAAGAACTTGACCCGGAGGGAGCGGCTAGAACTGAGGCGTTCGCACAATCCTG	878			
Query 841	CTGCTATACTACCTGCTACGCTCACCCTTCTATGACCGCTTCTCTGAAGCCAAGATCCTC	900			
Sbjct 879	CTGCTATACTACCTGCTACGCTCACCCTTCTATGACCGCTTCTCTGAAGCCAAGATCCTC	938			
Query 901	TTCTGCTCCAGCTGCTTACAGACCACATCCCTGGCGTGGGTCTGGTGGCAGGGCCGCTC	960			
Sbjct 939	TTCTGCTCCAGCTGCTTACAGACCACATCCCTGGCGTGGGTCTGGTGGCAGGGCCGCTC	998			
Query 961	ATGGACTACTTGCCCTCCTGGCAGAAAAATCTATTTCTACAGTTGGGGCTGA	1011			
Sbjct 999	ATGGACTACTTGCCCTCCTGGCAGAAAAATCTATTTCTACAGTTGGGGCTGA	1049			

pMSCVpuro_Pex16_rv

Alignments

[2_puro_Pex16_1_r_pMSCV_rv.fasta.txt - 1131 bp] 2_puro_Pex16_1_r_pMSCV_rv - Selection From [1] To [113]
 Sequence ID: lc|39299 Length: 1131 Number of Matches: 1
 Range 1: 209 to 1130

Score	Expect	Identities	Gaps	Strand	Frame
1688 bits(903)	0.0()	914/922(99%)	0/922(0%)	Plus/Minus	

Features:

Query	90	GGGCCTCAGTTACCTGCTGGCAGGTCGCTTCTCCGATTACACGAGCTGTCTGAACTGGT	149
Sbjct	1130	GGGCTTCAGTTACCTGCTGGCAGGTCGNNTTTCCGATTANMCGAGCTGTCTGAACTGGT	1071
Query	150	GTA	209
Sbjct	1070	KTATTC	1011
Query	210	AAAAAAGTTGCCTGTGTCGCTGTC	269
Sbjct	1010	AAAAAAGTTGCCTGTGTCGCTGTC	951
Query	270	GTGTGTGGAGGTGTTTCATGGAGATGGGGGCTGCCAAGGTGTGGGGCGAAGTAGGCCGTTG	329
Sbjct	950	GTGTGTGGAGGTGTTTCATGGAGATGGGGGCTGCCAAGGTGTGGGGCGAAGTAGGCCGTTG	891
Query	330	GCTCGTCATTGCTCTCATCCAGTTGGCCAAGGCCGTCCTGCGCATGCTCCTGTTGATCTG	389
Sbjct	890	GCTCGTCATTGCTCTCATCCAGTTGGCCAAGGCCGTCCTGCGCATGCTCCTGTTGATCTG	831
Query	390	GTTCAAGGCTGGCATTTCAGACATCACCCCCATTGTTCCACTGGACAGGGAAA	449
Sbjct	830	GTTCAAGGCTGGCATTTCAGACATCACCCCCATTGTTCCACTGGACAGGGAAA	771
Query	450	ACAGCCCTTGGATGGTGACCACAATCCGGGCAGCCAGGAGCCATCATATGTGGGGAAACG	509
Sbjct	770	ACAGCCCTTGGATGGTGACCACAATCCGGGCAGCCAGGAGCCATCATATGTGGGGAAACG	711
Query	510	GTACACAGAGTGGTGC	569
Sbjct	710	GTACACAGAGTGGTGC	651
Query	570	AGCCCTCAGCAGCGGGAAATTCGGCAGAAACAGCAGCAGGAGGAACTGAGCACACCC	629
Sbjct	650	AGCCCTCAGCAGCGGGAAATTCGGCAGAAACAGCAGCAGGAGGAACTGAGCACACCC	591
Query	630	AACACCTCTGGGGTTCAGGAGACCAATGCAGAGTCTTTGTACATCGCCCGGCCCTGCT	689
Sbjct	590	AACACCTCTGGGGTTCAGGAGACCAATGCAGAGTCTTTGTACATCGCCCGGCCCTGCT	531
Query	690	GCACTTGCTCAGCCTGGGCTTATGGGGTCAGCGATCGTGGACACCCCTGGCTACTGTCTGG	749
Sbjct	530	GCACTTGCTCAGCCTGGGCTTATGGGGTCAGCGATCGTGGACACCCCTGGCTACTGTCTGG	471
Query	750	TGTGGTAGATATGACTAGCCTGAGTCTCCTGAGTGACAGGAAGAACTTGACCCGGAGGGA	809
Sbjct	470	TGTGGTAGATATGACTAGCCTGAGTCTCCTGAGTGACAGGAAGAACTTGACCCGGAGGGA	411
Query	810	GCGGCTAGAACTGAGGCGTGCACAATCCTGCTGCTATACTACCTGCTACGCTCACCGTT	869
Sbjct	410	GCGGCTAGAACTGAGGCGTGCACAATCCTGCTGCTATACTACCTGCTACGCTCACCGTT	351
Query	870	CTATGACCGCTTCTCTGAAGCCAAGATCCTCTTCCTGCTCCAGCTGCTTACAGACCACAT	929
Sbjct	350	CTATGACCGCTTCTCTGAAGCCAAGATCCTCTTCCTGCTCCAGCTGCTTACAGACCACAT	291
Query	930	CCCTGGCGTGGGTCGGTGGCAAGGCCGCTCATGGACTACTTGCCTCCTGGCAGAAAAT	989
Sbjct	290	CCCTGGCGTGGGTCGGTGGCAAGGCCGCTCATGGACTACTTGCCTCCTGGCAGAAAAT	231
Query	990	CTATTCTACAGTTGGGGCTGA	1011
Sbjct	230	CTATTCTACAGTTGGGGCTGA	209

HisMaxC_Pex16_fw

Alignments

[7_HMC_Pex16_1_f_T7.fasta.txt - 1123 bp] 7_HMC_Pex16_1_f_T7 - Selection From [1] To [1123]

Sequence ID: lcl|31233 Length: 1123 Number of Matches: 1

Range 1: 299 to 1121

Score	Expect	Identities	Gaps	Strand	Frame
1517 bits(821)	0.00	822/823(99%)	0/823(0%)	Plus/Plus	
Features:					
Query	1	ATGGAGAAGCTACGGCTCCTGAGCCTCCGCTACCAGGAGTATGTGACTCGTCATCCAGCC			60
Sbjct	299	ATGGAGAAGCTACGGCTCCTGAGCCTCCGCTACCAGGAGTATGTGACTCGTCATCCAGCC			358
Query	61	GCCACGGCCCAAGTTGGAGACGGCTGTGCGGGCCCTCAGTTACCTGCTGGCAGGTGCGCTTC			120
Sbjct	359	GCCACGGCCCAAGTTGGAGACGGCTGTGCGGGCCCTCAGTTACCTGCTGGCAGGTGCGCTTC			418
Query	121	TCCGATTACACAGAGCTGTCTGAACTGGTGTACTCTGCCTCGAACTGCTGGTGTCTGCTC			180
Sbjct	419	TCCGATTACACAGAGCTGTCTGAACTGGTGTACTCTGCCTCGAACTGCTGGTGTCTGCTC			478
Query	181	AATGACGGGATCCTGAGGAAGGAGCTTCGAAAAAAGTTGCCTGTGTGCTGTCCCAGCAG			240
Sbjct	479	AATGACGGGATCCTGAGGAAGGAGCTTCGAAAAAAGTTGCCTGTGTGCTGTCCCAGCAG			538
Query	241	AAATTGCTGACATGGCTGAGTGTACTGGAGTGTGTGGAGGTGTTTCATGGAGATGGGGGCT			300
Sbjct	539	AAATTGCTGACATGGCTGAGTGTACTGGAGTGTGTGGAGGTGTTTCATGGAGATGGGGGCT			598
Query	301	GCCAAGGTGTGGGGCGAAGTAGGCCGTTGGCTCGTCATTGCTCTCATCCAGTTGGCCAAG			360
Sbjct	599	GCCAAGGTGTGGGGCGAAGTAGGCCGTTGGCTCGTCATTGCTCTCATCCAGTTGGCCAAG			658
Query	361	GCCGTCCTGCGCATGCTCCTGTTGATCTGGTTCAAGGCTGGCATTGAGACATCACCCCCC			420
Sbjct	659	GCCGTCCTGCGCATGCTCCTGTTGATCTGGTTCAAGGCTGGCATTGAGACATCACCCCCC			718
Query	421	ATTGTTCCACTGGACAGGGAAACTCAGGCACAGCCCTTGGATGGTGACCACAATCCGGGC			480
Sbjct	719	ATTGTTCCACTGGACAGGGAAACTCAGGCACAGCCCTTGGATGGTGACCACAATCCGGGC			778
Query	481	AGCCAGGAGCCATCATATGTGGGGAAACGGTCACACAGAGTGGTGCGAACCCCTCCAGAAC			540
Sbjct	779	AGCCAGGAGCCATCATATGTGGGGAAACGGTCACACAGAGTGGTGCGAACCCCTCCAGAAC			838
Query	541	AGCCCATCCCTGCACTCACGGTACTGGGGAGCCCTCAGCAGCGGGAAATTCGGCAGAAA			600
Sbjct	839	AGCCCATCCCTGCACTCACGGTACTGGGGAGCCCTCAGCAGCGGGAAATTCGGCAGAAA			898
Query	601	CAGCAGCAGGAGGAACTGAGCACACCCCAACACCTCTGGGGTTGCAGGAGACCATTGCA			660
Sbjct	899	CAGCAGCAGGAGGAACTGAGCACACCCCAACACCTCTGGGGTTGCAGGAGACCATTGCA			958
Query	661	GAGTCTTTGTACATCGCCCGGCCCTGCTGCACTTGCTCAGCCTGGGCTTATGGGGTCAG			720
Sbjct	959	GAGTCTTTGTACATCGCCCGGCCCTGCTGCACTTGCTCAGCCTGGGCTTATGGGGTCAG			1018
Query	721	CGATCGTGGACACCCCTGGCTACTGTCTGGTGTGGTAGATATGACTAGCCTGAGTCTCCTG			780
Sbjct	1019	CGATCGTGGACACCCCTGGCTACTGTCTGGTGTGGTAGATATGACTAGCCTGAGTCTCCTG			1078
Query	781	AGTGACAGGAAGAACTTGACCCGGAGGGAGCGGCTAGAACTGA		823	
Sbjct	1079	AGTGACAGGAAGAACTTGACCCGGAGGGAGCGGCTAGAACTGA		1121	

HisMaxC_Pex16_rv

Alignments

[2_puro_Pex16_1_r_pMSCV_rv.fasta.txt - 1131 bp] 2_puro_Pex16_1_r_pMSCV_rv - Selection From [1] To [113]
 Sequence ID: lcl|39299 Length: 1131 Number of Matches: 1
 Range 1: 209 to 1130

Score	Expect	Identities	Gaps	Strand	Frame
1688 bits(903)	0.0()	914/922(99%)	0/922(0%)	Plus/Minus	

Features:

Query	90	GGGCCTCAGTTACCTGCTGGCAGGTCGCTTCTCCGATTCACACGAGCTGTCTGAACTGGT	149
Sbjct	1130	GGGCTTCAGTTACCTGCTGGCAGGTCGNNNTTCCGATTCANMCGAGCTGTCTGAACTGGT	1071
Query	150	GTA CTCTGCCTCGAACCTGCTGGTGTCTGCTCAATGACGGGATCCTGAGGAAGGAGCTTCG	209
Sbjct	1070	KTATTCTGCCTCGAACCTGCTGGTGTCTGCTCAATGACGGGATCCTGAGGAAGGAGCTTCG	1011
Query	210	AAAAAAGTTGCCTGTGTGCTGTCCAGCAGAAAGTTGCTGACATGGCTGAGTGTACTGGA	269
Sbjct	1010	AAAAAAGTTGCCTGTGTGCTGTCCAGCAGAAAGTTGCTGACATGGCTGAGTGTACTGGA	951
Query	270	GTGTGTGGAGGTGTTTCATGGAGATGGGGGCTGCCAAGGTGTGGGGCGAAGTAGGCCGTTG	329
Sbjct	950	GTGTGTGGAGGTGTTTCATGGAGATGGGGGCTGCCAAGGTGTGGGGCGAAGTAGGCCGTTG	891
Query	330	GCTCGTCATTGCTCTCATCCAGTTGGCCAAGGCCGTCCTGCGCATGCTCCTGTTGATCTG	389
Sbjct	890	GCTCGTCATTGCTCTCATCCAGTTGGCCAAGGCCGTCCTGCGCATGCTCCTGTTGATCTG	831
Query	390	GTTCAAGGCTGGCATTGACATCAACCCCATTTGTTCCACTGGACAGGGAAACTCAGGC	449
Sbjct	830	GTTCAAGGCTGGCATTGACATCAACCCCATTTGTTCCACTGGACAGGGAAACTCAGGC	771
Query	450	ACAGCCCTTGGATGGTGACCAATCCGGGCAGCCAGGAGCCATCATATGTGGGGAAACG	509
Sbjct	770	ACAGCCCTTGGATGGTGACCAATCCGGGCAGCCAGGAGCCATCATATGTGGGGAAACG	711
Query	510	GTCACACAGAGTGGTGCAGAACCTCCAGAACAGCCCATCCCTGCACTCACGGTACTGGGG	569
Sbjct	710	GTCACACAGAGTGGTGCAGAACCTCCAGAACAGCCCATCCCTGCACTCACGGTACTGGGG	651
Query	570	AGCCCTCAGCAGCGGGAAATTCGGCAGAAAACAGCAGGAGGAACTGAGCACACCCCC	629
Sbjct	650	AGCCCTCAGCAGCGGGAAATTCGGCAGAAAACAGCAGGAGGAACTGAGCACACCCCC	591
Query	630	AACACCTCTGGGGTTGCAGGAGACCAATTGCAGAGTCTTTGTACATCGCCCGGCCCTGCT	689
Sbjct	590	AACACCTCTGGGGTTGCAGGAGACCAATTGCAGAGTCTTTGTACATCGCCCGGCCCTGCT	531
Query	690	GCACTTGCTCAGCCTGGGCTTATGGGGTCAGCGATCGTGGACACCCCTGGCTACTGTCTGG	749
Sbjct	530	GCACTTGCTCAGCCTGGGCTTATGGGGTCAGCGATCGTGGACACCCCTGGCTACTGTCTGG	471
Query	750	TGTGGTAGATATGACTAGCCTGAGTCTCCTGAGTGACAGGAAGAACTTGACCCGGAGGGA	809
Sbjct	470	TGTGGTAGATATGACTAGCCTGAGTCTCCTGAGTGACAGGAAGAACTTGACCCGGAGGGA	411
Query	810	GCGGCTAGAACTGAGGCGTCGCACAATCCTGCTGCTATACTACCTGCTACGCTCACCGTT	869
Sbjct	410	GCGGCTAGAACTGAGGCGTCGCACAATCCTGCTGCTATACTACCTGCTACGCTCACCGTT	351
Query	870	CTATGACCGCTTCTCTGAAGCCAAGATCCTCTTCCTGCTCCAGCTGCTTACAGACCACAT	929
Sbjct	350	CTATGACCGCTTCTCTGAAGCCAAGATCCTCTTCCTGCTCCAGCTGCTTACAGACCACAT	291
Query	930	CCCTGGCGTGGGTCTGGTGGCAAGGCCGCTCATGGACTACTTGCCCTCCTGGCAGAAAAT	989
Sbjct	290	CCCTGGCGTGGGTCTGGTGGCAAGGCCGCTCATGGACTACTTGCCCTCCTGGCAGAAAAT	231
Query	990	CTATTCTACAGTTGGGGCTGA	1011
Sbjct	230	CTATTCTACAGTTGGGGCTGA	209

pTK-Luc_Pex16_Peak1_fw, pTK-Luc_Pex16_Peak2_fw

Alignments

[4_pTK_x3_Peak1_M13.fasta - 1110 bp] 4_pTK_x3_Peak1_M13 - Selection From [1] To [1110]
 Sequence ID: lcl|236315 Length: 1110 Number of Matches: 1
 Range 1: 1 to 372

Score	Expect	Identities	Gaps	Strand	Frame
678 bits(367)	0.0()	372/374(99%)	2/374(0%)	Plus/Plus	
Features:					
Query	1033	TTGTAAC	TACGCAGGCGCCAAAGACAGCCAACCAAGGAGGCTGCAGATCGGGTGCCAGAAG	1092	
Sbjct	1	TTGT-ACTACGCAGGCGCC-AGACAGCCAACCAAGGAGGCTGCAGATCGGGTGCCAGAAG		58	
Query	1093	CTCTAGAGAGCTTCAGGGCCGAGAGAGAAGGAGCCAATGGCTGGAAAGGAGGGAGGGTGGG	1152		
Sbjct	59	CTCTAGAGAGCTTCAGGGCCGAGAGAGAAGGAGCCAATGGCTGGAAAGGAGGGAGGGTGGG	118		
Query	1153	AGCTCCCGGTCTCGGGGAGGAGGCGCTAGAGATGGGGTGAAGGGGCGTTTCAGGGGCTCCG	1212		
Sbjct	119	AGCTCCCGGTCTCGGGGAGGAGGCGCTAGAGATGGGGTGAAGGGGCGTTTCAGGGGCTCCG	178		
Query	1213	CGGGTCTAAGTCTCTCGGGCTGCGGAAAGTTGAGCAACCGGGAGGCGGGCTTAGGGCCGG	1272		
Sbjct	179	CGGGTCTAAGTCTCTCGGGCTGCGGAAAGTTGAGCAACCGGGAGGCGGGCTTAGGGCCGG	238		
Query	1273	AAGCAGGAAGGAGGGGCTCAGGACGCAGGGCGCCGCTGCCAGCCTTGCTGTGCGCCGGTGG	1332		
Sbjct	239	AAGCAGGAAGGAGGGGCTCAGGACGCAGGGCGCCGCTGCCAGCCTTGCTGTGCGCCGGTGG	298		
Query	1333	GACTGTCAGTGGCCAGAGCAGGATGGAGAAGCTACGGCTCCTGAGCCTCCGCTACCAGGA	1392		
Sbjct	299	GACTGTCAGTGGCCAGAGCAGGATGGAGAAGCTACGGCTCCTGAGCCTCCGCTACCAGGA	358		
Query	1393	GTATGTGACTCGTC	1406		
Sbjct	359	GTATGTGACTCGTC	372		

Alignments

[3_pTK_x3_Peak2_M13.fasta - 1110 bp] 3_pTK_x3_Peak2_M13 - Selection From [1] To [1110]
 Sequence ID: lcl|18831 Length: 1110 Number of Matches: 1
 Range 1: 1 to 380

Score	Expect	Identities	Gaps	Strand	Frame
658 bits(358)	0.0()	359/380(94%)	1/380(0%)	Plus/Plus	
Features:					
Query	1356	TGGAGAA-GCTACGGCTCCTGAGCCTCCGCTACCAGGAGTATGTGACTCGTCATCCAGCC	1414		
Sbjct	1	TGGAGAAAGCTACGGCTCCTGAGCCTCCGCTACCAGGAGTATGTGACTCGTCATCCAGCC	60		
Query	1415	GCCACGGCCAGTGGAGACGGCTGTGCGGGGCTCAGTTACCTGCTGGCAGGTGCCACA	1474		
Sbjct	61	GCCACGGCCAGTGGAGACGGCTGTGCGGGGCTCAGTTACCTGCTGGCAGGTGCCACA	120		
Query	1475	CTGACCTTTGACCCATTTCTTGGGGACTCTGACCCAGGAACCCATATGGCTCTTTGCCTGC	1534		
Sbjct	121	CTGACCTTTGACCCATTTCTTGGGGACTCTGACCCAGGAACCCATATGGCTCTTTGCCTGC	180		
Query	1535	TGACCCAGGGTAGTGGTTCGCGGTGCTTCAGTTCTGTCTGGGTTCCCTGTGGCGTAGAGGAA	1594		
Sbjct	181	TGACCCAGGGTAGTGGTTCGCGGTGCTTCAGTTCTGTCTGGGTTCCCTGTGGCGTAGAGGAA	240		
Query	1595	ACTAGAGAAACCCAAAGCCGAGGGTAAAACAGACGCTCACCAACGCCTTCTATACCTTCT	1654		
Sbjct	241	ACTAGAGAAACCCAAAGCCGAGGGTAAAACAGACGCTCACCAACGCCTTCTATACCTTCT	300		
Query	1655	TCCCTAGGTCGCTTCTCCGATTACACGAGCTGTCTGAACTGGGTAAAGTTGGACTCTGGG	1714		
Sbjct	301	TCCCTAGGTCGCTTCTCCGATTACACGAGCTGTCTGAACTGGGTAAAGTTGGACTCTGGG	360		

pTK-Luc_Pex16_Peak1+2_fw

Alignments

[2_pTK_x3_Peak1_2_M13.fasta - 1130 bp] 2_pTK_x3_Peak1_2_M13 - Selection From [1] To [1130]

Sequence ID: lcl|9885 Length: 1130 Number of Matches: 1

Range 1: 6 to 691

Score	Expect	Identities	Gaps	Strand	Frame	
1247 bits(675)	0.0()	685/689(99%)	3/689(0%)	Plus/Plus		
Features:						
Query	1026	CCGCAAGTTGTA	ACTACGCAGGCGCC	AAGACAGCC	AACCAAGGAGGCTGCAGATCGGGTG	1085
Sbjct	6	CCGC-AGTTGT-ACTACGCAGGCGCC-AGACAGCC	AACCAAGGAGGCTGCAGATCGGGTG			62
Query	1086	CCAGAAGCTCTAGAGAGCTTCAGGGCGGAGAGAGAAGGAGCC	AATGGCTGGAAGGAGGGGA			1145
Sbjct	63	CCAGAAGCTCTAGAGAGCTTCAGGGCGGAGAGAGAAGGAGCC	AATGGCTGGAAGGAGGGGA			122
Query	1146	GGGTGGGAGCTCCCGGTCTCGGGGAGGAGGCGCTAGAGATGGGGTGAAGGGGCGTTCAGG				1205
Sbjct	123	GGGTGGGAGCTCCCGGTCTCGGGGAGGAGGCGCTAGAGATGGGGTGAAGGGGCGTTCAGG				182
Query	1206	GGCTCCGCGGGTCTAAGTCTCTCGGGTGCAGGAAAGTTGAGCAACCGGGAGGCGGGCTTA				1265
Sbjct	183	GGCTCCGCGGGTCTAAGTCTCTCGGGTGCAGGAAAGTTGAGCAACCGGGAGGCGGGCTTA				242
Query	1266	GGGCCGGAAGCAGGAAGGAGGGCTCAGGACGCAGGGCGCCGCTGCCAGCCTTGCTGTCGG				1325
Sbjct	243	GGGCCGGAAGCAGGAAGGAGGGCTCAGGACGCAGGGCGCCGCTGCCAGCCTTGCTGTCGG				302
Query	1326	CCGGTGGGACTGTCAGTGGCCAGAGCAGGATGGAGAAGCTACGGCTCCTGAGCCTCCGCT				1385
Sbjct	303	CCGGTGGGACTGTCAGTGGCCAGAGCAGGATGGAGAAGCTACGGCTCCTGAGCCTCCGCT				362
Query	1386	ACCAGGAGTATGTGACTCGTCAATCCAGCCGCCACGGCCAGTTGGAGACGGCTGTGCGGG				1445
Sbjct	363	ACCAGGAGTATGTGACTCGTCAATCCAGCCGCCACGGCCAGTTGGAGACGGCTGTGCGGG				422
Query	1446	GCCTCAGTTACCTGCTGGCAGGTGCCCACTGACCTTTGACCCATTTCTTGGGGACTCTG				1505
Sbjct	423	GCCTCAGTTACCTGCTGGCAGGTGCCCACTGACCTTTGACCCATTTCTTGGGGACTCTG				482
Query	1506	ACCCAGGAACCCCTATGGCTCTTTGCTGCTGACCCAGGGTAGTGGTCGCGGTGCTTCAGT				1565
Sbjct	483	ACCCAGGAACCCCTATGGCTCTTTGCTGCTGACCCAGGGTAGTGGTCGCGGTGCTTCAGT				542
Query	1566	TCTGTCTGGGTTCCCTGTGGCGTAGAGGAAACTAGAGAACCCAAAGCCGCGGGTAAAAACA				1625
Sbjct	543	TCTGTCTGGGTTCCCTGTGGCGTAGAGGAAACTAGAGAACCCAAAGCCGCGGGTAAAAACA				602
Query	1626	GACGCTCACCAACGCCTTCTATACCTTCTTCCCTAGGTCGCTTCTCCGATTACACAGAGC				1685
Sbjct	603	GACGCTCACCAACGCCTTCTATACCTTCTTCCCTAGGTCGCTTCTCCGATTACACAGAGC				662
Query	1686	TGTCGAACTGGGTAAGTTGGACTCTGGG	1714			
Sbjct	663	TGTCGAACTGGGTAAGTTGGGCTCTGGG	691			

pTK-Luc_Pex16_Peak3s_fw, pTK-Luc_Pex16_Peak3I_fw

Alignments

[1_pTK_x3_Peak3_M13.fasta - 1207 bp] 1_pTK_x3_Peak3_M13 - Selection From [1] To [1207]
 Sequence ID: lcl|73877 Length: 1207 Number of Matches: 1
 Range 1: 5 to 321

Score	Expect	Identities	Gaps	Strand	Frame
580 bits(314)	1e-168()	317/318(99%)	1/318(0%)	Plus/Plus	
Features:					
Query	2145	TTGGCTGTTTGGAAACATGACAGGCAGTTTTTGGAGCAGCTCAGTAACCCAGTGTGTCCAGCA			2204
Sbjct	5	TTGGCTGTTTGG-ACATGACAGGCAGTTTTTGGAGCAGCTCAGTAACCCAGTGTGTCCAGCA			63
Query	2205	GAGCAAGGGCTGGCTTGTCACTCCAATCAGCTCATTTCCTACTGGCTCAGATGTCATCAT			2264
Sbjct	64	GAGCAAGGGCTGGCTTGTCACTCCAATCAGCTCATTTCCTACTGGCTCAGATGTCATCAT			123
Query	2265	GGAGAGAAATGGGGCTCTGAGGTAGTGGGCGGAGAGGCTTGTGGTTTCCACACAGTCTGT			2324
Sbjct	124	GGAGAGAAATGGGGCTCTGAGGTAGTGGGCGGAGAGGCTTGTGGTTTCCACACAGTCTGT			183
Query	2325	GGGTAGCTGTGATCGGTAGGGCTCTGGGGTAAGGGTGAGAGGGGTGAAGGCCACAGCAGG			2384
Sbjct	184	GGGTAGCTGTGATCGGTAGGGCTCTGGGGTAAGGGTGAGAGGGGTGAAGGCCACAGCAGG			243
Query	2385	GCCGGCCTCTCAAGACCACAATCTGCTTCTCAGTGTACTCTGCCTCGAACCTGCTGGTGC			2444
Sbjct	244	GCCGGCCTCTCAAGACCACAATCTGCTTCTCAGTGTACTCTGCCTCGAACCTGCTGGTGC			303
Query	2445	TGCTCAATGACGGGATCC	2462		
Sbjct	304	TGCTCAATGACGGGATCC	321		

Alignments

[3_pTK_Luc_peak3_M13.fasta - 1122 bp] 3_pTK_Luc_peak3_M13 - Selection From [1] To [1122]
 Sequence ID: lcl|50251 Length: 1122 Number of Matches: 1
 Range 1: 5 to 485

Score	Expect	Identities	Gaps	Strand	Frame
848 bits(458)	0.0()	481/482(99%)	1/482(0%)	Plus/Plus	
Features:					
Query	2144	TTTGGCTGTTTGGAAACATGACAGGCAGTTTTTGGAGCAGCTCAGTAACCCAGTGTGTCCAGC			2203
Sbjct	5	TTTGGCTGTTTGG-ACATGACAGGCAGTTTTTGGAGCAGCTCAGTAACCCAGTGTGTCCAGC			63
Query	2204	AGAGCAAGGGCTGGCTTGTCACTCCAATCAGCTCATTTCCTACTGGCTCAGATGTCATCA			2263
Sbjct	64	AGAGCAAGGGCTGGCTTGTCACTCCAATCAGCTCATTTCCTACTGGCTCAGATGTCATCA			123
Query	2264	TGGAGAGAAATGGGGCTCTGAGGTAGTGGGCGGAGAGGCTTGTGGTTTCCACACAGTCTG			2323
Sbjct	124	TGGAGAGAAATGGGGCTCTGAGGTAGTGGGCGGAGAGGCTTGTGGTTTCCACACAGTCTG			183
Query	2324	TGGGTAGCTGTGATCGGTAGGGCTCTGGGGTAAGGGTGAGAGGGGTGAAGGCCACAGCAG			2383
Sbjct	184	TGGGTAGCTGTGATCGGTAGGGCTCTGGGGTAAGGGTGAGAGGGGTGAAGGCCACAGCAG			243
Query	2384	GGCCGGCCTCTCAAGACCACAATCTGCTTCTCAGTGTACTCTGCCTCGAACCTGCTGGTGC			2443
Sbjct	244	GGCCGGCCTCTCAAGACCACAATCTGCTTCTCAGTGTACTCTGCCTCGAACCTGCTGGTGC			303
Query	2444	CTGCTCAATGACGGGATCCTGAGGAAGGAGCTTCGAAAAAAGTTGCCTGTGGTGAGAACT			2503
Sbjct	304	CTGCTCAATGACGGGATCCTGAGGAAGGAGCTTCGAAAAAAGTTGCCTGTGGTGAGAACT			363
Query	2504	TTGCCAGGAGCTGGGGGTGGGAAGCTCAGGGACTTGGGAGGAAAAACAGTAATGACCAGCA			2563
Sbjct	364	TTGCCAGGAGCTGGGGGTGGGAAGCTCAGGGACTTGGGAGGAAAAACAGTAATGACCAGCA			423
Query	2564	CGTGTGGTACATGTCGTTGTCTCAGAGAGTGAGGCATGCCCA	2605		
Sbjct	424	CGTGTGGTACATGTCGTTGTCTCAGAGAGTGAGGCATGCCCA	465		

pGI4.26_Pex16_Peak1_fw, pGI4.26_Pex16_Peak1_rv

Alignments

[1_Pex16_Peak1_fw_Pex16_Peak1_2_fw.fasta - 1137 bp] 1_Pex16_Peak1_fw_Pex16_Peak1_2_fw - Selection From [1] To [1137]
 Sequence ID: lcl|33325 Length: 1137 Number of Matches: 1
 Range 1: 2 to 349

Score	Expect	Identities	Gaps	Strand	Frame
634 bits(343)	0.0()	348/350(99%)	2/350(0%)	Plus/Plus	
Features:					
Query	1057	AGCCAACCAAGGAGGCTGCAGATCGGGTGCCAGAAAGCTCTAGAGAGCTTCAGGGCGGAGA	1116		
Sbjct	2	AGCC-ACC-AGGAGGCTGCAGATCGGGTGCCAGAAAGCTCTAGAGAGCTTCAGGGCGGAGA	59		
Query	1117	GAGAAGGAGCCAAATGGCTGGAAAGGAGGGAGGGTGGGAGCTCCCGGTCTCGGGGAGGAGGC	1176		
Sbjct	60	GAGAAGGAGCCAAATGGCTGGAAAGGAGGGAGGGTGGGAGCTCCCGGTCTCGGGGAGGAGGC	119		
Query	1177	GCTAGAGATGGGGTGAAGGGGCGTTCAGGGGCTCCGCGGGTCTAAGTCTCTCTGGGCTGC	1236		
Sbjct	120	GCTAGAGATGGGGTGAAGGGGCGTTCAGGGGCTCCGCGGGTCTAAGTCTCTCTGGGCTGC	179		
Query	1237	GGAAAGTTGAGCAACCGGGAGGCGGGCTTAGGGCCGGAAGCAGGAAGGAGGGCTCAGGACG	1296		
Sbjct	180	GGAAAGTTGAGCAACCGGGAGGCGGGCTTAGGGCCGGAAGCAGGAAGGAGGGCTCAGGACG	239		
Query	1297	CAGGGCGCCCTGCCAGCCTTGTCTGTCGGCCGGTGGGACTGTCACTGGCCAGAGCAGGAT	1356		
Sbjct	240	CAGGGCGCCCTGCCAGCCTTGTCTGTCGGCCGGTGGGACTGTCACTGGCCAGAGCAGGAT	299		
Query	1357	GGAGAAGCTACGGCTCCTGAGCCTCCGCTACCCAGGAGTATGTGACTCGTC	1406		
Sbjct	300	GGAGAAGCTACGGCTCCTGAGCCTCCGCTACCCAGGAGTATGTGACTCGTC	349		

Alignments

[2_Pex16_Peak1_rv_Pex16_Peak1_rv.fasta - 1164 bp] 2_Pex16_Peak1_rv_Pex16_Peak1_rv - Selection From [1] To [1164]
 Sequence ID: lcl|109391 Length: 1164 Number of Matches: 1
 Range 1: 3 to 359

Score	Expect	Identities	Gaps	Strand	Frame
856 bits(355)	0.0()	358/357(99%)	0/357(0%)	Plus/Minus	
Features:					
Query	1013	CTGTTTCAGCCTGCCCGCAAGTTGTAACCTACGCAAGGCGCCAAAGACAGCCAAACCAAGGAGGC	1072		
Sbjct	359	CTGTTTCAGCCTGCCCGCAAGTTGTAACCTACGCAAGGCGCCAAAGACAGCCAAACCAAGGAGGC	300		
Query	1073	TGCAGATCGGGTGCAGAAAGCTCTAGAGAGCTTCAGGGCGGAGAGAGAAAGGAGCCAAATGG	1132		
Sbjct	299	TGCAGATCGGGTGCAGAAAGCTCTAGAGAGCTTCAGGGCGGAGAGAGAAAGGAGCCAAATGG	240		
Query	1133	CTGGAAGGAGGGAGGGTGGGAGCTCCCGGTCTCGGGGAGGAGGGCGCTAGAGATGGGGTGA	1192		
Sbjct	239	CTGGAAGGAGGGAGGGTGGGAGCTCCCGGTCTCGGGGAGGAGGGCGCTAGAGATGGGGTGA	180		
Query	1193	AGGGGCGTTCAGGGGCTCCGCGGGTCTAAGTCTCTCTGGGCTGCGGAAGTTGAGCAACCG	1252		
Sbjct	179	AGGGGCGTTCAGGGGCTCCGCGGGTCTAAGTCTCTCTGGGCTGCGGAAGTTGAGCAACCG	120		
Query	1253	GGAGGCGGGCTTAGGGCCGGAAGCAGGAAGGAGGGCTCAGGACGAGGGGCGCCGCTGCCA	1312		
Sbjct	119	GGAGGCGGGCTTAGGGCCGGAAGCAGGAAGGAGGGCTCAGGACGAGGGGCGCCGCTGCCA	60		
Query	1313	GCCTTGTCTGTCGGCCGGTGGGACTGTCACTGGCCAGAGCAGGATGGAGAAGCTACGG	1369		
Sbjct	59	GCCTTGTCTGTCGGCCGGTGGGACTGTCACTGGCCAGAGCAGGATGGAGAAGCTACGG	3		

pGI4.26_Pex16_Peak2_fw, pGI4.26_Pex16_Peak2_rv

Alignments

[3_Pex16_Peak2_fw_Pex16_Peak2_fw.fasta - 1148 bp] 3_Pex16_Peak2_fw_Pex16_Peak2_fw - Selection From [1] To [1148]

Sequence ID: lcl|7189 Length: 1148 Number of Matches: 1

Range 1: 5 to 356

Score	Expect	Identities	Gaps	Strand	Frame
843 bits(348)	0.0()	351/352(99%)	1/352(0%)	Plus/Plus	
Features:					
Query	1362	AGCTACGGCTCCTGAG-CCTCCGCTACCAAGGATATGTGACTCGTCATCCAGCCGCCACG	1420		
Sbjct	5	AGCTACGGCTCCTGAGCCTCCGCTACCAAGGATATGTGACTCGTCATCCAGCCGCCACG	64		
Query	1421	GCCCAATTGGAGACGGCTGTGCGGGGCTCAGTTACCTGCTGGCAGGTGCCACACTGACC	1480		
Sbjct	65	GCCCAATTGGAGACGGCTGTGCGGGGCTCAGTTACCTGCTGGCAGGTGCCACACTGACC	124		
Query	1481	TTTGACCAATTTCTTGGGACTCTGACCAAGAAACCTATGGCTCTTTGCTGCTGACCC	1540		
Sbjct	125	TTTGACCAATTTCTTGGGACTCTGACCAAGAAACCTATGGCTCTTTGCTGCTGACCC	184		
Query	1541	AGGGTAGTGGTCGCGGTGCTTCAGTTCTGTCTGGGTTCCCTGTGGCGTAGAGGAACTAGA	1600		
Sbjct	185	AGGGTAGTGGTCGCGGTGCTTCAGTTCTGTCTGGGTTCCCTGTGGCGTAGAGGAACTAGA	244		
Query	1601	GAACCCAAAGCCGACGGTAAAACAGACGCTCACCACGCTTCTATACCTTCTCCCTA	1660		
Sbjct	245	GAACCCAAAGCCGACGGTAAAACAGACGCTCACCACGCTTCTATACCTTCTCCCTA	304		
Query	1661	GGTCGTTCTCCGATTCACACGAGCTGTCTGAACGGGTAAGTTGGACTCTG	1712		
Sbjct	305	GGTCGTTCTCCGATTCACACGAGCTGTCTGAACGGGTAAGTTGGACTCTG	356		

Alignments

[4_Pex16_Peak2_rv_Pex16_Peak1_2_rv.fasta - 1158 bp] 4_Pex16_Peak2_rv_Pex16_Peak1_2_rv - Selection From [1] To [1158]

Sequence ID: lcl|6973 Length: 1158 Number of Matches: 1

Range 1: 1 to 355

Score	Expect	Identities	Gaps	Strand	Frame
847 bits(350)	0.0()	354/356(99%)	1/356(0%)	Plus/Minus	
Features:					
Query	1319	CTGTCCGCGGTGGGACTGTCAATGGCCAGAGCAGGATGGAGAAGCTACGGCTCCTGAGC	1378		
Sbjct	355	CTGTCCGCGGTGGGACTGTCAATGGCCAGAGCAGGATGGAGAAGCTACGGCTCCTGAGC	296		
Query	1379	CTCCGCTACCAAGGATATGTGACTCGTCATCCAGCCGCCAGGCCAGTTGGAGACGGCT	1438		
Sbjct	295	CTCCGCTACCAAGGATATGTGACTCGTCATCCAGCCGCCAGGCCAGTTGGAGACGGCT	236		
Query	1439	GTGCGGGGCTCAGTTACCTGCTGGCAGGTGCCACACTGACCTTTGACCAATTTCTTGGG	1498		
Sbjct	235	GTGCGGGGCTCAGTTACCTGCTGGCAGGTGCCACACTGACCTTTGACCAATTTCTTGGG	176		
Query	1499	GACTCTGACCCAGGAACCTATGGCTCTTTGCTGCTGACCCAGGGTAGTGGTCGCGGTG	1558		
Sbjct	175	GACTCTGACCCAGGAACCTATGGCTCTTTGCTGCTGACCCAGGGTAGTGGTCGCGGTG	116		
Query	1559	CTTCAGTTCTGTCTGGGTTCTGTGGCGTAGAGGAACTAGAGAACCCAAAGCCGACGGG	1618		
Sbjct	115	CTTCAGTTCTGTCTGGGTTCTGTGGCGTAGAGGAACTAGAGAACCCAAAGCCGACGGG	56		
Query	1619	TAAAACAGACGCTCACCACGCTTCTATACCTTCTTCCCTAGGTCGCTTCTCCGA	1674		
Sbjct	55	TAAAACAGACGCTCACCACGCTTCTATACCTTCTTCCCTAGGTCGCTN-TCCGA	1		

pGI4.26_Pex16_Peak1+2_fw_pGI4.26_Pex16_Peak1+2_rv

Alignments

[5_Pex16_Peak12_f_Pex16_Peak1_2_fw.fasta - 1147 bp] 5_Pex16_Peak12_f_Pex16_Peak1_2_fw - Selection From [1] To [1147]
Sequence ID: lcl|8007 Length: 1147 Number of Matches: 1
Range 1: 4 to 649

Score	Expect	Identities	Gaps	Strand	Frame
1194 bits(848)	0.0()	848/848(100%)	0/848(0%)	Plus/Plus	
Features:					
Query 1067	GGAGGCTGCAGATCGGGTGCCAGAACTCTAGAGAGCTTCAGGGCGGAGAGAGAGGAGC	1126			
Sbjct 4	GGAGGCTGCAGATCGGGTGCCAGAACTCTAGAGAGCTTCAGGGCGGAGAGAGAGGAGC	63			
Query 1127	CAATGGCTGGAAGGAGGGAGGGTGGGAGCTCCCGGTCTCGGGGAGGAGGCGCTAGAGATG	1186			
Sbjct 64	CAATGGCTGGAAGGAGGGAGGGTGGGAGCTCCCGGTCTCGGGGAGGAGGCGCTAGAGATG	123			
Query 1187	GGGTGAAGGGGCGTTCAGGGGCTCCGCGGGTCTAAGTCTCTCTGGGCTCGGAAATTGAG	1246			
Sbjct 124	GGGTGAAGGGGCGTTCAGGGGCTCCGCGGGTCTAAGTCTCTCTGGGCTCGGAAATTGAG	183			
Query 1247	CAACCGGAGGCGGGCTTAGGGCCGGAAGCAGGAAGGAGGGCTCAGGACGCAGGGCGCCG	1306			
Sbjct 184	CAACCGGAGGCGGGCTTAGGGCCGGAAGCAGGAAGGAGGGCTCAGGACGCAGGGCGCCG	243			
Query 1307	CTGCCAGCCTTGCTGTCCGGCGGTGGGACTGTCACTGGCCAGAGCAGGATGGAGAAGCTA	1366			
Sbjct 244	CTGCCAGCCTTGCTGTCCGGCGGTGGGACTGTCACTGGCCAGAGCAGGATGGAGAAGCTA	303			
Query 1367	CGGCTCTGAGCCTCCGCTACCAAGGATATGTACTCGTCAATCCAGCCGCCAGGGCCCG	1426			
Sbjct 304	CGGCTCTGAGCCTCCGCTACCAAGGATATGTACTCGTCAATCCAGCCGCCAGGGCCCG	363			
Query 1427	TTGGAGACGGCTGTGCGGGGCTCACTTACCTGCTGGCAGGTGCCACTGACCTTTGAC	1486			
Sbjct 364	TTGGAGACGGCTGTGCGGGGCTCACTTACCTGCTGGCAGGTGCCACTGACCTTTGAC	423			
Query 1487	CCATTTCTTGGGACTCTGACCCAGGAACCTATGGCTCTTTGCTGCTGACCCAGGGTA	1546			
Sbjct 424	CCATTTCTTGGGACTCTGACCCAGGAACCTATGGCTCTTTGCTGCTGACCCAGGGTA	483			
Query 1547	GTGGTCGCGGTGCTTCAGTCTCTGGGTTCTGTGGCGTAGAGAAACTAGAGAACC	1606			
Sbjct 484	GTGGTCGCGGTGCTTCAGTCTCTGGGTTCTGTGGCGTAGAGAAACTAGAGAACC	543			
Query 1607	AAAGCCGACGGTAAAAACAGACGCTCAACCAACGCTTCTATACTTCTTCCCTAGGTGCG	1666			
Sbjct 544	AAAGCCGACGGTAAAAACAGACGCTCAACCAACGCTTCTATACTTCTTCCCTAGGTGCG	603			
Query 1667	TTCTCCGATTCACACGAGCTGTGAACTGGGTAAGTTGGACTCTG	1712			
Sbjct 604	TTCTCCGATTCACACGAGCTGTGAACTGGGTAAGTTGGACTCTG	649			

Alignments

[6_Pex16_Peak12_r_Pex16_Peak1_2_rv.fasta - 1158 bp] 6_Pex16_Peak12_r_Pex16_Peak1_2_rv - Selection From [1] To [1158]
Sequence ID: lcl|21799 Length: 1158 Number of Matches: 1
Range 1: 8 to 680

Score	Expect	Identities	Gaps	Strand	Frame
1210 bits(855)	0.0()	855/855(100%)	0/855(0%)	Plus/Minus	
Features:					
Query 1013	CTGTTACGCTGCCCGCAAGTTGTAACCTACGACGGCCCAAGACAGCCCAACCAAGGAGGC	1072			
Sbjct 660	CTGTTACGCTGCCCGCAAGTTGTAACCTACGACGGCCCAAGACAGCCCAACCAAGGAGGC	601			
Query 1073	TGCAGATCGGGTGCCAGAACTCTAGAGAGCTTCAGGGCGGAGAGAGAGGAGCCAAATGG	1132			
Sbjct 600	TGCAGATCGGGTGCCAGAACTCTAGAGAGCTTCAGGGCGGAGAGAGAGGAGCCAAATGG	541			
Query 1133	CTGGAAGGAGGGAGGGTGGGAGCTCCCGGTCTCGGGGAGGAGGCGCTAGAGATGGGGTGA	1192			
Sbjct 540	CTGGAAGGAGGGAGGGTGGGAGCTCCCGGTCTCGGGGAGGAGGCGCTAGAGATGGGGTGA	481			
Query 1193	AGGGGCGTTACGGGGCTCCGCGGGTCTAAGTCTCTCTGGGCTGCGGAAATTGAGCAACG	1252			
Sbjct 480	AGGGGCGTTACGGGGCTCCGCGGGTCTAAGTCTCTCTGGGCTGCGGAAATTGAGCAACG	421			
Query 1253	GGAGGCGGGCTTAGGGCCGGAAGCAGGAAGGAGGGCTCAGGACGCAGGGCGCCGCTGCCA	1312			
Sbjct 420	GGAGGCGGGCTTAGGGCCGGAAGCAGGAAGGAGGGCTCAGGACGCAGGGCGCCGCTGCCA	361			
Query 1313	GCCTTGCTGTGCGCGGGTGGGACTGTCACTGGCCAGAGCAGGATGGAGAAGCTACGGCTC	1372			
Sbjct 360	GCCTTGCTGTGCGCGGGTGGGACTGTCACTGGCCAGAGCAGGATGGAGAAGCTACGGCTC	301			
Query 1373	CTGAGCCTCCGCTACCAAGGATATGTACTCGTCAATCCAGCCGCCAGGGCCAGTTGGAG	1432			
Sbjct 300	CTGAGCCTCCGCTACCAAGGATATGTACTCGTCAATCCAGCCGCCAGGGCCAGTTGGAG	241			
Query 1433	ACGGCTGTGCGGGGCTCACTTACCTGCTGGCAGGTGCCACTGACCTTTGACCCATT	1492			
Sbjct 240	ACGGCTGTGCGGGGCTCACTTACCTGCTGGCAGGTGCCACTGACCTTTGACCCATT	181			
Query 1493	CTTGGGGACTCTGACCCAGGAACCTATGGCTCTTTGCTGCTGACCCAGGGTAGTGGTC	1552			
Sbjct 180	CTTGGGGACTCTGACCCAGGAACCTATGGCTCTTTGCTGCTGACCCAGGGTAGTGGTC	121			
Query 1553	CGGGTCTTCACTTCTGTCTGGGTTCTGTGGCGTAGAGAAACTAGAGAACC	1612			
Sbjct 120	CGGGTCTTCACTTCTGTCTGGGTTCTGTGGCGTAGAGAAACTAGAGAACC	61			
Query 1613	GCAGGGTAAAAACAGACGCTCAACCAACGCTTCTATACTTCTTCCCTAGGTGCGCT	1672			
Sbjct 60	GCAGGGTAAAAACAGACGCTCAACCAACGCTTCTATACTTCTTCCCTAGGTGCGCT	6			

pGI4.26_Pex16_Peak3_fw, pGI4.26_Pex16_Peak3_rv

Alignments

[7_Pex16_Peak3_fw_Pex16_Peak3_fw.fasta - 1199 bp] 7_Pex16_Peak3_fw_Pex16_Peak3_fw - Selection From [1] To [1199]
 Sequence ID: lcl|8689 Length: 1199 Number of Matches: 1
 Range 1: 1 to 481

Score	Expect	Identities	Gaps	Strand	Frame
843 bits(458)	0.0()	480/482(99%)	1/482(0%)	Plus/Plus	
Features:					
Query	2145	TTGGCTGTTTGGAAACATGACAGGCAGTTTTGAGCAGCTCAGTAACCAAGTCTGTCCAGCA			2204
Sbjct	1	TTGGCTGTTTGG-ACNTGACAGGCAGTTTTGAGCAGCTCAGTAACCAAGTCTGTCCAGCA			59
Query	2205	GAGCAAGGGCTGGCTTGTCACTCCAATCAGCTCAITTTCTTACTGGCTCAGATGTCATCAT			2264
Sbjct	60	GAGCAAGGGCTGGCTTGTCACTCCAATCAGCTCAITTTCTTACTGGCTCAGATGTCATCAT			119
Query	2265	GGAGAGAATGGGGCTCTGAGGTAGTGGGCGGAGAGGCTTGTGGTTTCCACACAGTCTGT			2324
Sbjct	120	GGAGAGAATGGGGCTCTGAGGTAGTGGGCGGAGAGGCTTGTGGTTTCCACACAGTCTGT			179
Query	2325	GGGTAGCTGTGATCGGTAGGGCTCTGGGGTAAGGGTGAGAGGGGTGAAGGCCACAGCAGG			2384
Sbjct	180	GGGTAGCTGTGATCGGTAGGGCTCTGGGGTAAGGGTGAGAGGGGTGAAGGCCACAGCAGG			239
Query	2385	GCCGGCTCTCAGACCAACAATCTGCTTCTCAGTGTACTCTGCTCGAACTGCTGGTGC			2444
Sbjct	240	GCCGGCTCTCAGACCAACAATCTGCTTCTCAGTGTACTCTGCTCGAACTGCTGGTGC			299
Query	2445	TGCTCAATGACGGGATCCTGAGGAAGGAGCTTCGAAAAAAGTTGCTGTGGTGAAGACTT			2504
Sbjct	300	TGCTCAATGACGGGATCCTGAGGAAGGAGCTTCGAAAAAAGTTGCTGTGGTGAAGACTT			359
Query	2505	TGCCAGGAGCTGGGGTGGGAAGCTCAGGGACTTGGGAGGAAAAAGTAATGACCAAGCAC			2564
Sbjct	360	TGCCAGGAGCTGGGGTGGGAAGCTCAGGGACTTGGGAGGAAAAAGTAATGACCAAGCAC			419
Query	2565	GTGTGGTACATGTCGTTGCTCAGAGAGTGAGGCATGCCAC			2606
Sbjct	420	GTGTGGTACATGTCGTTGCTCAGAGAGTGAGGCATGCCAC			461

Alignments

[8_Pex16_Peak3_rv_Pex16_Peak3_rv.fasta - 1130 bp] 8_Pex16_Peak3_rv_Pex16_Peak3_rv - Selection From [1] To [1130]
 Sequence ID: lcl|181849 Length: 1130 Number of Matches: 1
 Range 1: 8 to 460

Score	Expect	Identities	Gaps	Strand	Frame
833 bits(451)	0.0()	452/453(99%)	0/453(0%)	Plus/Minus	
Features:					
Query	2112	GAGAGCAAAGATGAGTTGGTGGGACCAACAATTTGGCTGTTTGGAAACATGACAGGCAGTT			2172
Sbjct	460	GAGAGCAAAGATGAGTTGGTGGGACCAACAATTTGGCTGTTTGGAAACATGACAGGCAGTT			401
Query	2172	TTGAGCAGCTCAGTAACCAAGTCTGTCCAGCAGAGCAAGGGCTGGCTTGTCACTCCAATC			2232
Sbjct	400	TTGAGCAGCTCAGTAACCAAGTCTGTCCAGCAGAGCAAGGGCTGGCTTGTCACTCCAATC			341
Query	2232	AGCTCAITTTCTTACTGGCTCAGATGTCATCATGGAGAGAATGGGGCTCTGAGGTAGTGGG			2292
Sbjct	340	AGCTCAITTTCTTACTGGCTCAGATGTCATCATGGAGAGAATGGGGCTCTGAGGTAGTGGG			281
Query	2292	CGGAGAGGCTTGTGGTTTCCACACAGTCTGTGGGTAGCTGTGATCGGTAGGGCTCTGGG			2352
Sbjct	280	CGGAGAGGCTTGTGGTTTCCACACAGTCTGTGGGTAGCTGTGATCGGTAGGGCTCTGGG			221
Query	2352	GTAAGGGTGAGAGGGGTGAAGGCCACAGCAGGGCCGGCTCTCAAGACCAACAATCTGCTT			2412
Sbjct	220	GTAAGGGTGAGAGGGGTGAAGGCCACAGCAGGGCCGGCTCTCAAGACCAACAATCTGCTT			161
Query	2412	CTCAGTGTACTCTGCTCGAACTGCTGGTGTGCTCAATGACGGGATCCTGAGGAAGGA			2472
Sbjct	160	CTCAGTGTACTCTGCTCGAACTGCTGGTGTGCTCAATGACGGGATCCTGAGGAAGGA			101
Query	2472	GCTTCGAAAAAAGTTGCTGTGGTGAGAACTTTGCCAGGAGCTGGGGTGGGAAGCTCAG			2532
Sbjct	100	GCTTCGAAAAAAGTTGCTGTGGTGAGAACTTTGCCAGGAGCTGGGGTGGGAAGCTCAG			41
Query	2532	GGACTTGGGAGGAAAAAGTAATGACCAAGCACG			2565
Sbjct	40	GGACTTGGGAGGAAAAAGTAATGACCAAGCACG			8

Bibliography

- [1] Kim PK and Mullen RT. PEX16: a multifaceted regulator of peroxisome biogenesis. *Front. Physiol.*, 4:241, 2013.
- [2] Bagattin A, Hugendubler L, and Mueller E. Transcriptional coactivator PGC-1 α promotes peroxisomal remodeling and biogenesis. *PNAS*, 107 (47):20376–20381, 2010.
- [3] Kramar R. Die Beteiligung von Peroxisomen am Lipidstoffwechsel. *J. Clin. Chem. Clin. Biochem.*, 24(2):109–118, 1986.
- [4] Kim PK, Mullen RT, Schumann U, and Lippincott-Schwartz J. The origin and maintenance of mammalian peroxisomes involves a de novo PEX16-dependent pathway from the ER. *J Cell Biol.*, 173(4):521–532, 2006.
- [5] Eitzen GA, Szilard RK, and Rachubinski RA. Enlarged Peroxisomes Are Present in Oleic Acid-grown *Yarrowia lipolytica* Overexpressing the PEX16 Gene Encoding an Intraperoxisomal Peripheral Membrane Peroxin. *J Cell Biol.*, 137(6):1265–1278, 1997.
- [6] Titorenko VI, Ogrydziak DM, and Rachubinski RA. Four distinct secretory pathways serve protein secretion, cell surface growth, and peroxisome biogenesis in the yeast *Yarrowia lipolytica*. *Mol Cell Biol.*, 17(9):5210–5226, 1997.
- [7] Titorenko VI and Rachubinski RA. Mutants of the yeast *Yarrowia lipolytica* defective in protein exit from the endoplasmic reticulum are also defective in peroxisome biogenesis. *Mol Cell Biol.*, 18(5):2789–2803, 1998.
- [8] Honsho M, Hiroshige T, and Fujiki Y. The membrane biogenesis peroxin Pex16p. Topogenesis and functional roles in peroxisomal membrane assembly. *J Biol Chem.*, 277(46):44513–44524, 2002.
- [9] Honsho M, Tamura S, Shimozawa N, Suzuki Y, Kondo N, and Fujiki Y. Mutation in PEX16 Is Causal in the Peroxisome-Deficient Zellweger Syndrome of Complementation Group D. *Am. J. Hum. Genet.*, 63(6):1622–1630, 1998.
- [10] Fransen M, Wylin T, Brees C, Mannaerts GP, and Van Veldhoven PP. Human Pex19p Binds Peroxisomal Integral Membrane Proteins at Regions Distinct from Their Sorting Sequences. *Mol Cell Biol.*, 21(13):4413–4424, 2001.

- [11] Yonekawa S, Furuno A, Baba T, Fujiki Y, Ogasawara Y, Yamamoto A, Tagaya M, and Tani K. Sec16B is involved in the endoplasmic reticulum export of the peroxisomal membrane biogenesis factor peroxin 16 (Pex16) in mammalian cells. *Proc Natl Acad Sci USA.*, 108(31):12746–12751, 2011.
- [12] Matsuzaki T and Fujiki Y. The peroxisomal membrane protein import receptor Pex3p is directly transported to peroxisomes by a novel Pex19p- and Pex16p- dependent pathway. *J Cell Biol.*, 183(7):1275–1286, 2008.
- [13] Heiland I and Erdmann R. Biogenesis of peroxisomes. Topogenesis of the peroxisomal membrane and matrix proteins. *FEBS J.*, 272(10):2362–2372, 2005.
- [14] Baerends RJ, Rasmussen SW, Hilbrands RE, van der Heide M, Faber KN, Reuvekamp RT, Kiel JA, Cregg JM, van der Klei IJ, and Veenhuis M. The *Hansenula polymorpha* PER9 gene encodes a peroxisomal membrane protein essential for peroxisome assembly and integrity. *J Biol Chem.*, 271(15):8887–8894, 1996.
- [15] Schliebs W and Kunau WH. Peroxisome membrane biogenesis: the stage is set. *Curr Biol.*, 14(10):R397–R399, 2004.
- [16] Waterham HR and Ebberink MS. Genetics and molecular basis of human peroxisome biogenesis disorders. *Biochim Biophys Acta.*, 1822(9):1430–1441, 2012.
- [17] Gould SG, Valle D, Raymond GV, eds. Scriver CR, Beaudet AL, Sly WS, and Valle D. "The peroxisome biogenesis disorders". In *The Metabolic and Molecular Bases of Inherited Disease*, volume 8, pages 3181–3217. McGraw-Hill, New York, 2001.
- [18] Titorenko VI and Rachubinski RA. The peroxisome: orchestrating important developmental decisions from inside the cell. *J Cell Biol.*, 164(5):641–645, 2004.
- [19] Wanders RJ, Vreken P, Ferdinandusse S, Jansen GA, Waterham HR, Van Roermund CW, and Van Grunsven EG. Peroxisomal fatty acid alpha- and beta-oxidation in humans: enzymology, peroxisomal metabolite transporters and peroxisomal diseases. *Biochem Soc Trans*, 29:250–267, 2001.
- [20] Reddy JK. Nonalcoholic Steatosis and Steatohepatitis. III. Peroxisomal β - oxidation, PPAR α , and steatohepatitis. *Am J Physiol Gastrointest Liver Physiol*, 281(6):G1333–G1339, 2001.
- [21] Subramani S. Components involved in peroxisome import, biogenesis, proliferation, turnover, and movement. *Physiol Rev*, 78(1):171–188, 1998.
- [22] Islinger M, Cardoso MJ, and Schrader M. Be different- the diversity of peroxisomes in the animal kingdom. *Biochim Biophys Acta*, 1803(8):881–897, 2010.

- [23] Desvergne B and Wahli W. Peroxisome proliferator-activated receptors: nuclear control of metabolism. *Endocr. Rev.*, 20(5):649–688, 1999.
- [24] Michalik L, Desvergne B, Dreyer C, Gavillet M, Laurini N, and Wahli W. PPAR expression and function during vertebrate development. *Int J Dev Biol.*, 46(1):105–114, 2002.
- [25] Di-Poi N, Tan NS, Michalik L, Wahli W, and Desvergne B. Antiapoptotic role of PPAR β in keratinocytes via transcriptional control of the Akt1 signaling pathway. *Mol Cell.*, 10(4):721–733, 2002.
- [26] Kersten S, Desvergne B, and Wahli W. Roles of PPARs in health and disease. *Nature*, 405(6785):421–424, 2000.
- [27] Martens K, Bottelbergs A, Peeters A, Jacobs F, Espeel M, Carmeliet P, Van Veldhoven PP, and Baes M. Peroxisome deficient aP2-Pex5 knockout mice display impaired white adipocyte and muscle function concomitant with reduced adrenergic tone. *Mol Genet Metab.*, 107(4):735–747, 2012.
- [28] Ahlaba I and Barnard T. Observations on peroxisomes in brown adipose tissue of the rat. *J Histochem Cytochem.*, 19(11):670–675, 1971.
- [29] Pavelka M, Goldenberg H, Hüttinger M, and Kramar R. Enzymic and morphological studies on catalase positive particles from brown fat of cold adapted rats. *Histochemistry*, 50(1):47–55, 1976.
- [30] Kramar R, Hüttinger M, Gmeiner B, and Goldenberg H. Beta-oxidation in peroxisomes of brown adipose tissue. *Biochim Biophys Acta.*, 531(3):353–356, 1978. PM: 216397.
- [31] Ortiz de Montanello P. *Cytochrome P450 Structure, Mechanism, and Biochemistry (2nd ed.)*. New York Plenum, 1995.
- [32] Johnson EF, Palmer CN, Griffin KJ, and Hsu MH. Role of the peroxisome proliferator-activated receptor in cytochrome P450 4A gene regulation. *FASEB J*, 10(11):1241–1248, 1996.
- [33] Mannaerts GP, Van Veldhoven PP, and Casteels M. Peroxisomal lipid degradation via β - and α - oxidation in mammals. *Cell Biochem Biophys.*, 32:73–87, 2000.
- [34] Reddy JK and Hashimoto T. Peroxisomal β -oxidation and peroxisome proliferator-activated receptor α : an adaptive metabolic system. *Annu Rev Nutr*, 21:193–230, 2001.
- [35] Zhu Y, Qi C, Cao WQ, Yeldandi AV, Rao MS, and Reddy JK. Cloning and characterization of PIMT, a protein with a methyltransferase domain, which interacts with and enhances nuclear receptor coactivator PRIP function. *Proc Natl Acad Sci USA*, 98(18):10380–10385, 2001.

- [36] Lazarow PB and ed. Sies H. Compartmentation of β - oxidation of fatty acids in peroxisomes. In *Metabolic compartmentation.*, pages 317–329. Academic Press, New York, 1982.
- [37] Xie WD, Wang H, Zhang JF, Li JN, Can Y, Qing L, Kung HF, and Zhang YO. Enhanced peroxisomal β - oxidation metabolism in visceral adipose tissues of high-fat diet-fed obesity-resistant C57BL/6 mice. *Exp Ther Med.*, 2(2):309–315, 2011.
- [38] Mangurian LP and Donaldson RP. Development of peroxisomal beta-oxidation activities in brown fat of perinatal rabbits. *Biol Neonate.*, 57(6):349–357, 1990. PM: 1973620.
- [39] Brites P, Ferreira AS, da Silva TF, Sousa VF, Malheiro AR, Duran M, Waterham HR, Baes M, and Wanders RJ. Alkyl-glycerol rescues plasmalogen levels and pathology of ether-phospholipid deficient mice. *PLoS One*, 6(12):e28539, 2011.
- [40] Sacksteder KA, Jones JM, South ST, Li X, Liu Y, and Gould SJ. PEX19 Binds Multiple Peroxisomal Membrane Proteins, Is Predominantly Cytoplasmic, and Is Required for Peroxisome Membrane Synthesis. *J Cell Biol.*, 148(5):931–944, 2000.
- [41] Rosen ED and Spiegelman BM. What We Talk About When We Talk About Fat. *Cell*, 156(1-2):20–44, 2014.
- [42] Cannon B and Nedergaard J. Brown Adipose Tissue: Function and Physiological Significance. *Physiological Reviews*, 84(1):277–359, 2004.
- [43] Gao AW and Houtkooper RH. Mitochondrial fission: firing up mitochondria in brown adipose tissue. *EMBO J*, 33(5):401–402, 2014.
- [44] Seale P. Brown adipose tissue biology and therapeutic potential. *Front. Endocrinol.*, 4:14, 2013.
- [45] Birerdinc A, Jarrar M, Stotish T, Randhawa M, and Baranova A. Manipulating molecular switches in brown adipocytes and their precursors: A therapeutic potential. *Prog Lipid Res.*, 52(1):51–61, 2013.
- [46] Klein J, Fasshauer M, Klein HH, Benito M, and Kahn CR. Novel adipocyte lines from brown fat: a model system for the study of differentiation, energy metabolism, and insulin action. *BioEssays*, 24(4):382–388, 2002.
- [47] Kim JB, Wright HM, Wright M, and Spiegelman BM. ADD1/SREBP1 activates PPARgamma through the production of endogenous ligand. *Proc Natl Acad Sci USA*, 95(8):4333–4337, 1998.